

## Distribution Agreement

In presenting this thesis or dissertation as a partial fulfillment of the requirements for an advanced degree from Emory University, I hereby grant to Emory University and its agents the non-exclusive license to archive, make accessible, and display my thesis or dissertation in whole or in part in all forms of media, now or hereafter known, including display on the world wide web. I understand that I may select some access restrictions as part of the online submission of this thesis or dissertation. I retain all ownership rights to the copyright of the thesis or dissertation. I also retain the right to use in future works (such as articles or books) all or part of this thesis or dissertation.

Signature:

---

Harrison Carroll Brown

---

Date

Bioengineering Viral Transgenes for the Treatment of the Hemophilias

By

Harrison Carroll Brown  
Doctor of Philosophy

Graduate Division of Biological and Biomedical Science  
Molecular and Systems Pharmacology

---

Chris Doering, Ph.D.  
Advisor

---

Trent Spencer, Ph.D.  
Committee Member

---

Renhao Li, Ph.D.  
Committee Member

---

Edward Morgan, Ph.D.  
Committee Member

Accepted:

---

Lisa A. Tedesco Ph.D.  
Dean of the James T. Laney School of Graduate Studies

---

Date

Bioengineering Viral Transgenes for the Treatment of the Hemophilias

By

Harrison Carroll Brown  
B.B.A, Emory University Goizueta Business School, 2009

Advisor: Chris Doering, Ph.D.

An abstract of a dissertation submitted to the Faculty of the  
James T. Laney School of Graduate Studies of Emory University  
in partial fulfillment of the requirements for the degree of  
Doctor of Philosophy  
in the Graduate Division of Biological and Biomedical Science,  
Molecular and Systems Pharmacology  
2016

## Abstract

### Bioengineering Viral Transgenes for the Treatment of the Hemophilias

By Harrison Carroll Brown

Since its inception in the mid-1960s, gene therapy has remained an attractive yet elusive strategy for the treatment of inherited genetic disease. The first successful introduction of therapeutic DNA into a human was performed in 1990, where a gene encoding adenosine deaminase was introduced in cells from an adenosine deaminase deficiency severe combined immunodeficiency (ADA-SCID) patient. Since then, over 2,300 clinical trials have been conducted worldwide, and over \$7 billion were invested in commercial gene therapy in 2015 alone. Despite these efforts, only one clinical gene therapy product has been approved in a regulated market to date.

Over the last 15 years, there has been substantial scientific and financial investment in producing a clinically viable gene therapy for the hemophilias, A and B. At the time of writing, there are 8 active gene therapy clinical trials for hemophilia, with 4 actively recruiting. These trials propose to use adeno-associated virus to deliver therapeutic transgenes to the liver of patients with hemophilia. However, a second modality of using lentivirus to deliver the transgene to hematopoietic cells is also under pre-clinical investigation.

Experience with previous adeno-associated viral trials for hemophilia B have been hampered by low-levels of protein expression at clinically safe viral doses. This problem has been anticipated in ongoing trials, and substantial effort has been made to increase protein expression while maintaining a safe vector dose. The work presented herein furthers these efforts, both by expanding on previously utilized methods of increasing protein production as well as introducing novel strategies tailored toward gene therapy. We hypothesized that there are two primary factors limiting efficient protein production from these gene therapy systems. First, that the oversized nature of the transgene utilized in the context of AAV-mediated gene therapy limits the amount of functional vector DNA that is delivered to a patient's cells, and that this could be overcome by engineering smaller, more efficient regulatory control regions. Second, that the intracellular biosynthesis of the protein itself limits protein production, and that this could be overcome by both engineering the protein itself or by modifying the coding sequence of the vector DNA for optimal expression within the particular cellular milieu in which it is expressed. Through a combination of these techniques, we have developed AAV vectors for both hemophilia A and B that pre-clinical *in vivo* studies predict are of sufficient potency to delivery curative levels of protein expression at clinical safe viral vector doses, achieving a long-sought milestone in the history of viral gene therapy for the hemophilias.

Bioengineering Viral Transgenes for the Treatment of the Hemophilias

By

Harrison Carroll Brown  
B.B.A, Emory University Goizueta Business School, 2009

Advisor: Chris Doering, Ph.D.

A dissertation submitted to the Faculty of the  
James T. Laney School of Graduate Studies of Emory University  
in partial fulfillment of the requirements for the degree of  
Doctor of Philosophy  
in the Graduate Division of Biological and Biomedical Science,  
Molecular and Systems Pharmacology  
2016

## **Acknowledgements**

First and foremost, I would like to thank my advisor Dr. Chris Doering for taking a chance 8 years prior to this writing by accepting a business major undergraduate with no laboratory experience and a tenuous grasp of basic biology into his lab. Over the years of thoughtful teaching, guidance through mentorship, and endless patience, he has been instrumental in every phase of my scientific training and preparation for my future career. There is no way I can properly express my gratitude for all he has done for me throughout the years. With his boundless knowledge and positivity, he has made every step of the way a truly amazing experience. His mentorship has been an indispensable part of my training, and he has taught me lessons in science and beyond that will last a lifetime.

I also want to thank Dr. Trent Spencer, who has been a second mentor to me. His door has always been open to discuss a question or idea, and I have been very fortunate to have a mentor such as him. I also thank the other members of my committee, Dr. Renhao Li and Dr. Eddie Morgan for their open mindedness and insights toward my project. I thank them for the time and effort they have offered to me, consider myself lucky to have had a committee of this caliber.

I would like to thank Dr. Bagi Gangadharan, who taught me many if not most of the laboratory skills I know today. He has always been happy to be a board to bounce ideas off, even from abroad, and I am grateful for his ongoing insights and friendship. I also want to thank both my lab and the staff of Expression Therapeutics, who have always been there to lend a helping hand, and have made our lab a fun and friendly place to work. Finally, I want to thank John Healey and Ernie Parker, who often become graduate student mentors who did not sign up for the job. They never missed an opportunity to help or to teach, and have been an integral part of my training and that of the many others who had the fortune of working with them.

## **Table of Contents**

**Abstract**

**Acknowledgements**

**Table of Contents**

**List of Figures and Tables**

**List of Abbreviations**

<b>Chapter 1 – Introduction .....</b>	<b>1</b>
1.1 History of gene therapy .....	2
1.2 Types of gene therapy vectors .....	4
A. Integrating vectors .....	5
B. Non-integrating vectors.....	7
1.3 AAV as a gene therapy vector .....	9
1.4 History of the Hemophilias.....	13
1.5 Coagulation Physiology .....	15
1.6 Challenges in Modern Hemophilia Treatment.....	17
1.7 Landscape of Clinical AAV for the Hemophilias .....	20
1.8 Strategies for Improving AAV Vectors for the Hemophilias .....	24
A. Capsid Discover and Engineering.....	25
B. Protein Bioengineering.....	25
C. Size Reduction.....	26
D. Codon Optimization.....	27
1.9 Concluding Remarks .....	27
1.10 Thesis Hypothesis.....	29
<b>Chapter 2 – Bioengineered Coagulation Factor VIII Enables Long-Term Correction of Murine Hemophilia A Following Liver-Directed Adeno-Associate Viral Vector Delivery... 30</b>	
2.1 Abstract.....	31

2.2 Introduction.....	31
2.3 Materials and Methods.....	33
2.4 Results.....	38
2.5 Discussion.....	49
2.6 Acknowledgements.....	59
2.7 Supplemental Information.....	60
<b>Chapter 3 – Liver-directed bioengineering of AAV-FVIII transgenes.....</b>	<b>67</b>
3.1 Abstract.....	68
3.2 Introduction.....	68
3.3 Materials and Methods.....	70
3.4 Results.....	73
3.5 Discussion.....	89
3.6 Acknowledgements.....	94
3.7 Supplemental Information.....	95
<b>Chapter 4 – General Discussion.....</b>	<b>96</b>
4.1 Collective Results.....	97
4.2 Implications of Findings.....	99
4.3 Limitations and Future Directions.....	101
4.4 Conclusions.....	104
<b>References.....</b>	<b>106</b>

## List of Figures and Tables

<b>Figure 1.1 Schematic representation of AAV and lentiviral genomes</b> .....	6
<b>Figure 1.2 Tissue tropism and receptor usage of AAV serotypes 1-9</b> .....	12
<b>Figure 1.3 Schematic summary of primary and secondary hemostasis</b> .....	18
<b>Figure 1.4 Model of loss of vector potency with increasing transgene length</b> .....	28
<b>Figure 2.1: Viral Vector Design</b> .....	39
<b>Figure 2.2: Molecular assembly of rAAV-HCR-ET3 vector particles</b> .....	42
<b>Figure 2.3: Dose finding of rAAV-HCR-ET3 in a murine model of hemophilia A</b> .....	44
<b>Figure 2.4: Formation of FVIII inhibitors following rAAV-HCR-ET3 administration</b> .....	47
<b>Figure 2.5: <i>In vivo</i> viral genome copy number</b> .....	50
<b>Figure 2.6: Phenotypic correction of the bleeding diathesis</b> .....	51
<b>Supplemental Table 2.1: Biotinylated probes used for detection of AAV-HCR-ET3 viral genomes</b> .....	60
<b>Supplemental Table 2.2: Primers used for regional transgene analysis</b> .....	61
<b>Supplemental Table 2.3: Hydrodynamic injection of FVIII encoding AAV expression plasmids</b> .....	62
<b>Supplemental Figure 2.1: Standard curves for quantitative PCR analysis</b> .....	63
<b>Supplemental Figure 2.2: Sequence alignment of porcine-substituted Domains of ET3 and HSQ</b> .....	64
<b>Supplemental Figure 2.3: ET3 C2 domain sequence RNA is present in liver of treated mice</b> .....	69
<b>Figure 3.1 Promoter design and testing</b> .....	75
<b>Figure 3.2: Liver directed codon optimization</b> .....	79
<b>Figure 3.3: Expression and tissue specificity of HCO versus LCO</b> .....	83
<b>Figure 3.4: Expression and tissue specificity of LCO, MCO, and NoCo designs</b> .....	84
<b>Figure 3.5: In vivo expression of codon optimized designs</b> .....	86

<b>Figure 3.6: AAV delivery of optimized FVIII cassettes .....</b>	<b>88</b>
<b>Supplemental Figure 3.1: Schematics of size reduction of AAV-FVIII transgenes .....</b>	<b>95</b>

### **List of abbreviations**

AAP	assembly-activating protein
AAV	adeno-associated virus
ABP	$\alpha$ -microglobulin/Bikuni
ABPnat	$\alpha$ -microglobulin/Bikuni native
ABPshort	$\alpha$ -microglobulin/Bikuni short
ADA	adenosine deaminase
ADA	adenovirus
AFP	$\alpha$ -fetoprotein
An53	ancestral FVIII node 53
APOE	apolipoprotein
BDD	B-domain deleted
bGHPA	bovine growth hormone poly adenylation
BHK	baby hamster kidney
bp	base pair
BU	Bethesda units
Cap	capsid
CBER	Center for Biologics Evaluation and Research
CDS	coding DNA sequence
CFTR	cystic fibrosis transmembrane conductance regulator
CHO	Chinese hamster ovary
CMV	cytomegalovirus
CUB	codon usage bias
DHFR	the dihydrofolate reductase
ds	double stranded
ER	endoplasmic reticulum
FD	frequency deviation
FDA	the Food and Drug Administration
FIX	factor IX
FV	factor V
FVII	factor VII
FVIII	factor VIII
FX	factor X
hAAT	human alpha-1 antitrypsin
HCB	hepatic combinatorial bundle
HCO	human codon optimized
HEK	human embryonic kidney
HGPT	hypoxanthine-guanine phosphoribosyl transferase
HLP	hybrid liver promoter
HSC	hematopoietic stem cell
IM	intramuscular
ITI	immune tolerance induction
ITR	inverted terminal repeat

kb	kilobases
kg	kilogram
LCO	liver codon optimized
LPLD	lipoprotein lipase deficiency
LV	lentivirus
MCO	myeloid codon optimized
MHC	major histocompatibility
NoCo	non codon optimized
ORV	oncoretrovirus
PAGE	polyacrylamide gel electrophoresis
PBS	phosphate buffered saline
polyA	polyadenylation
rAAV	recombinant adeno-associated virus
rhFVIII	recombinant human factor VIII
rpFVIII	recombinant porcine factor VIII
SCID	severe combined immunodeficiency
SERPINA1	serine protease A1
ss	single stranded
SV40	Simian vacuolating virus 40
TF	tissue factor
TF	transcription factor
TRS	terminal resolution site
TSS	transcription start site
TTR	transthyretin
UTR	untranslated region
vg	vector genomes
vp	vector particles
VWF	von Willebrand factor

## **Chapter 1**

### **Introduction**

## 1.1 A history of Gene Therapy

In the United States, gene therapy is regulated by the Center for Biologics Evaluation and Research (CBER), one of the six main centers of the Food and Drug Administration (FDA), as enabled by the Public Health Service Act and the Federal Food Drug and Cosmetic Act (1). Gene therapy is defined by the FDA as therapies that “that mediate their effects by transcription and/or translation of transferred genetic material and/or by integrating into the host genome and that are administered as nucleic acids, viruses, or genetically engineered microorganisms. The products may be used to modify cells *in vivo* or transferred to cells *ex vivo* prior to administration to the recipient” (2).

Despite the regulatory pipeline to enable the approval of medicinal gene therapies, at the time of this writing the FDA has yet to approve any gene therapy product for use in the United States. To date, the European Commission is the only western regulatory body to grant marketing approval of a gene therapy product, Glybera® (alipogene tiparvovec), which was approved in October, 2012 for the treatment of familial lipoprotein lipase deficiency (LPLD) (3).

The earliest demonstration of experimental gene transfer may be traced to the 1928 work of Frederick Griffith, over 2 decades before the now famous Hershey Chase experiment confirmed DNA as the source of heritable genetic material (4; 5). In his seminal work, Griffith demonstrated that nonvirulent *Streptococcus pneumoniae* could be converted into a virulent phenotype by mixing it with a heat-inactivated virulent form of the bacteria. It would not be until 1944 that work by Oswald Avery and colleagues would show that the causative agent of the virulent transformation was DNA (6).

In 1962, the first proof-of-principle demonstration of heritable correction of a genetic defect in mammalian cells was demonstrated by Szybalska *et al* (7). In this experiment, Szybalska established a line of bone marrow-derived cells with defective hypoxanthine-guanine phosphoribosyl transferase (HGPRT), an enzyme critical for the *de novo* synthesis of purines when the dihydrofolate reductase (DHFR) pathway is inhibited. When both of these pathways are disrupted, purine

synthesis is shut down and the cell subsequently dies. Syblaska showed that as expected, when the DHFR pathway is blocked by the addition of aminopterin, the HGPT<sup>(-)</sup> cells failed to proliferate and subsequently died. However, by transforming these cells with DNA extracted from HGPT<sup>(+)</sup> cells, the HGPT pathway was salvaged, and the cells grown in the presence of aminopterin survived and proliferated. Furthermore, the daughter cells of the transformed HGPT<sup>(-)</sup> retained the phenotype of the transformed parental cells, for the first time demonstrating the possibility of heritable correction of a genetic defect.

The next pivotal finding in the history of gene transfer came from the work of Joseph Sambrook in 1968. Sambrook and colleagues were investigating the state of viral DNA in cells that had been infected from Simian vacuolating virus 40 (SV40). Surprisingly, multiple copies of viral DNA were found to have been stably integrated into the host cell's chromosomal DNA (8). This work demonstrated that not only could viruses transfer genetic information cells, but that they could permanently and heritably modify the genome of the recipient cell.

Building on this knowledge, in 1975 Terheggen *et al* attempted the first published attempt at gene therapy in humans (9). In this study, wild-type Shope papilloma virus, which was believed to carry a virally coded arginase, was delivered to three hyperargininemic patients, with the hope that the virally delivered arginase gene would correct the underlying metabolic disorder. Unfortunately, this experiment resulted in no change in serum arginine levels in these patients. It was not until the genome of the Shope papilloma virus was fully sequenced in 1985 that it was discovered that the virus does not carry an arginase encoding gene (10).

It would not be until 1990 that the first successful therapeutic introduction of recombinant DNA into humans was achieved. In this trial, two children with adenosine deaminase severe combined immunodeficiency (ADA-SCID) received T-cells which were modified *ex vivo* using retroviral-mediated gene transfer to express adenosine deaminase (11). The results of this study were mixed, yet promising. One patient showed persistent benefit from the therapy, with improvements in both

cellular ADA levels as well as both cellular and humoral immune function. The second patient showed only transient improvement.

A second gene therapy trial for ADA-SCID was initiated in 1995, again using retroviral-mediated *ex vivo* transduction, but in contrast to the 1990 trial, both peripheral lymphocytes as well as bone marrow cells were gene modified. The two patients that received this therapy exhibited persistent benefit from the treatment (12). Fate mapping of the gene modified cells demonstrated rapid but short term immune reconstitution was achieved with the gene modified peripheral lymphocytes, while delayed but long term reconstitution was achieved with modified bone marrow cells. This benefit persisted in the years reported following the gene therapy.

Since these initial clinical trials, over 2,300 clinical trials have been initiated across 36 countries, for indications ranging from cardiovascular disease, ocular disorders, cancer, hematological malignancies and beyond (13).

## **1.2 Types of Gene Therapy Vectors**

In early gene therapy trials, the choice of viral vector was largely made out of convenience and availability. This is perhaps most poignantly demonstrated by the 1975 trial using the Shope papilloma virus, where it was hoped the wild-type virus would on its own confer the therapeutic gene with no further manipulation. However, as knowledge of molecular genetics and virology have advanced, a wide variety of gene therapy vectors have become available. As this panel grew, it became apparent that each vector would have a vastly different profile in terms of safety and efficacy, and that the holy grail of a one size fits all viral vector for gene therapy was unlikely to be found. Indeed, it has become increasingly clear that under the current paradigm of gene therapy, each gene therapy protocol will likely need to carefully select a vector tailored to a specific disease and even a specific patient.

Of particular consideration when choosing a vector are the durability of gene expression, the ability to infect dividing or quiescent cells, the immunogenicity of the vector, the prevalence of preexisting inhibitory antibodies to the vector, the tropism of the virus, as well as the practical

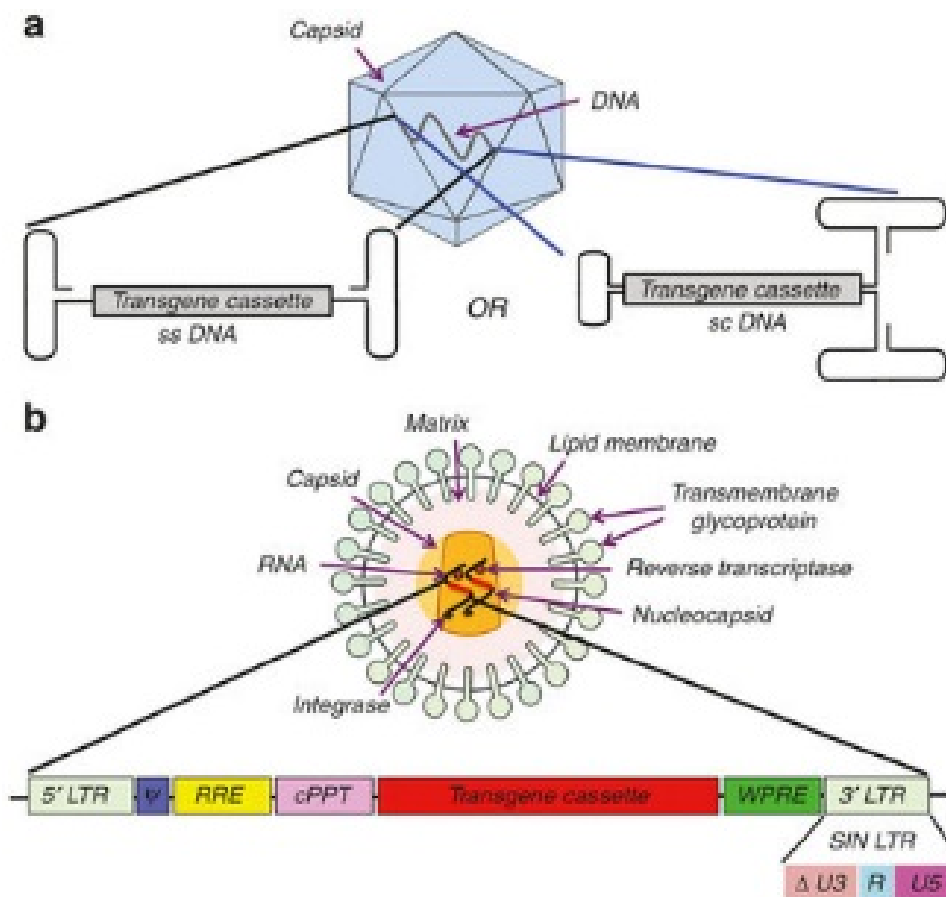
considerations of the cost of vector manufacture and supply chain infrastructure necessary for global distribution. In this section, we will explore the benefits and shortcomings of some of the most widely utilized viral gene therapy vectors. However, it is worth noting that several non-viral gene delivery approaches, including naked plasmid delivery (14), liposome encapsulated nucleic acids (15), polymer nanoparticle and mechanical mediated approaches to gene transfer are also being explored for clinical gene therapy (16; 17).

Viral gene therapy vectors may be broadly divided into two categories: integrating and non-integrating. Integrating viruses stably incorporate their genetic cargo into the chromosomal DNA of the host cells. One particular benefit of these viruses is that the modified DNA is passed to daughter cells, providing durable gene expression over the life of that cell's and that of its progeny. However, this comes at the risk of heritable disruption or activation of endogenous gene function. Non-integrating viruses, conversely, do not modify the DNA of the host cells, and instead persist as episomes capable of gene expression but not replication. As a result, these episomes are diluted out during cell division, providing gene expression for the life of the parent cell, but decreasing expression in each successive generation of progeny. As these viral tools have been further developed, the lines between integrating and non-integrating viruses are becoming increasingly blurred. Non-integrating viruses may be engineered to deliver transposons and or gene editing systems, where the host cell DNA is modified a while sparing integration of the viral transgene itself (18-20). Alternatively, non-integrating variants of naturally integrating vectors have also been developed (21). The genomic structure of two prototypical gene therapy vectors is contrasted in

### **Figure 1.1**

#### **A. Integrating Vectors**

Due to the permanent inheritability of gene modification, integrating viral vectors are an attractive and obvious choice for gene therapy. Within this class, the vectors being most rigorously developed for gene therapy can be subdivided into two classes: oncoretroviruses (ORVs) and

**Figure 1.1**

**Figure 1.1 Schematic representation of AAV and lentiviral genomes. A)** The non-integrating AAV vector utilizes a compact genome and simple structure containing only vector DNA surrounded by protein capsid. **B)** The integrating lentiviral vector utilizes a more complex genome and viral structure containing both viral RNA and viral proteins contained in a lipid membrane envelope. Abbreviations: ssDNA: single stranded DNA, scDNA: self complimentary DNA, LTR: long terminal repeat, cPPT: central polypurine tract, WPRE: woodchuck's posttranscriptional response element, SIN: self inactivating, This figure was adapted from [Molecular Therapy – Methods & Clinical Development](#). It was originally created by Sandeep Kumar and Roland Herzog and is licensed under [CC BY-NC license](#).

lentiviruses (LVs). LVs are the most broadly utilized vectors, while ORVs, which were utilized in the first ADA-SCID trials, are restricted in use due to their dangerous integration profiles.

Despite their popularity in early clinical trials, ORVs suffer from two distinct disadvantages. First, these viruses have been found to poorly infect quiescent cells, as breakdown of the nuclear envelope during cell division is required for efficient infection, with infection of quiescent cells being as much as 100-fold lower than those that are actively dividing (22). Due to this requirement, the use of these vectors has largely been limited to *ex vivo* modification, where cells such as peripheral lymphocytes or their progenitors may be stimulated to actively divide and permit efficient transduction. The second limitation of ORVs is their propensity to integrate in the non-coding gene enhancers and promoters proximal to active genes. Due to this preference, these viruses have been documented to activate proto-oncogenes, leading to loss of cell cycle control, which is then passed to the rapidly proliferating daughter cells (23; 24).

Unlike ORVs, LVs are capable of efficiently infecting both dividing and terminally differentiated, quiescent cells (25). Like ORVs, LVs are capable of infecting dividing cells *ex vivo*, however, cells that are quiescent *in vivo* such as hepatocytes, neurons, or myofibers are also permissive to infection. Additionally, LVs have a much more favorable integration profile than ORVs in terms of clinical safety. LVs tend to integrate more randomly through the genome, with a preference for integration within the coding of actively transcribing genes (26). While this leaves the potential for gene disruption, in most cases the second copy of the gene would be sufficient to provide protection against disruption of any anti-oncogenic gene. For these reasons, LVs are becoming the vector of choice over ORV for gene therapy applications.

## **B. Non-integrating Vectors**

While the permanent heritability of integrating vectors offers a clear advantage to their clinical application, strategies of non-integrating gene therapy are also under active development. These approaches are attractive when either permanent gene expression may not be desired, such as gene editing systems, or when the target cells are under long term quiescence or undergoing slow

turnover, such as in neurons and hepatocytes, respectively. In these cases, non-integrating vectors may provide years to a lifetime of benefit despite their non-heritable nature. The two lead non-integrating vectors under current development for clinical gene therapy are adenovirus and adeno-associated virus.

Adenovirus (Ad) is a large (100nm) virus known to efficiently transfer genes to the cells of most human organs *in vivo* (27). This discovery made adenovirus a front runner in early gene therapy vector designs. However, adenovirus is well documented to elicit a potent, dose responsive immune response in persons treated with the vector, with the potential to induce a strong innate and cellular immune response against the infected cells, resulting in destruction of the infected cells, the loss of gene expression, and the potential of escalating to life-threatening systemic inflammatory response (28; 29). While toxicities have tempered enthusiasm for the use of this virus for the treatment of hereditary genetic disease, adenovirus remains an attractive vector for targeting of some cancers. In 2004, China's State Food and Drug Administration approved Gendicine, an adenoviral gene therapy vector, for the treatment of head and neck squamous cell carcinoma (30).

Originally discovered as a contaminating factor to adenoviral preparations, adeno-associated virus (AAV) is quickly becoming the preferred vector for many gene therapy applications (31-34). AAV is a small, single stranded virus that causes no known pathogenicity in humans (35). Due to its small size, the DNA packaging capacity of the virus is limited to about 4.7 kilobases (kb), which limits its ability to carry larger transgenes, such as the cystic fibrosis transmembrane conductance regulator (CFTR) or coagulation factor VIII (FVIII). Despite this limitation, AAV continues to be developed and applied clinically to treat a wide variety of genetic disease. A particular benefit of AAV is that a large library of both naturally-occurring and synthetically-derived serotypes have been well characterized, with over 100 naturally occurring variants described to date (36). While each serotype has a similar DNA packaging capacity, the unique viral capsid structure of these vectors allows for broad or specific tissue tropism based on the needs of the therapy (37; 38).

### 1.3 AAV as a gene therapy vector

Adeno associated virus (AAV) is a small, helper-dependent DNA virus of the *Dependovirus* genus of parvoviruses that infects humans and other primates. With the exception of mild immune response, AAV causes no known pathogenicity. AAV is able to infect a wide variety of both dividing and quiescent cells, and due to this favorable profile of robust infectivity as well as safety, AAV has become an attractive vector for human gene therapy applications, with over 170 clinical trials having been conducted, representing 7.2% of all gene therapy clinical trials to date (39).

Wildtype AAV uses a compact, 4.7kb single-stranded DNA genome that is reliant co-infection with helper viruses such as adenovirus or herpes simplex virus to produce a productive infection. Cellular infection with AAV may take two non-exclusive pathways: latent or productive. In the presence of helper virus co-infection, there is sufficient functionality to allow for successful viral genome reproduction and packaging of DNA into nascent viral particles. In the absence of helper virus coinfection, the AAV-encoded Rep proteins guide the viral DNA to integrate into a specific locus on human chromosome 19, where it may persist in latency until it is later rescued by infection with a helper virus.

While over 100 variants of AAV have been isolated from various host species, these viruses all share the same genome structure (36). AAV genomes are generated from double stranded (ds) DNA precursor, which serves as both template for DNA replication and substrate itself for packaging into preformed viral capsids as single stranded (ss) DNA fragments, with both strand polarities (+ or -) packaged with equal efficiencies (40). The single stranded genome is flanked on both ends by non-coding T-shaped hairpin structures known as inverted terminal repeats (ITRs). These ITRs serve as important elements for the replication, integration, rescue, and packaging of the AAV genome. Between these ITRs are two open reading frames, which through alternative splicing are translated into four non-structural (Rep40, Rep52, Rep68, and Rep78), and three structural (VP1, VP2, and VP3) proteins, which code for capsid (Cap) proteins. An alternative

ORF within the VP gene codes for the non-structural assembly-activating protein (AAP), which is required for capsid assembly (41). All other functions needed for AAV reproduction and assembly are provided by the host cell or helper virus coinfection.

The basis for use of AAV as a gene therapy vector is that, in absence of the Rep/Cap proteins or viral coinfection, the host cell alone is capable of uncoating the viral capsid, converting the ssDNA genome to dsDNA, and utilizing DNA repair pathways to form stable extrachromosomal episomes directed by the structure of the ITRs (42). A therapeutic AAV vector is created by replacing the rep/cap genes of the AAV genome with a therapeutic gene expression cassette. Under this design, the recombinant genome is delivered, converted, stabilized, and expressed in the same manner as the wildtype genome, but lacking the rep/cap genes, is unable to reproduce.

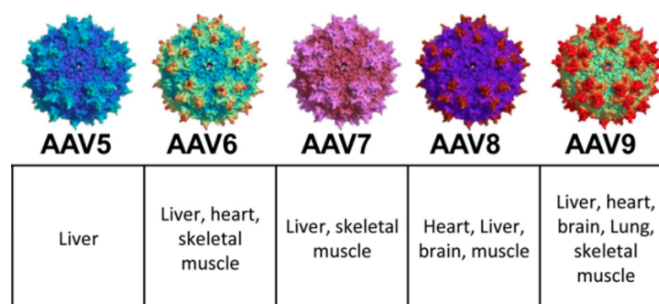
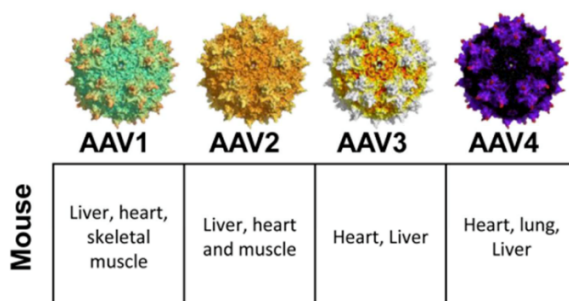
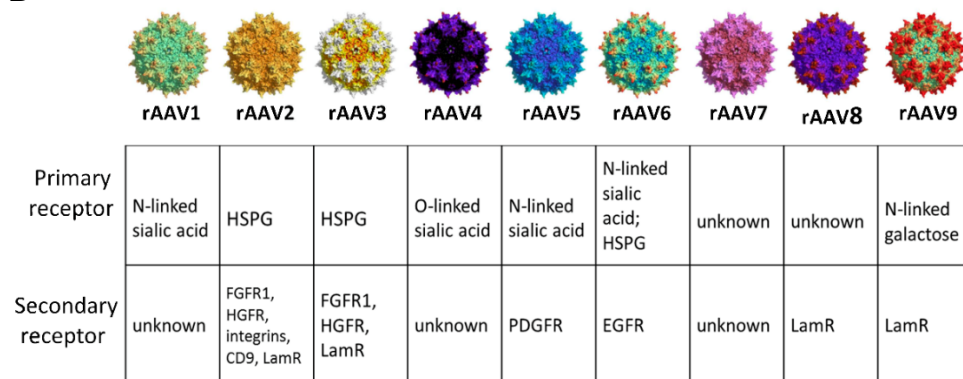
Packaging of a recombinant AAV genome into an AAV capsid minimally requires the ITRs to be *in cis* with the DNA expression cassette. To generate a functional AAV viral vector free from AAV coding DNA, the proteins required for viral replication (rep, cap, AAP, and helper virus proteins) are provided *in trans* during virus production. The necessary elements (the ITR flanked expression cassette, rep/cap genes, and helper virus genes) are brought together in producer cell lines by standard gene transfer techniques, such as plasmid transfection or viral transduction. Within the producer cells, rep/cap and helper proteins are expressed, and in a process analogous to a productive wildtype infection, the ITR flanked genome is rescued from the dsDNA plasmid template and packaged as ssDNA into preformed viral capsids. These capsids may then be purified by standard chromatography or centrifugation techniques.

The tissue specificity and immunogenic properties of AAVs are determined by the structure of the viral capsid, which is composed of the three structural proteins VP1, VP2, and VP3 assembled in a 1:1:10 ratio. When assembled, these proteins form a 20nm shell of icosahedral symmetry. While structurally similar, the particular topology of the surface of the capsid shell of the different AAV serotypes may radically alter the cell binding and immunogenic profile of a

particular serotype (37; 43). AAVs utilize multiple cell surface glycans as anchors for cellular attachment and entry, with the particular binding profile of each serotype determined by the structure of the capsid shell. AAV vector transgenes may be cross-packaged into different capsid serotypes depending on the tissues targeted for gene transfer. The tissue tropism and receptor usage of AAV serotypes 1-9 are shown in **Figure 1.2**.

These therapeutic particles may be delivered either systemically or directly to the target tissue. Upon binding to cell surface receptors, AAV vectors are internalized through clathrin coated pits, however, the potential for intracellular signaling through surface receptor binding remains an unanswered question (44). While the spatiotemporal nature of the pathways and mechanisms of viral trafficking and uncoating remain incompletely understood, it is generally accepted that minimally AAV particles are trafficked through endosomal pathways, ultimately resulting in nuclear transport. However, visualization of intact AAV particles throughout the cell suggests that alternative, non-mutually exclusive pathways of nuclear entry may exist (45). Within the nucleus, the single-stranded DNA genome undergoes conversion to dsDNA by utilizing the self-complimentary end of the 3' ITR as a self-priming motif, allowing cellular polymerases to extend second strand synthesis across the length of the genome. However, this step has been shown to be rate-limiting and potentially detrimental to recombinant AAV vectors (46). To relieve this restriction, AAV may be packaged as double stranded DNA by deleting the terminal resolution site within the 3' ITR. This site is the target for cleavage by the AAV rep protein, which is necessary for single stranded packaging. Lacking this motif, vector DNA is packaged as self-complimentary dsDNA, which is believed to increase vector potency by eliminating the necessity of second strand synthesis.

Despite the favorable safety profile and increasing interest in AAV as a gene therapy vectors, the biology of the virus imposes several limitations on its use as a therapeutic tool. The small size of the assembled capsid (20nm) places a physical constraint on the amount of DNA that may be packaged. The precise capacity of the virus remains debated, however, it is generally

**Figure 1.2****A****B****Figure 1.2 The tissue tropism and receptor usage of adeno-associated virus serotypes 1-9. A)**

The adeno-associated virus (AAV) capsid structure dictates the tissue tropism of the vector when injected intravenously. **B)** The alternative receptor usage of AAV capsids is a key determinant in

the tissue tropism of the vector. Abbreviations: HSPG: heparan sulfate proteoglycan, FGFR1:

Fibroblast growth factor receptor 1, HGFR: hepatocyte growth factor receptor, PDGFR: platelet

derived growth factor receptor, EGFR: endothelium growth factor receptor. This figure was

adapted from [InTech Open](#). It was originally created by Melisa Vance and Richard J. Samulski

and is licensed under [CC BY-NC 4.0](#) license.

recognized to be under 5.0kb of total DNA, with efficiency of vector production, heterogeneity of vector product, and potency of the virus improving as transgene size approaches the 4.7kb wildtype genome (47). This places particular constraints on the treatment of diseases caused deficiencies in proteins coded by long cDNAs, such as the cystic fibrosis transmembrane conductance regulator in cystic fibrosis, dystrophin in muscular dystrophy, or coagulation factor FVIII for hemophilia A. In these cases, the size of the cDNA approaches or exceeds the ideal packaging capacity of the virus on its own, while still requiring the addition of ITRs and non-coding regulatory control features. While vectors larger than 5.0kb are frequently utilized, these vectors package as genome fragments, which rely on intracellular reassembly after coinfection with a viral fragment containing a partially overlapping, complimentary strand containing the missing regions of transgene DNA, which greatly reduces vector potency (48). Because of this constraint, transgene size is a critical parameter in the design of AAV vectors. This is of particular concern for self-complimentary, dsDNA designs, which are limited to half the coding length of ssDNA designs.

In addition to the size constraints, pre-existing immunity to AAV is an additional obstacle in AAV administration. As natural hosts to AAV, 22-56% of humans are estimated to have pre-existing inhibitory antibodies against AAV serotype 2, with antibodies frequently cross-reacting to other serotypes (49; 50). Systemic administration of AAV to these individuals is rendered ineffective by this pre-existing immunity, however, several strategies have been proposed to circumvent this obstacle. Pharmacologic intervention, local administration, the use of “decoy” capsids to saturate antibody binding, and the use of alternative natural or artificial capsid serotypes hold promise to allow broader administration of AAV vectors to populations with high prevalence of pre-existing immunity (51).

#### **1.4 History of the Hemophilias**

The hemophilias are a primarily an X-linked inherited bleeding disorder resulting from deficiencies in functional circulating blood coagulation factors. Lacking these factors, the body's ability to control bleeding is impaired, resulting in a pro-hemorrhagic state that leads to prolonged

bleeding, excessive bruising, and greatly increased risk of hemarthrosis and cerebral hemorrhage. Left untreated, hemophilia is universally fatal by the age of 30 (52). Hemophilia may be considered the first instance of a documented inherited disease, where the 5<sup>th</sup> century Babylonian Talmud, a collection of rabbinical writings on Jewish law and tradition, provides an exemption to the ritual of circumcision for sons of a mother who has previously had two sons die from the operation (53). While the discovery of the mechanisms of gene transmission remained over a millennium away, this writing importantly identified both the familial and maternal nature of the disease inheritance. The disease was first identified in medical literature by the Arabic 12<sup>th</sup> century physician Albucasis, who specifically described families with males who died from seemingly minor injuries (54).

The first description of hemophilia in modern times was by physician John Conrad Otto, who in 1803, some 700 years after the writings of Albucasis would again describe a familial bleeding disorder which specifically effected males (55), however, the etiology of the disease would not begin to be understood until the next century. In 1916, Minot and Lee described that whole blood transfusion from healthy donors decreased bleeding time in patients with hemophilia, and in 1937, Patek and Taylor would discover that a specific component extracted from blood plasma, which they described as “*anti-hemophilic globulin*” was sufficient to control bleeding time (56). In 1944, it was discovered that the blood from one person with hemophilia could correct the bleeding from another person with hemophilia, and vice versa (57). This finding showed that there existed at least two forms of hemophilia, which would later become known as hemophilia A, which results from deficient levels of coagulation factor VIII (FVIII), and hemophilia B, which occurs from the deficiency of coagulation factor IX (FIX). These discoveries of the early 20<sup>th</sup> century for the first time allowed efficacious treatment of the hemophilias, however, due to the limited volume of blood able to be transfused at a single time, complete correction of bleeding was unachievable and morbidity and mortality remained high.

A breakthrough in treatment for the hemophilias came in 1964, when it was discovered that fractions from cryoprecipitated blood plasma contained concentrated amounts of clotting factors

(58). These factor concentrates for the first time allowed near complete correction of bleeding diathesis, allowing for surgery and control of severe bleeding. Over the next two decades, increased availability of clotting factor concentrates allowed for improved treatment protocols, allowing for at-home prophylactic injection of clotting factor, leading to significantly improved quality of life and decreased burden on healthcare systems and providers. Tragically, the increased use of these blood-derived concentrates throughout the 70s and early 80s coincided with the rise of the worldwide HIV and hepatitis epidemic. As these pooled blood-derived products were not screened for viral contamination at this time, by the mid 80's 40% of persons with hemophilia were positive for hepatitis C, and over 50% were positive for HIV (59; 60).

Fortunately, the discovery of the viral contamination of blood-derived products coincided with the emergence practical gene sequencing methods, and by 1985 the DNA sequences of FIX and FVIII had been determined (61; 62). This complete sequence allowed the development of recombinantly expressed FIX and FVIII concentrates, which are produced free from human blood and greatly improved the safety of protein replacement therapies, while improved viral detection methods increased the safety of blood-derived products. Through these developments over the last century, the hemophilias have transformed from a lethal pediatric disease to a chronic condition that when properly managed allows near normal life expectancy.

### **1.5 Coagulation physiology**

Approximately 800 million years ago, the multicellular eukaryotic kingdom Metazoa emerged. The rise of this kingdom marked a significant departure in the body plan of early organisms, where their multicellular nature allowed an expansion in size and complexity. While early organisms relied on simple diffusion for the transport of nutrients and oxygen, as body size increased there was a need for organized transport systems, a scheme that may broadly be classified as circulatory systems. In both vertebrate and invertebrate lineages, closed circulatory systems, wherein blood remains distinctly separated from the tissues of the body, arose to meet these demands. These closed systems rely on a propulsive force to drive blood through diverging branches of vessels to distribute

blood throughout body. A consequence of propulsive force within a closed system is pressurization. While these pressurized systems allowed for large and efficient body plans, an uncontrolled breach of this closed system would result in a fatal compromise of the distribution of nutrients and removal of wastes. From this, a strong evolutionary pressure to control such hemorrhages emerged (63).

Hemostasis is the process that emerged to protect organisms from injury to the vascular system (64). This process is highly conserved within mammals, and ultimately results in the local transformation of blood from a liquid to a gel. This process may be divided into two separate yet interrelated parts: primary and secondary hemostasis. Primary hemostasis is the process in which platelets adhere to the site of injury to form a plug which controls hemorrhage, while secondary hemostasis is the process in which insoluble fibrin is incorporated into this plug, strengthening and stabilizing it from disruption. Despite the names of primary and secondary, these two processes occur simultaneously. Upon injury to the endothelial lumen of a blood vessel, the pro-thrombotic subendothelial matrix becomes exposed to circulating blood, initiating the process of hemostasis. Within the subendothelial matrix lies immobilized von Willebrand factor (VWF) and collagen, which bind to platelet receptors GPIb-IX-V and GPVI, respectively (65; 66). This binding results in integrin-dependent platelet activation, ultimately resulting in platelet-activating agonists releasing from the platelets themselves, causing feedback activation of nearby platelets and further aggregation of the local platelet plug (67).

During the formation of the platelet plug, secondary hemostasis initiates from the exposure of subendothelial tissue factor (TF), which binds the circulating serine protease coagulation factor VII (FVII). Upon binding, FVII is activated to FVIIa as a result of cleavage from several proteases, including thrombin and the FVIIa-TF complex itself. The TF-FVIIa complex activates coagulation factors IX (FIX) and X (FX) to FIXa and FXa, respectively. This activation initiates a feedback loop, wherein the presence of its cofactor activated coagulation factor VIII (FVIIIa), FIXa will itself activate FX to FXa. FXa, and in the presence of its cofactor activated coagulation factor V (FVa), form the prothrombinase complex, which activates pro-thrombin to thrombin. The now

active thrombin feeds back to activate FVIII to FVIIIa, FV to FVa, and FVII to FVIIa, as well as to convert soluble fibrinogen to insoluble fibrin which is deposited within the growing platelet plug, forming a mesh that stabilizes the plug against disruption. In the absence of functional FVIII (hemophilia A) or FIX (hemophilia B), this thrombin-generating feedback loop is disrupted, resulting in impaired fibrin deposition and significantly impaired clotting, however, the FVIIa-TF complex by itself provides low levels of FX activation, permitting low-levels of thrombin activation and fibrin deposition (68). This process is summarized in **Figure 1.3**. In persons with hemophilia, FVIII or FIX protein concentrate may be supplied by intravenous injection, restoring the thrombin generating feedback loop and enabling normal hemostasis.

### **1.6 Challenges in Modern Hemophilia Treatment**

While the past century has brought tremendous improvements in the treatment of hemophilia, from the genetic and biomolecular etiology of the disease to the availability and use of recombinant protein replacement therapies, patients and practitioners are still left with many challenges in managing the disease. In countries and communities with access to advanced health care resources, prophylactic protein replacement is well established as the standard of care for the hemophilias (69). Under this regimen, patients generally self-administer clotting factor concentrates intravenously 2 to 3 times per week, with a goal of constantly maintaining therapeutic levels of clotting factor activity. This treatment generally provides patients with protection from the rigors of everyday life, however, additional factor concentrate may be utilized to protect against anticipated trauma, such as high impact sporting events, dental procedures, or surgery.

While this treatment modality offers an unprecedented opportunity for improved life expectancy and quality of life, many challenges still face patients, practitioners, and health care systems around the world. Even under ideal circumstances, prophylactic treatment remains highly invasive, resulting in poor patient compliance. Due to its invasive nature, over 10% of patients with access to prophylactic protein replacement decline the treatment, while only 60% of those who



choose treatment accurately follow the treatment regimen (70). Unfortunately, across the world access to prophylactic treatment is the exception rather than the norm. Globally, approximately 80% of persons with hemophilia receive either no or inadequate treatment (71), largely arising from the high cost of prophylactic treatment of hemophilia A and B, which cost approximately \$150,000 and \$200,000 per patient year, respectively (72).

However, even in locations with sufficient resources to provide advanced healthcare, treating hemophilia remains problematic. The primary complication with treatment is the formation of inhibitory antibodies (inhibitors) against the exogenous FVIII and FIX, which occurs in 33% and 3% of patients, respectively (73). In these patients, antibodies binding to the FVIII or FIX proteins block their procoagulant activity, rendering protein replacement ineffective. Treatment options for these patients is cumbersome and expensive. A primary strategy for treating patients with inhibitors is immune tolerance induction (ITI), wherein large amounts of factor concentrate are given at regular intervals until central and peripheral immune tolerance to the protein is achieved. This strategy is effective in approximately 50% of inhibitor patients with hemophilia A, while data on hemophilia B is limited (74). While this strategy has proven effective, the high doses of factor concentrate which are given over the course of months to over a year, carries a significant cost burden, with estimated lifetime costs of \$1.7 million per patient (75). Lacking availability or response to ITI, patient care becomes additionally complex. Bypassing agents, such as FVIIa or concentrates of FX and thrombin may be given, but these agents do not provide the same levels of protection against bleeding as FIX or FVIII concentrates. A recently approved strategy for managing inhibitor patients is the use of recombinant porcine FVIII, which the antibodies of some inhibitor patients fail to bind, allowing effective restoration of hemostatic activity (76).

Despite the growing portfolio of approved products for the treatment of hemophilia, the high cost of treatment, invasiveness of injections, and development of inhibitors pose challenges largely unmet by currently available therapies. Gene therapy, which ultimately seeks to provide a single dose cure of the disease, offers a potential solution to these challenges. The goal of gene therapy

for hemophilia is the use of DNA transfer technology to enable a person with hemophilia to endogenously produce therapeutic levels of their deficient coagulation factor. The hemophilias have long been identified as ideal target diseases for gene therapy. As circulating plasma proteins, FVIII and FIX could conceptually be produced and secreted by any cell with access to the vasculature, and phenotypic benefit may be easily quantified by routine clinical assay of coagulation factor activity. An important aspect of hemophilia gene therapy is the broad therapeutic window of coagulation factor activity. Coagulation factor activity is measured by correlation to the activity of pooled normal human plasma, which is self-defined as 100% activity. For both hemophilia A and B, restoration of even 1% of normal factor activity has clinical benefit, while levels of 30% or more would result in nearly complete phenotypic correction (77). Multiple modalities of gene therapy for the hemophilias have been developed in small and large animal models, and have now advanced into early stage clinical trials.

### **1.7 Landscape of Clinical AAV for the Hemophilias**

Due to the limited packaging capacity of AAV for the large FVIII transgene, combined with the poor biosynthetic efficiency of the FVIII protein itself, early efforts in clinical gene therapy for the hemophilias have centered on hemophilia B. Like hemophilia A, hemophilia B is an attractive target for gene therapy as only modest increases in FIX expression (>1% of normal) confer phenotypic improvement. However, due to the small size of the FIX cDNA (1.39kb) and more efficient biosynthesis of the FIX protein, AAV-FIX vectors are not encumbered by the same challenges of AAV-FVIII, making these vectors an excellent platform for AAV gene therapy vector development.

The first AAV clinical trials for hemophilia B were conducted by Avigen, Inc in the early 2000s. The first study published investigated the safety of intramuscular (IM) injection of an AAV-FIX vector (78-80). While pre-clinical studies in dogs supported the safety and efficacy of this approach, this trial would be the first IM directed AAV clinical trial in humans (81). The vector chosen for this study utilized the AAV2 capsid carrying a wild-type human FIX driven by a

cytomegalovirus (CMV) promoter. As safety was the primary outcome measured in this study, it was designed as a dose escalation study, with cohorts of subjects receiving between  $2 \times 10^{11}$  and  $1.8 \times 10^{12}$  vector genomes (vg) / kilogram (kg). The AAV was administered through a series of 10-12 injections to the anterior thigh under local anesthesia, and patients were followed for over 4 years after vector administration. Although one patient developed transient thrombocytopenia, there were no other vector related toxicities noted in the study, nor did any patients develop inhibitory antibodies to the FIX protein. PCR-based studies showed the presence of vector transgene in the muscle in 8/10 patients, however, only 2 of these patients showed measurable increases in circulation FIX, with these levels being  $<2\%$ .

The second Avigen AAV trial, published in 2006, investigated intrahepatic delivery of AAV-FIX (82). Like the IM trial, this study utilized an AAV2 capsid carrying wildtype FIX, however, instead of a CMV promoter, this vector utilized a synthetic variation of the human alpha-1 antitrypsin (hAAT) promoter generated by fusing the apolipoprotein (APOE) hepatic control region (HCR) enhancer to the serine protease A1 (SERPINA1) promoter, which provided liver-directed expression of the transgene. The vector itself was targeted toward the liver by angiographic guidance to the hepatic portal vein. Designed as a dose escalation combined phase I/II clinical trial, this study investigated both the safety and efficacy of the treatment.

The vector was administered in three doses,  $8 \times 10^{10}$  vg/kg,  $4 \times 10^{11}$  vg/kg, and finally  $2 \times 10^{12}$  vg/kg. At the lowest dose, the recipient showed no vector related toxicity, but FIX expression remained undetectable at  $<1\%$  of normal. In the medium dose ( $4 \times 10^{11}$  vg/kg), no FIX expression was seen in any of the four patients treated, however, one patient exhibited a modest rise in liver transaminase levels, a response indicative of hepatotoxicity, which resolved without intervention over the next 4 weeks. In the high dose ( $2 \times 10^{12}$  vg/kg) cohort, the two treated subjects showed an increase in circulating FIX levels to 3% and 11% of normal. However, this expression dropped to  $<1\%$  of normal in both patients over the next 12 weeks. While no toxicities were noted in the patient whose FIX levels increased to 3%, a significant rise in liver transaminase levels to  $>20x$  normal were

noted in the patient expressing 11% of normal FIX. This transaminitis resolved without intervention with kinetics similar to the decline in FIX expression. Further investigation found that the transaminitis and decline in FIX expression was due to an AAV capsid-specific memory CD8<sup>+</sup> T-cell response directed against capsid proteins displayed by major histocompatibility (MCH) presentation on the surface of infected cells, resulting in specific cytotoxic destruction of the gene modified cells (82; 83). This study demonstrated the safety of liver-directed AAV at low doses, but suggested a dose limiting toxicity at levels of 2e12 vg/kg, as well as uncovering the need for vector designs capable of conferring efficacious expression FIX at low vector doses.

Building on the experiences of the Avigen trials, St. Jude Children's Research Hospital in 2007 sponsored an AAV-FIX trial using a vector developed at the University College, London (84). This vector incorporated several new technologies designed to increase the efficacy of the virus at lower vector doses. While the Avigen trials utilized AAV serotype 2, this vector utilized the AAV8 capsid. First isolated in 2002, this serotype was found to transduce hepatocytes 10-100 more efficiently than other serotypes (85). The vector encoded a wildtype FIX protein, however, the coding region was codon optimized for increased biosynthesis in the context of expression within a human liver cell. This optimized cDNA was driven by a variant of the hAAT promoter, consisting of the core regions of the HCR enhancer fused to the core hAAT promoter. Finally, this design incorporated a self-complimentary genome design, wherein a deletion of the terminal resolution site (TRS) in the 3' ITR results in packaging of the viral genome, relieving the vector of the need for second strand synthesis and improving transgene expression (86).

This study was performed as a dose escalation study, with participants receiving 2e11 vg/kg, 6e11 vg/kg, or 2e12 vg/kg. In the low-dose cohort, the two patients showed FIX expression levels of 2% of normal, that remained stable for the for the 6 to 16 month follow-up after vector infusion with no signs of transaminitis indicative of cytotoxic T-cell response. The mid dose group showed stable FIX expression at 3-4% of normal during the follow-up period, again with no signs of transaminitis. In the high dose group, the two participants showed peak FIX levels of 8 and 12%.

However, this expression was accompanied by a concurrent rise in transaminase levels and subsequent decline in FIX expression. The participants were immediately started on a regimen of prednisolone to control the cytotoxic T-cell response. At the resolution of the transaminitis, FIX expression in the first participant remained stable at 3% of normal, while the second participant stabilized at levels between 8 and 12%. This study showed that the dose limiting toxicity of AAV at  $2 \times 10^{12}$  vg/kg was replicated with AAV8, however, with advanced knowledge of the underlying mechanism, FIX expression was spared through pharmacological immune modulation. While the hepatotoxicity noted in this study was not severe enough to qualify as a severe adverse event, it highlighted the need for further improved vectors capable of providing curative levels of FIX expression at low vector doses.

The promising results from these initial studies generated substantial commercial interest in generating a commercially viable AAV-FIX vector. As of September, 2016, four AAV-FIX gene replacement clinical trials have been initiated by for-profit entities. Recognizing the need for more efficacious vectors, these industry efforts have incorporated novel technologies in an attempt to further improve FIX expression at clinically safe vector doses. Amsterdam-based Uniqure, BV, whose portfolio contains Glybera, the only gene therapy approved for human use in the west, has initiated human trials utilizing a vector transgene comparable to that used by in the 2007 St. Jude trial, with the notable difference of utilizing an AAV5 capsid. At a 9-month follow up, patients receiving this vector are stably expressing FIX levels of approximately 5% of normal (87). Baxalta, formerly a wholly-owned subsidiary of Baxter International, in 2016 conducted an AAV-FIX trial utilizing a self-complementary AAV8 vector encoding a variant of human FIX containing a mutation of arginine 338 to leucine, which has been previously shown to increase the specific activity of FIX by over 700%, this time being driven by the liver-directed transthyretin (TTR) promoter (88; 89). Since this trial initiated, Baxter was purchased by Shire, Plc, which has since discontinued the trial due to inconsistent performance of the vector (90). Dimension Therapeutics, in partnership with Bayer AG, has initiated a trial utilizing wild-type FIX packaged into an

AAVrh10 capsid (91). Finally, Spark Therapeutics has released what may be the most promising results to date. This trial utilizes the same high specific activity FIX variant as the Bayer trial, packaged in an undescribed capsid designated “Spark100” and driven by an undisclosed, liver-directed promoter. At 4-6 months after dosing at  $5 \times 10^{11}$  vg/kg, patients in this trial are stably expressing FIX at levels of 20-40% of normal with no signs of hepatotoxicity (92).

In Q4 2015, BioMarin Pharmaceutical initiated the first AAV gene therapy clinical trial for hemophilia A. This vector utilizes an AAV5 capsid and codon optimized human FVIII driven by a minimally sized promoter. This trial utilized higher vector doses than the previous trials for hemophilia B. The first patient was dosed with  $6 \times 10^{12}$  vg/kg, with doses escalating to  $2 \times 10^{13}$  and  $6 \times 10^{13}$  vg/kg. At the lowest vector dose, no FVIII activity was detected, however, at the mid and high doses, FVIII expression ranged from 2% to 50% of normal in all patients treated. However, consistent with previous results, these high vector doses resulted in transaminitis which was partially controlled by steroid administration. Two of the patients met criteria for halting enrollment, and the trial was put on hold until October 2016 (93).

From these developments, the future of AAV gene therapy for the hemophilias is bright. However, further development of these vectors is warranted to improve factor expression, reduce vector toxicity, and enable efficient vector manufacture to allow distribution of an affordable product in the global market.

### **1.8 Strategies for improving AAV Vectors for the Hemophilias**

Increasing the per viral particle factor expression conferred by AAV therapies remains an important goal in both academic and commercial gene therapy. By increasing the potency of the virus, higher and potentially curative levels of expression may be obtained while using lower vector doses. With lower vector doses comes improved safety through the avoidance of cellular immunity against gene modified cells, as well as reduced per-patient cost of vector manufacture. AAV vectors essentially contain just two parts: the protein capsid and DNA transgene. Both of these components offer opportunities for improving the pharmacologic properties of clinically oriented vectors.

## **A. Capsid Discovery and Engineering**

To date, over 100 variants of AAV have been isolated from various host species, including humans (36). While structurally similar, each variant has a potential for altered profiles of tissue tropism, infectivity, and immunogenicity. AAVs utilize multiple cell surface glycans as anchors for cellular attachment and entry, with the particular binding profile of each serotype determined by the structure of the capsid shell. It is this variation in receptor binding that provides the variety the specificity of tissue tropism of the various AAV serotypes, however, post-entry viral restriction may inhibit viral uncoating and gene expression in certain tissues (94). In addition to exploiting the natural variation in AAV capsids, there has been substantial effort in engineering or evolving capsids to improve their properties as a gene therapy vector. Efforts to rationally direct the tropism of AAV capsids have included modifying the capsid subunits with antibody domains and targeting peptides to allow anchoring to non-native cellular receptors (95; 96). Alternatively, directed evolution has been utilized to generate novel capsids without pre-existing knowledge of the resultant structure (97). Both of these approaches have developed novel capsid structures with potentially beneficial alterations in tropism, immunogenicity, and post-entry uncoating.

## **B. Protein Bioengineering**

Modification of the primary amino acid sequence of the protein product of AAV vectors has shown promise to improve the potency of the vectors. To do this, novel FVIII and FIX protein designs have been explored to both increase the biosynthetic efficiency of protein production, resulting in increased levels of circulating protein, or to increase the specific activity of the molecule, resulting in higher coagulation factor activity at the same levels of protein expression. FVIII is expressed at levels 2-3 orders of magnitude lower than similarly sized proteins (98). This low-level expression has been spatially and temporally located to poor trafficking between the endoplasmic reticulum and Golgi apparatus due to engagement of the unfolded protein response (99; 100). As shown in **Figure 2.1A**, FVIII is organized in domains structure of A1-A1-B-C1-C2, where the B domain is a largely unorganized sequence with no known biological function, and

frequently substituted with a short peptide linker in recombinant FVIII designs. The A domains share homology with the A domains of the copper-binding protein ceruloplasmin, while the C domains mediate membrane binding. Substitution of porcine FVIII A1 and A3 domains has been shown to relieve this constraint, increasing FVIII expression 100-fold over the native human sequence (99). Incorporation of such a molecule into AAV-FVIII designs would be expected to significantly increase the potency of the vector. Recently, there was described a naturally occurring pro-thrombotic mutation in FIX that has been shown to increase the specific activity of the protein 5-10 fold (89). Similar to the incorporation of the porcine domains in FVIII, incorporation of this gain of function mutation would similarly be expected to increase the potency of AAV-FIX vectors.

### **C. Size reduction**

The limited DNA packaging capacity of AAV of approximately 4.9 kilobases presents a substantial constraint on the design of AAV-FVIII vectors, where the FVIII cDNA itself occupies 4.4kb of available space. While vectors larger than 5.0kb are frequently utilized, the potency of the virus is substantially reduced due to the need of intracellular reassembly of the resulting fragmented vector genomes (47; 48). An AAV-FVIII vector minimally contains a promoter, FVIII cDNA, polyadenylation signal (polyA), and flanking pairs of AAV inverted terminal repeats (ITRs). At 145 base pairs (bp) each, the ITRs in combination with the FVIII cDNA minimally occupy 4.7kb, leaving only 200bp for the promoter, polyA signal, and any intervening sequences. A common feature of many AAV vector designs is the inclusion of unnecessary wild-type AAV genome sequence, often occupying over 100bp of space. Through DNA synthesis technologies, these genomic regions, which were initially utilized to facilitate molecular cloning into the wildtype genome, can be eliminated. Another attractive approach is the design of minimally sized promoters. There is a recently described minimally sized yet highly potent promoter called the “super core promoter” (101). At just 81 base pairs in length, this promoter demonstrates that minimally sized promoters are capable of driving robust gene activity. By incorporating a minimally sized promoter and polyadenylation signal, in addition to removal of unnecessary viral DNA remnants, the creation

of a sub 4.9kb AAV-FVIII vector becomes a possibility, which would be expected to improve vector potency, in addition to reducing intraparticle heterogeneity and allowing for increased efficiencies in vector manufacture. The theoretical loss in vector potency with increasing transgene length is modeled in **Figure 1.4**.

#### **D. Codon Optimization**

Codon optimization is a frequently used a process wherein synonymous codon substitutions are introduced to a cDNA to increase protein production. With the exception of methionine and tryptophan, all other 18 standard amino acids are encoded by two or more synonymous codon, however, it is well documented that organisms do not use these codons equally (102). Rather, each organism has a particular bias toward usage of certain codons and avoidance of others. Termed “codon usage bias”, this phenomenon is believed to result from coevolution of accumulation of synonymous codon changes to reflect alterations in the physical pools of cognate tRNAs with an organism. By maintaining parity of codon usage levels to the corresponding tRNA levels, protein transcription occurs more efficiently, as a balanced pool of tRNA isoacceptors are available during the translational process. It is routinely shown that by introducing synonymous codon changes to cDNA to better match the codon usage preference of the organism, protein expression levels are increased in a process termed “codon optimization” (103). This strategy is now commonly used in the design of AAV gene therapy vectors to increase vector potency. Codon optimization strategies utilize the entire genomic cDNA of a host species to derive the codon usage bias of the organism as a whole, which is assumed to be reflective of the physical tRNA pools within its cells, originally described as the “tRNA adaptation theory” (104-107). However, recent work has shown that the physical tRNA pools within different tissues vary (108). Therefore, there exists an opportunity to improve upon this paradigm by optimizing codon usage to the particular tissue of gene expression, rather than to expression in the organism as a whole.

#### **1.10 Concluding Remarks**

Figure 1.4

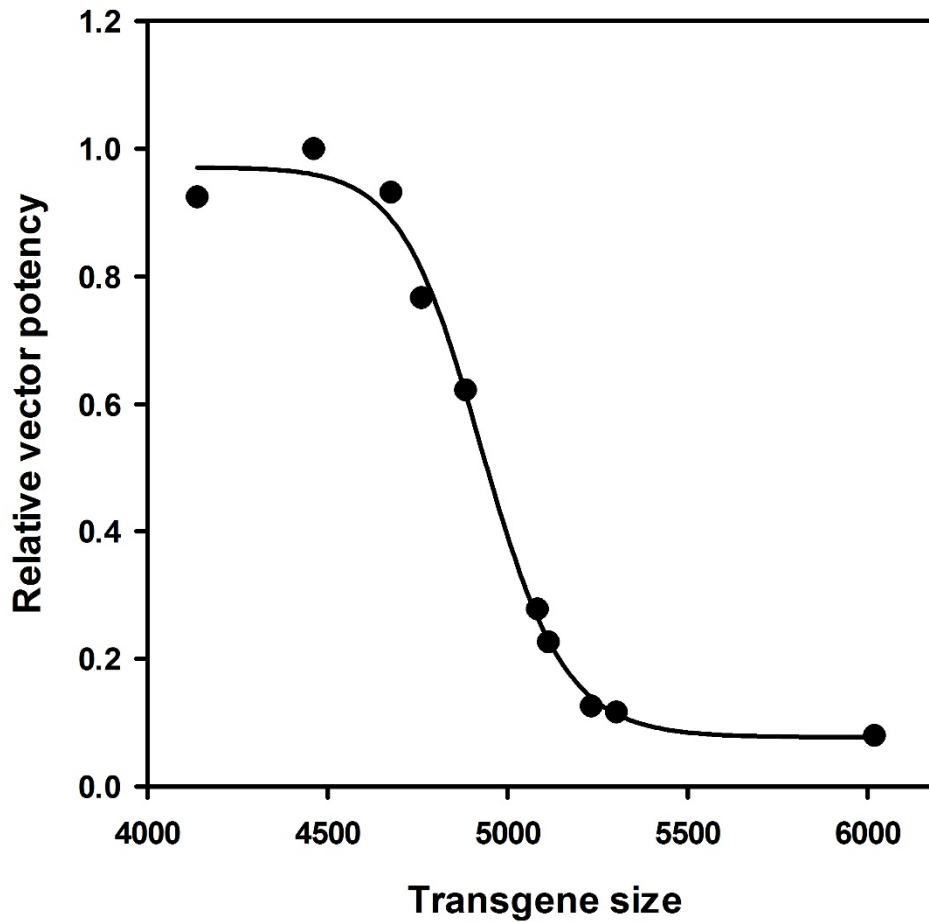


**Figure 1.4 Model of loss of vector potency with increasing transgene length.** Due to the limited packaging capacity of AAV vectors of approximately 5.0kb, exceeding this length results in fragmented transgene packaging and reduced vector potency. This graph and model were generated from data originally reported by Dong *et al* (47).

In the last two decades, there has been enormous effort, both from academia and industry, in developing clinically viable vectors for human gene therapy. AAV has emerged as one of the most promising vectors to achieve this goal. Due to its excellent safety profile and ease of administration, AAV remains the vector of choice for the treatment of many diseases, including the hemophilias. However, several challenges remain to be addressed before these vectors will be sufficient for global distribution and routine clinical use. Vector related cytotoxicity limits the dose of virus that may safely be administered. At these vector doses, low-level protein expression often remains insufficient to offer a *bone fide* cure. Increasing vector potency will enable higher levels of protein expression at safe vector doses. This will both increase the efficacy of treatment as well as decrease the per patient cost of vector manufacture. There are multiple approaches to achieve this goal. Protein engineering, vector shortening, and novel methods of codon optimization all present novel yet viable means of increasing potency and achieving the long desired goal of curative levels of gene expression at clinically safe vector doses.

### **1.10 Thesis Hypothesis**

In this thesis, multiple modalities of AAV vector transgene bioengineering are investigated for their potential to increase FVIII expression conferred by the vector. Since FVIII suffers from intrinsically poor biosynthetic efficiency, it is hypothesized that substitution of porcine FVIII A1 and A3 domains will increase per particle FVIII activity conferred by an AAV-FVIII vectors. Since AAV vectors of over 5.0kb are known to suffer from decreased vector potency, it is hypothesized that utilizing smaller regulatory control elements will increase vector potency. Finally, since FVIII is being expressed exogenously in the liver, it is hypothesized that altering the codon usage bias of the FVIII cDNA to match the predicted tRNA milieu of the liver will increase vector potency. This thesis supports that combination of these modifications results in a vector of sufficient potency to provide high levels of FVIII expression at clinically safe vector doses.

## Chapter 2

### **Bioengineered Coagulation Factor VIII Enables Long-Term Correction of Murine Hemophilia A Following Liver-Directed Adeno-Associated Viral Vector Delivery**

This research was published in *Molecular Therapy Methods & Clinical Development*.

Brown HC, Wright JF, Zhou S, Lytle AM, Shields JE, Spencer HT, Doering CB.

[Bioengineered Coagulation Factor VIII Enables Long-Term Correction of Murine Hemophilia A Following Liver-Directed Adeno-Associated Viral Vector Delivery](#)

*Molecular Therapy Methods & Clinical Development*. 2013. 1: 14036.

© 2014 American Society of Gene & Cell Therapy

Harrison Brown designed and cloned expression cassettes, performed and designed the experiments, and wrote and edited the paper

Fraser Wright and Shangzhen Zhou produced and characterized AAV virus

Alison Lytle and Jordan Shields performed experiments

Trent Spencer and Chris Doering conceived the experiments and edited the paper

## 2.1 ABSTRACT

Clinical data support the feasibility and safety of adeno-associated viral (AAV) vectors in gene therapy applications. Despite several clinical trials of AAV-based gene transfer for hemophilia B, a unique set of obstacles impede the development of a similar approach for hemophilia A. These include 1) size of the factor VIII (FVIII) transgene, 2) humoral immune responses to FVIII, 3) inefficient biosynthesis of FVIII, and 4) AAV vector immunity. Through bioengineering approaches, a novel FVIII molecule, designated ET3, was generated and shown to demonstrate 10-100 fold improvement in biosynthetic efficiency. In the current study, the utility of ET3 was assessed in the context of liver-directed, AAV-mediated gene transfer into hemophilia A mice. Due to the large transgene size and use of proven, but not minimized regulatory elements, the AAV-ET3 genomes packaged into viral particles as partial genome fragments. Despite this potential limitation, a single peripheral vein administration of AAV-ET3 into immune-competent hemophilia A mice resulted in correction of the FVIII deficiency at lower vector doses than previously reported for similarly oversized AAV-FVIII vectors. Therefore, ET3 appears to improve vector potency and mitigate several of the critical barriers to AAV-based clinical gene therapy for hemophilia A.

## 2.2 INTRODUCTION

Hemophilia A is an X-linked congenital bleeding disorder characterized by a deficiency in functional coagulation factor VIII (FVIII) in the blood compartment. Recently, clinical advancements have been made using recombinant adeno-associated virus (rAAV) -based gene transfer for hemophilia B. However, a unique set of obstacles impede the development of a similar approach for the related and more common bleeding disorder hemophilia A (109). These obstacles include 1) inefficient biosynthesis of human fVIII (hFVIII) (98), 2) limited packaging capacity of rAAV (4.7 kb) (47; 110) which is exceeded by FVIII expression cassettes as B domain deleted (BDD) FVIII cDNAs alone are approximately 4.4 kb, 3) humoral immune responses to the

transgene product (*i.e.* FVIII) (111), and 4) capsid-mediated cytotoxicity of the virus itself, which has been proposed to be as low as  $2 \times 10^{12}$  vector particles (vp)/kg (112).

FVIII is a large glycoprotein containing a domain structure (A1-A2-B-*ap*-A3-C1-C2) that is secreted at levels up to 3 orders of magnitude lower than other similarly sized secreted glycoproteins *in vivo* and *in vitro*. This low secretory rate has been spatially and temporally linked to inefficient posttranslational trafficking from the endoplasmic reticulum (ER) to the Golgi (98; 113-117). The primary determinants of this biosynthetic limitation are specific amino acid sequences within the A1 and A3 domains of the molecule itself that cannot be overcome by standard transgene expression technologies such as more efficient DNA regulatory elements (e.g. promoters/enhancers), transgene copy number, targeted integration at genomic “hotspots” for transcription, and codon optimization. Instead, bioengineering of the FVIII molecule itself appears to be required to overcome inefficient secretion. We have developed such a bioengineered FVIII molecule (herein designated ET3 and previously referred to as HP47) using knowledge gained from the characterization of B-domain deleted (BDD) recombinant porcine FVIII (rpFVIII) (118; 119). Both rpFVIII and ET3 are secreted 10-100 fold more efficiently than other FVIII constructs through diminished interactions with ER resident chaperones and attenuated induction of the unfolded protein response (117-120). The enhanced secretory capacity of ET3 is enabled through the substitution of “high expression” rpFVIII sequences in the A1 and *ap*-A3 domains into recombinant human FVIII (rhFVIII), which, despite retaining 91 percent overall amino acid identity, have been shown to be necessary and sufficient to confer 10 – 100-fold improved biosynthesis (119). In addition to the A1 and *ap*-A3 domain substitutions, the BDD hfVIII protein, designated HSQ, substitutes the 14 amino acid human-derived SQ linker sequence for the B-domain, whereas ET3 utilizes the 24 amino acid porcine-derived OL linker sequence, which have been previously described and shown to produce similar levels of FVIII expression when substituted into porcine FVIII (118).

In the present study, proof of concept of a liver-directed rAAV vector encoding ET3 to confer long-term expression of therapeutic levels of FVIII in immune-competent hemophilia A mice was investigated. The vector design was based on an rAAV vector previously shown to effectively deliver and express the human coagulation factor IX (FIX) transgene (121). This current vector, designated rAAV-HCR-ET3, has a total genome size of 5.9 kb, which is 125% of the 4.7 kb endogenous rAAV genome and therefore is oversized. Recently published data from Samulski and colleagues suggest that oversized AAV genomes are packaged into preformed viral capsids as incomplete single stranded (ss) DNA fragments with either strand polarity likely containing overlapping portions of the transgene, which are heterogeneously truncated during the packaging process. Intracellular reassembly of these transgene fragments was suggested to confer transgene product expression levels 25-37 fold lower than that attained from smaller, non-fragmented transgenes (47; 110; 122; 123). The standard mechanism of AAV reassembly and second strand synthesis has been previously reviewed (124). Given the limitations of generating complete rAAV vectors for large transgenes such as FVIII, understanding the mechanisms and efficiencies of oversized rAAV genome packaging and transgene cassette reassembly are critical to the development of the next generation of rAAV vectors.

## 2.3 MATERIALS AND METHODS

*Vector Cloning* - The previously described HP47/ET3 transgene (119) was released from the ReNeo vector backbone by digesting with NotI followed by Klenow fragment fill-in and subsequent *SpeI* digestion. The previously described AAV2 vector backbone AAV-HCR-hAAT-FIX (121) was digested with *BglII* followed by Klenow fragment fill in and subsequent *NheI* digest. The AAV-HCR-hAAT vector backbone was ligated to the ET3 transgene, generating the rAAV-HCR-ET3 viral vector expression plasmid. An equivalent AAV expression vector encoding a previously described non-bioengineered BDD hFVIII construct (designated HSQ) (125) was generated by releasing HSQ with *NotI* followed by Klenow fragment fill in and subsequent *XhoI*

digestion. AAV-HCR-hAAT-FIX was digested with *BglIII* followed by Klenow fragment fill in and subsequent *Sall* digestion. AAV-HCR-hAAT was ligated to the HSQ transgene, generating the rAAV-HCR-HSQ viral vector expression plasmid.

*Transient Transfection* - Naïve human hepatocellular liver carcinoma (HepG2) cells were grown to 75% confluency in 6 well plates. Cells were transfected with 2 $\mu$ g of rAAV-HCR-ET3 or rAAV-HCR-HSQ viral expression plasmid using 6  $\mu$ L Lipofectamine 2000 (Life Technologies, Carlsbad, CA) in DMEM supplemented with 10% fetal bovine serum. Twenty-four and 48 hours post transfection, media was replaced with 1 mL AIM-V serum free medium (Life Technologies). Seventy-two hours after transfection, conditioned media was collected and analyzed for FVIII activity by one stage clot assay as previously described (125).

*Vector Production* - The recombinant AAV8 vector encoding ET3 was produced as described previously (126). Briefly, human embryonic kidney (HEK) 293 cells were transfected by calcium phosphate using the following plasmids: 1) the adenovirus helper plasmid AdHP encoding adenovirus helper proteins E2 and E4, 2) the AAV8 packaging plasmid AAV8PK encoding AAV2 Rep and AAV8 Cap, and 3) the vector plasmid encoding the transgene expression cassette. The transfected cells were harvested 72 hours after transfection, lysed by homogenization, clarified by centrifugation, and vectors purified by precipitation with 8% polyethylene glycol and two rounds of cesium chloride gradient ultracentrifugation. Purified vectors were dialyzed into phosphate buffered saline (PBS) and supplemented with Pluronic F68 (0.001% final concentration). The empty capsid free vector preparations were quantified by SDS-polyacrylamide gel electrophoresis (PAGE) with silver staining by comparing VP1, 2 and 3 staining intensity by scanning densitometry with an established AAV reference vector.

*Molecular Studies* - Viral ssDNA was isolated from virus stocks using the QIAmp MinElute Virus Spin Kit (Qiagen, Hilden, Germany) according to the manufacturer's instructions. Preparations for size analysis were prepared free of carrier RNA. Size analysis was performed by alkaline gel electrophoresis and subsequent Southern blot. DNA was probed using a cocktail of

biotinylated probes directed against the A2, C2, and bovine polyadenylation sequences (**Table S1**) and detected using the North2South Chemiluminescent Detection kit (Thermo Fisher, Waltham, MA) according to the manufacturer's instructions. Sizing analysis was performed by interpolating from the distances migrated by a DNA standard run in the alkaline gel to that of a single-stranded DNA ladder. Cellular DNA was extracted from liver tissue following perfusion for 10 minutes with 0.9% saline solution using the DNeasy Blood and Tissue Kit (Qiagen) according to the manufacturer's instructions. All qPCR was performed using a StepOne real-time PCR platform (Life Technologies) and analyzed on the device's software. QPCR quantitation was performed using a standard curve generated from dilutions of rAAV-HCR-ET3 viral expression plasmid. For determination of FVIII mRNA quantity in HepG2 cells transfected with AAV-FVIII expression plasmids, mRNA was extracted from cells using the Qiagen RNEasy kit, and quantitative reverse-transcription PCR was performed as previously described (118). Quantitation of regions of the viral genome was performed in separate experiments using sets of primers directed against regions that spanned the length of the rAAV-HCR-ET3 transgene (**Table 1.S2**). To control for any differences in primer efficiency, each reaction was quantitated separately against plasmid standard curves generated using each region-specific primer pair (**Figure 1.S1**). Isolated viral ssDNA was added to 2x Power SYBR green PCR master mix (Life Technologies) with final concentrations of 0.3125  $\mu$ M each of forward and reverse primers to a final volume of 20  $\mu$ L. The data shown is the mean of two qPCR reactions. As all virus used in this study was generated in a single production run, error bars are not shown to avoid confusion between the inter-assay variability and variability due to independent virus preparations. For determination of liver transgene copy numbers, 40 ng of cellular DNA was used as template in 2x Power SYBR Green PCR master mix with final primer concentrations of 0.3125  $\mu$ M each. The primer set directed against the A2 domain (**Table 1.S2**) was used for determination of transgene copy number in transduced livers. Quantitation was performed using a standard curve generated from rAAV-HCR-ET3 viral expression plasmid. Forty ng of naïve liver genomic DNA was added to each standard curve reaction to mimic the cellular

DNA environment of the experimental samples. To determine the presence of full-length mRNA in the livers of treated mice, RNA was extracted from liver tissue using the RNeasy kit (Qiagen) according to the manufacturer's instructions. One  $\mu\text{g}$  of RNA was subject to DNA removal and reverse transcribed using the Quantitect reverse transcription kit (Qiagen) according to the manufacturer's instructions. PCR was performed using the primer set directed against the C2 region of ET3 (**Table S2**).

*Animal Studies* - All animal studies were performed under the guidelines set by the Emory University Institutional Animal Care and Use Committee. Immune competent, exon 16 disrupted C57BL/6 backcrossed mice were used as a murine model of hemophilia A (127) and C57BL6 background mice used as healthy control. Hydrodynamic plasmid injections were performed in unanesthetized four to six week old hemophilia A mice. For these studies, 10 $\mu\text{g}$  of plasmid was diluted into 2.1mL Transit-EE hydrodynamic delivery solution (Mirus) and delivered by tail vein injection over the course of seven to ten seconds. Blood plasma was collected 24 hours after injection. AAV administration studies were performed in eight to twelve week old mice, which were administered a single tail vein injection of AAV viral vector diluted to a volume of 200  $\mu\text{L}$  in sterile filtered DPBS containing Pluronic F68 (0.001%). For both *in vivo* studies, citrated plasma was collected by retro-orbital bleed into one-tenth volume 3.8% trisodium citrate. FVIII activity was measured using the commercially available COATEST SP fVIII assay (Coatest SP, Diapharma, West Chester, OH, USA) according to the manufacturer's instructions using a standard curve generated from pooled citrated human plasma (George King, Overland Park, KS). Using this standard curve, the limit of detection for the assay was empirically determined to be 0.015 units (U) of fVIII/mL. Baseline determinations of fVIII activity in untreated hemophilia A mice were determined to be below the limit of detection of the assay. Circulating antibodies against fVIII were detected by enzyme-linked immunosorbent assay (ELISA) (128). Antibodies to fVIII were captured using immobilized recombinant hfVIII (Kogenate, Bayer, Leverkusen, Germany) bound to microtiter plates and detected using alkaline phosphatase conjugate of goat anti-mouse IgG as

previously described (125; 129). Absorbance at 405 nm was measured from dilutions of test plasma and plotted against the logarithm of the plasma dilution. The resulting sigmoidal curves were fit to the 4-parameter logistic equation by non-linear regression using the Levenberg-Marquardt algorithm. ELISA titer was defined empirically as a dimensionless value calculated from the reciprocal plasma dilution resulting in an optical density of 0.3 from the fitted curves (129). The presence of inhibitory antibodies was confirmed by Bethesda assay, performed as previously described (130; 131). Bethesda titer was calculated as the average of dilutions of inhibitor found to produce between 25% and 75% residual activity.

*In vivo specific activity of rAAV-derived FVIII* - Antigen concentrations were determined using a capture ELISA designed to detect the heavy chain of FVIII. Monoclonal antibody (421C) directed towards a porcine A1 domain epitope was immobilized on 96 well high binding polystyrene plates (Corning, Corning, NY) and used to capture FVIII antigen from plasma samples diluted in HBS Tween-80. Samples were then incubated with a biotinylated secondary monoclonal antibody (4C7) directed towards a human A2 domain epitope for one hour in blocking buffer containing 1% BSA. Full length FVIII was measured using goat anti-mouse IgG antibody conjugated to alkaline phosphatase and *p*-nitrophenylphosphate. Absorbance at 405nm was read 30 minutes after the addition of the chromogenic substrate. Antigen concentrations were extrapolated from a standard curve derived from purified FVIII protein serially diluted in E-16 disrupted hemophilia A mouse plasma. Specific activity of mouse plasma samples were determined by plotting antigen concentration against FVIII activity measured by COATEST SP FVIII assay kit. Linear regression analysis was performed, comparing AAV treated mouse plasma samples to the standard curve.

*Tail Transection Assay* - Tail transection bleeding assay was performed as previously described (130). Briefly, mice were anesthetized under isoflurane and their tails were warmed for 10 minutes in a 37 °C water bath. Tails then were transected 4 mm from the tip using a scalpel and immediately placed into 14 mL vials containing 0.9% saline solution held at 37 °C. Tails were

allowed to bleed freely for 45 minutes, at which time they were removed from the vials. Blood loss during 45 minutes was measured by mass of blood accumulated in the tube and normalized to body weight while controlling for evaporative loss.

## 2.4 RESULTS

*Viral vector construction and in vitro comparison of BDD hFVIII and ET3 expression.* The rAAV vector design was based on constructs previously used to express the human coagulation factor IX transgene from liver tissue (121). The ET3 transgene, which consists of human FVIII sequences in the A2, C1, and C2 domains and porcine FVIII sequences in the A1 and *ap*-A3 domains, or alternatively, a BDD hFVIII transgene with a 14 amino acid linker (SQ), designated HSQ, were cloned into an AAV expression cassette controlled by a liver-specific ApoE hepatic control region (HCR)/human alpha-1 antitrypsin (hAAT) enhancer/promoter and flanked by AAV2 inverted terminal repeats (ITRs) (**Figure 2.1a**). Alignment of HSQ and ET3 amino acid sequences reveals 91 percent identity (**Figure 2.S2**). We have previously shown that the increased expression of ET3 is conferred through enhanced post-translational processing of the nascent FVIII peptide (119). To determine if the post-translational biosynthetic efficiency of ET3 expression compared to HSQ is recapitulated by the two AAV expression plasmid constructs in the context of the liver-directed transcriptional control elements in the rAAV-HCR-hAAT vector backbone, an *in vitro* transfection experiment utilizing the human hepatocellular carcinoma HepG2 cell line was performed. rAAV-HCR-ET3 and rAAV-HCR-HSQ expression plasmids were transiently transfected into HepG2 cells, and FVIII activity in the conditioned medium and quantity of FVIII mRNA transcripts were determined. Interestingly, a greater number of ET3 mRNA transcripts per cell (850, +/- 39), were determined compared to HSQ transcripts per cell (284, +/- 69). However, this 3-fold increase in mRNA resulted in over a 20-fold increase in FVIII secretion into the medium (0.70 units/mL +/- 0.24 ET3, and 0.034 units/mL +/- 0.010 HSQ). Together, these findings show that the rAAV-HCR-ET3 transfected HepG2 cells demonstrated 7-fold higher levels of FVIII

Figure 2.1

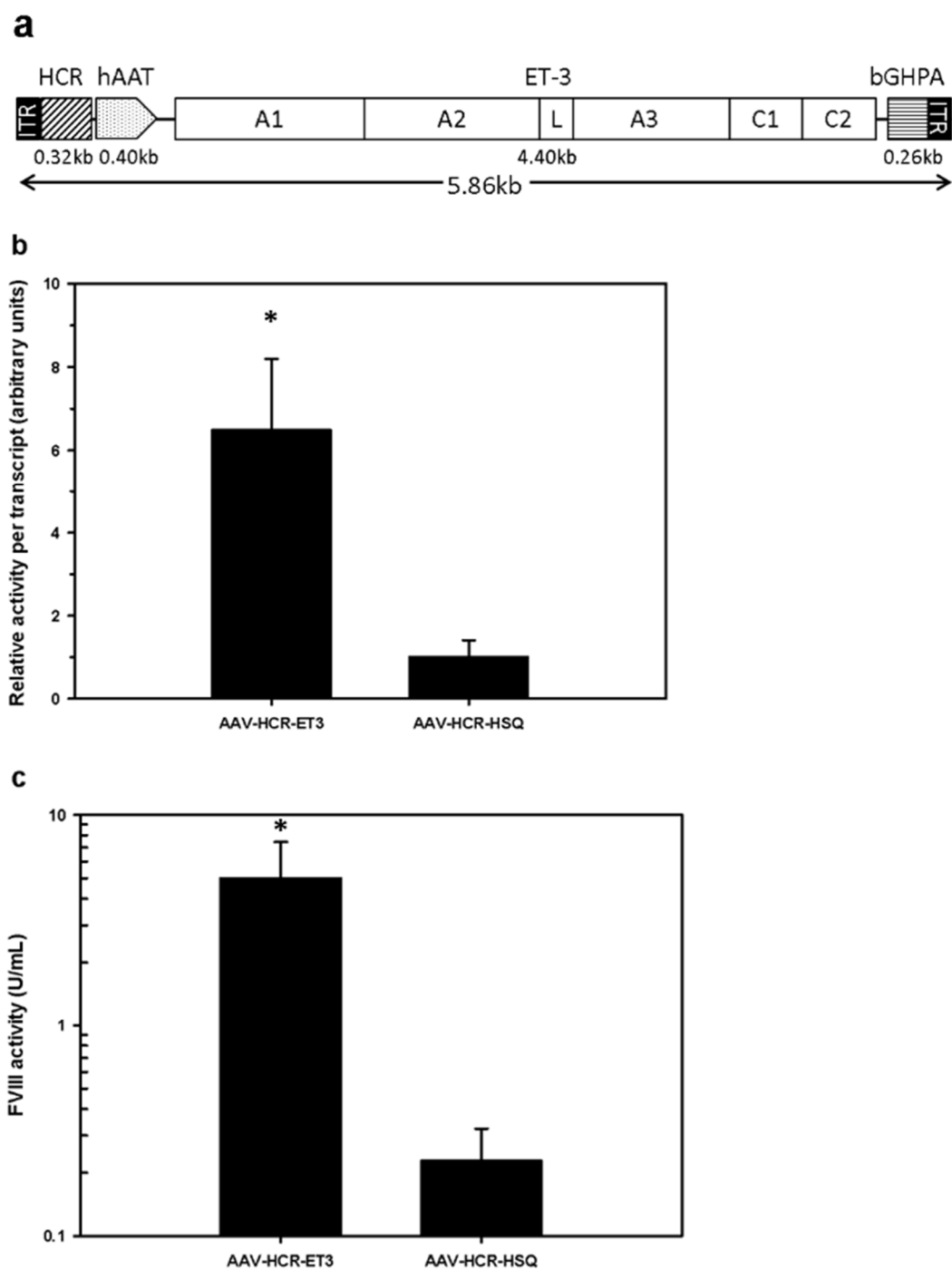


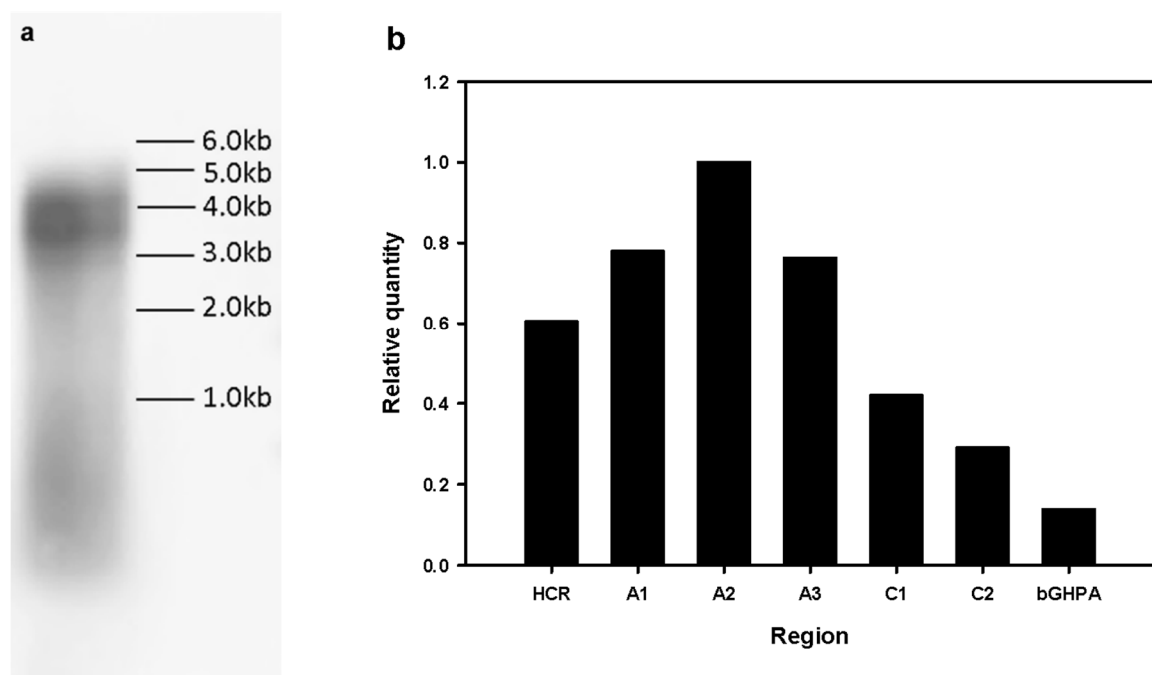
**Figure 2.1: Viral Vector Design** The 5.86 kb rAAV-HCR-ET3 genome encodes the high expression bioengineered FVIII molecule ET3, which consists of porcine FVIII sequences in the A1 and *ap*-A3 domains and human sequence in the A2, C1, and C2 domains. The ET3 transgene is under the control of a liver-specific hAAT promoter/ApoE HCR enhancer sequence, and

termination is governed by a bovine growth hormone poly adenylation signal (bGHPA). The genome is flanked by AAV2 ITRs on both the 5' and 3' ends (**A**). FVIII activity was measured in conditioned medium of HepG2 cells that were transiently transfected with rAAV-HCR viral expression vectors encoding ET3 or the non-bioengineered BDD hFVIII construct HSQ, and activity normalized to quantity of FVIII mRNA transcripts per cell (**B**). Plasma FVIII activity was measured in hemophilia A mice that were hydrodynamically injected with rAAV-HCR viral expression plasmid encoding ET3 or HSQ (**C**). Baseline FVIII levels were determined to be below the limit of detection for all mice (data not shown). All error bars show one sample standard deviation, N=3 for *in vitro* studies and 3-4 for *in vivo* studies. (\* =  $p < 0.05$  by 2-way t-test)

activity per mRNA transcript into the conditioned medium than the rAAV-HCR-HSQ transfected cells (**Figure 2.1b**), suggesting that the post-translational biosynthetic efficiency of ET3 expression is the primary determinant of its enhanced secretion in the context of liver-directed expression. We cannot rule out, however, that increased transcriptional efficiency or mRNA stability may further contribute to the enhanced expression of ET3 compared to HSQ. To further examine the finding of enhanced expression of ET3, an *in vivo* comparison of the two vector-transgene designs by hydrodynamic injection of the expression plasmids was performed. In this experimental system, rAAV-HCR-ET3 expression plasmid conferred 20-fold higher plasma levels of FVIII activity than rAAV-HCR-HSQ expression plasmid again supporting the claim of enhanced expression of ET3 compared to HSQ (**Figure. 2.1c, Table 2.S3**).

*rAAV vector production and characterization* - AAV particles encoding the rAAV-HCR-ET3 transgene were generated by transient transfection of HEK293 cells and subsequent purification of the vector particles from supernatants and cell lysates as previously described (126). rAAV-HCR-ET3 was designed with a vector genome of 5.9 kb from ITR to ITR, which exceeds the endogenous rAAV genome size by 25%. Despite its oversized design, production of approximately  $1.2 \times 10^{13}$  total rAAV-HCR-ET3 vp at concentrations of  $5.3 \times 10^{12}$  vp per mL was achieved.

To assess the effect of the oversized genome on rAAV packaging, viral ssDNA obtained from cesium chloride gradient purified rAAV-HCR-ET3 was subjected to alkaline gel electrophoresis followed by Southern blot analysis using probes directed to the A2 and C2 domain sequences of FVIII and the bovine polyadenylation signal sequence (**Figure 2.2a**). The rAAV-HCR-ET3 vector preparation did not contain detectable genetic material at the position expected for full-length genomes (5.9 kb). Rather, a heterogeneous smear of viral ssDNA approaching 5.0kb was observed suggesting that the majority of viral genomic DNA was packaged as truncated fragments. It has been suggested previously that oversized transgenes, such as that encoded by rAAV-HCR-ET3, may extend beyond the capsid, exposing free 5' ends of ssDNA on the outside

**Figure 2.2**

**Figure 2.2: Molecular assembly of rAAV-HCR-ET3 vector particles.** ssDNA from rAAV-HCR-ET3 viral particles were purified, subjected to alkaline gel electrophoresis, and detected by Southern blot (a). The molecular composition of the packaged viral genomes was determined by quantitative PCR directed against specific regions of the vector genome and normalized to the quantity of the A2 region (b).

of the viral particles. A comparison of Southern blot analysis of viral particles treated with DNase prior to disruption of the viral capsid to those that were not DNase treated failed to detect a difference in genome size, suggesting that vector genomic ssDNA does not extend beyond the viral capsid (data not shown).

The composition of the truncated rAAV-HCR-ET3 genome fragments was assessed by qPCR using primer sets directed against different genome regions spanning from ITR to ITR (**Figure 2.2b**). Although this analysis could not distinguish strand polarity, it did show that sequences corresponding to the A2 domain of FVIII, which are located near the center of the designed viral genome, were the most prevalent. Comparatively, the terminal sequences, both encompassing either the promoter or poly A signal sequence, were up to 7.3-fold less prevalent than the central A2 sequences. This result is consistent with the current theory that oversized AAV viral genomes are packaged from one of the 3' ITRs of either polarity and truncated prematurely before reaching the other ITR.

*In vivo expression of FVIII rAAV-HCR-ET3* - A dose finding study was performed to determine the ability of rAAV-HCR-ET3 to provide therapeutic levels of circulating fVIII activity *in vivo*. Immune-competent 8-12 week old male mice were administered a single peripheral vein injection of the vector at doses ranging from  $6.2 \times 10^{10}$  to  $2.0 \times 10^{13}$  vp/kg. A long term (50 week) study was performed on a first cohort of mice receiving high vector doses ( $4 \times 10^{12}$  –  $2 \times 10^{13}$  vp/kg), while follow-up on the second cohort that received lower doses ( $1 \times 10^{12}$  –  $8 \times 10^{12}$  vp/kg) was shorter (24 weeks). Lastly, as the lower dose limit was not attained in the second cohort, a third cohort of mice was dosed with rAAV-HCR-ET3 at even lower levels ( $6.2 \times 10^{10}$  –  $5 \times 10^{11}$  vp/kg) and was followed out to 11 weeks post-AAV injection. Starting two weeks after vector administration, circulating plasma was assayed for FVIII activity at scheduled time points. Male mice receiving rAAV-HCR-ET3 showed dose responsive increases in circulating FVIII activity (**Figures 2.3a-c**). Supraphysiologic FVIII levels, at over  $>3$  units (U)/mL, were achieved at the dose of  $1 \times 10^{13}$  vp/kg. For reference, the FVIII activity level observed in pooled normal human plasma is defined as 1 U/mL, while clinical

Figure 2.3

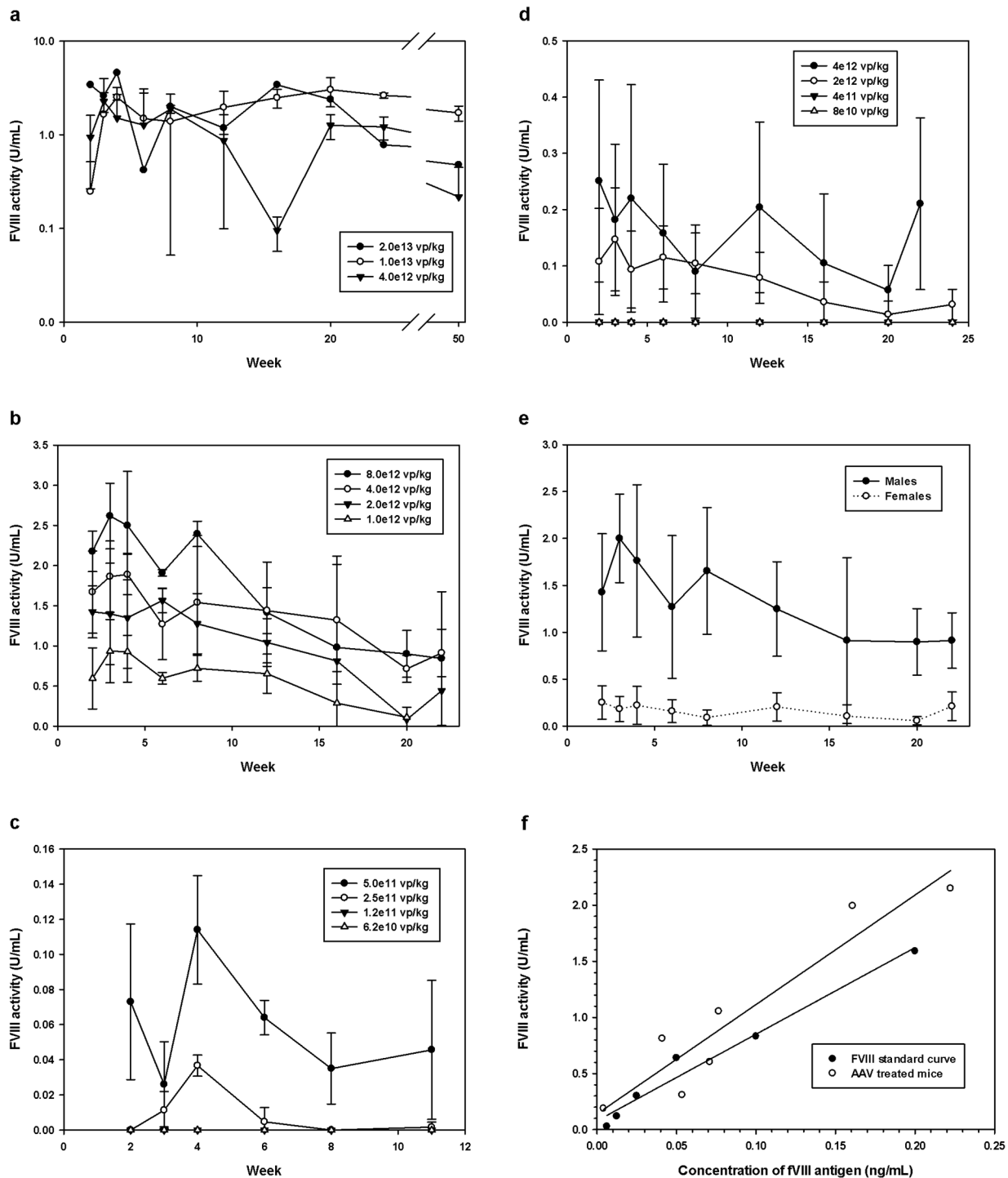


**Figure 2.3: Dose finding of rAAV-HCR-ET3 in a murine model of hemophilia A.** Dose finding studies were performed in male and female immune-competent hemophilia A mice. FVIII activity is presented from mice that did not form neutralizing antibodies. In male mice, a long term, high dose study (**a**), a medium duration, mid-dose extension study (**b**) and a short term, minimum effective dose study (**c**) were performed. In female mice, a shorter duration dose finding study was performed (**d**). A comparison between male and female mice receiving  $4 \times 10^{12}$  vg/kg (**e**) shows the intersex difference in FVIII levels. Baseline determination of FVIII activity in all mice tested was below the limit of detection of the assay (data not shown).  $N=2-4$  for all doses, error bars show one sample standard deviation. To determine the specific activity of in vivo rAAV derived FVIII, the specific activity of a panel of plasmas from rAAV-HCR-ET3 treated mice (open circles) was compared to a standard curve generated from purified ET3 protein serially diluted in hemophilia A mouse plasma (closed circles) (**f**). Antigen concentrations were determined using a capture ELISA and FVIII activity was determined using a chromogenic substrate activity assay.

hemophilia A disease classifications are severe – <1%, moderate 1 – 5%, and mild 5 – 40% normal FVIII activity. Correction to curative levels (>0.4 U/mL or 40% normal human FVIII activity level) was achieved at doses as low as 1.0e12 vp/kg, and partial correction (>0.05 U/mL) was seen at doses as low as 5e11 vp/kg. FVIII expression was maintained throughout the duration of the experiment in all but the lowest doses of vector administered. However, there was a trend toward activity loss over the duration of the experiment, which is consistent with gradual liver tissue turnover and loss of the episomal AAV genomes.

*Formation of anti-FVIII inhibitors* - Two mice that received high doses of rAAV-HCR-ET3 (2e13 and 1e13 vp/kg) displayed sudden and sustained losses of circulating FVIII activity at weeks 8 and 12, respectively (**Figure 2.4**). Prior to the losses in plasma FVIII activity, both mice were expressing ET3 at supraphysiologic levels (>250% of normal). As repeated intravenous administration of recombinant rFVIII (rFVIII) to naïve hemophilia A mice is known to be immunogenic, all mice were tested for inhibitory antibodies to FVIII by ELISA. In the two mice that lost FVIII activity, positive anti-FVIII ELISA titers of 512 and 668 were observed at week 12 post rAAV-HCR-ET3 infusion, suggesting that these animals had mounted neutralizing humoral immune responses against the transgene product, which persisted for the duration of the study. The antibodies were confirmed to be inhibitory by Bethesda assay at week 16, which showed inhibitor titer of 320 and 118 Bethesda units (BU) per mL. Development of inhibitors, as detected either by loss of FVIII activity or ELISA titer, was not detected in any of the other experimental mice throughout the course of the long term follow-up (data not shown).

*Expression of FVIII rAAV-HCR-ET3 in female mice* - Previously, it has been reported that rAAV has reduced ability to mediate liver gene transfer in female mice (132). Therefore, a limited dose finding study for rAAV-HCR-ET3 was performed in 8 – 12 week old immune-competent female mice. At doses ranging from 8e10 to 4e12 vp/kg, female mice showed an attenuated response to rAAV-HCR-ET3 gene transfer, with doses as low as 2e12 vp/kg resulting in partial correction of FVIII activity, which was maintained for the duration of the study (**Figure 2.3d**). No

Figure 2.4

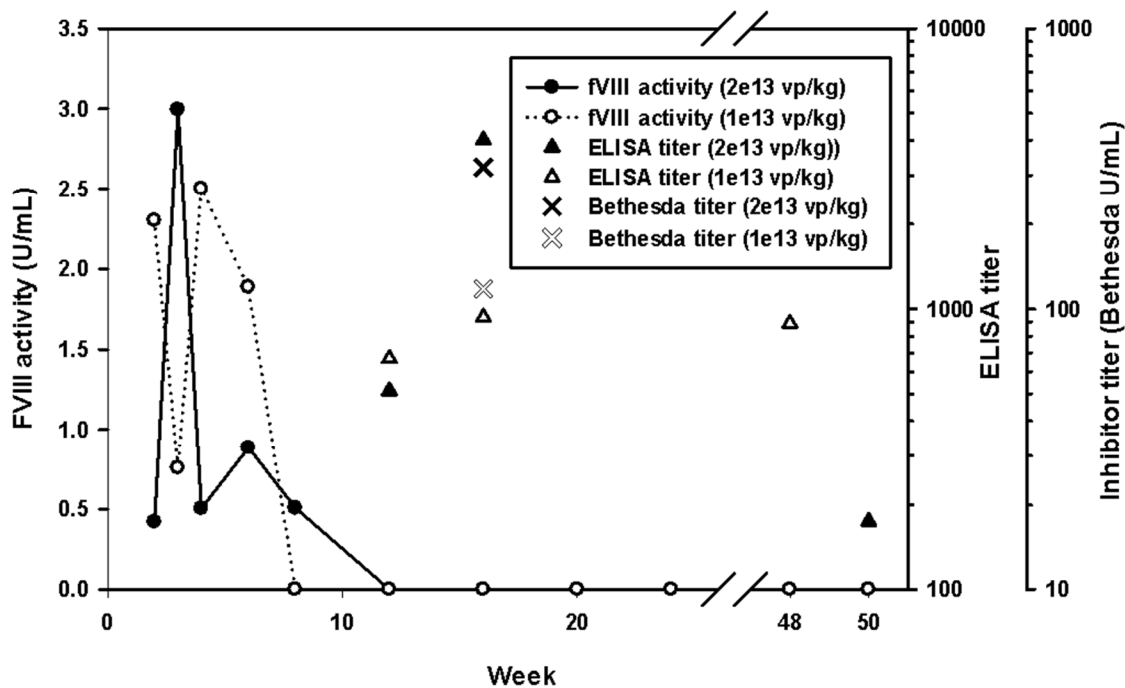


**Figure 2.4: Formation of FVIII inhibitors following rAAV-HCR-ET3 administration.** Two mice that received one of the high doses of rAAV-HCR-ET3 (2e13 vp/kg and 1e13 vp/kg) experienced sudden and persistent loss of FVIII activity at between 8 and 12 weeks after vector administration. Anti-ET3 ELISA assay confirmed these mice had developed IgG antibodies to FVIII, which persisted for the duration of the study. A Bethesda assay was performed at week 16 to confirm the presence of neutralizing antibodies against FVIII.

female mice developed neutralizing antibodies to fVIII at the vector doses tested. With respect to the results obtained in male hemophilia A mice, circulating fVIII activity levels in female mice were approximately 8-fold lower at all doses tested, which is consistent with previous reports (**Figure 2.3e**).

*Molecular composition of rAAV-derived FVIII* - Our molecular studies of the rAAV viral vectors suggests that the majority of viral transgenes package as sub-5.0kb fragments, which lack either the necessary 5' transcriptional control region or 3' FVIII coding sequence and poly(A) signal necessary to confer expression of full-length FVIII protein. To confirm the expression of complete ET3 mRNA sequences in mice treated with viral vector, RNA extracted from the livers of treated and untreated mice were subjected to reverse transcription PCR analysis for the presence of ET3 C2 domain RNA sequence, a region spanning position 5036 to 5205 at the 3' end of the transgene predicted to be truncated during the packaging process (**Figure 2.S3**). Truncation at the 5' end, which includes the promoter region, would preclude transcription of ET3 mRNA, whereas truncation at the 3' end would result in loss of template for the PCR reaction. The detection of this mRNA region therefore supports the presence of full-length mRNA from the truncated viral ssDNA genomes.

While this analysis supports the presence of full length FVIII mRNA transcripts, it does not exclude the possibility that only a small proportion of mRNA transcripts in treated animals contain the complete FVIII coding sequence. The presence of mRNA transcripts coding a truncated FVIII sequence could lead to the production of a heterogeneous population of dysfunctional FVIII molecules. To interrogate the presence of dysfunctional FVIII protein in rAAV-treated mice, we determined the *in vivo* specific activity of rAAV-derived FVIII in vector-treated hemophilia A mice. Antigen concentrations, measured using a capture ELISA designed to detect the heavy chain of FVIII, a region not predicted to be truncated from the promoter region of the antisense-coding vector genomes, were plotted against the FVIII activity of each sample and compared to a standard curve of purified FVIII protein serially diluted in hemophilia A mouse plasma. The specific activity

of the AAV treated mouse samples was found to be similar to that of the standard curve, indicating that the majority of mRNA transcripts encode a fully functional FVIII molecule.

*Viral genome copy number in transduced livers* - QPCR analysis of viral genome target sequences within the centrally-located A2 domain of FVIII was performed using DNA extracted from livers of all transduced male mice (**Figure 2.5**). rAAV-HCR-ET3 proviral genomes containing the A2 domain sequence persisted as long as 1 year after treatment. There were approximately 2 viral transgenes per cell in mice receiving  $2 \times 10^{13}$  vp/kg, and a dose responsive decrease in transgene number at the lower doses, with mice receiving the lowest doses ( $6.4 \times 10^{10}$  vp/kg) approaching the limit of detection.

*Correction of bleeding phenotype* - Correction of the hemophilia A bleeding phenotype was assessed by tail transection bleeding assay on animals that received varying doses of rAAV-HCR-ET3 (**Figure 2.6**). Overall, mice that received rAAV-HCR-ET3 treatment demonstrated less blood loss than saline-treated control mice. Specifically, all mice that received one of the high vector doses ( $8 \times 10^{12}$ –  $2 \times 10^{13}$  vp/kg) showed no detectable blood loss while mice that received medium ( $1 \times 10^{12}$  –  $4 \times 10^{12}$  vp/kg) or low ( $6.2 \times 10^{10}$  –  $5.0 \times 10^{11}$  vp/kg) doses demonstrated dose responsive decreases in blood loss that, both as individuals groups and as a whole, were significantly less than saline treated controls ( $p < 0.005$ , Mann-Whitney U test).

## 2.5 DISCUSSION

The favorable safety profile, ease of delivery, durable expression and lack of innate immune stimulation position rAAV as a promising vector for clinical gene therapy of hemophilia A. However, large transgene size, potential humoral immunogenicity and poor biosynthetic efficiency of human FVIII present as significant obstacles hindering clinical translation. This point is supported by the observation that five clinical trials of AAV-factor IX vectors for the treatment

Figure 2.5

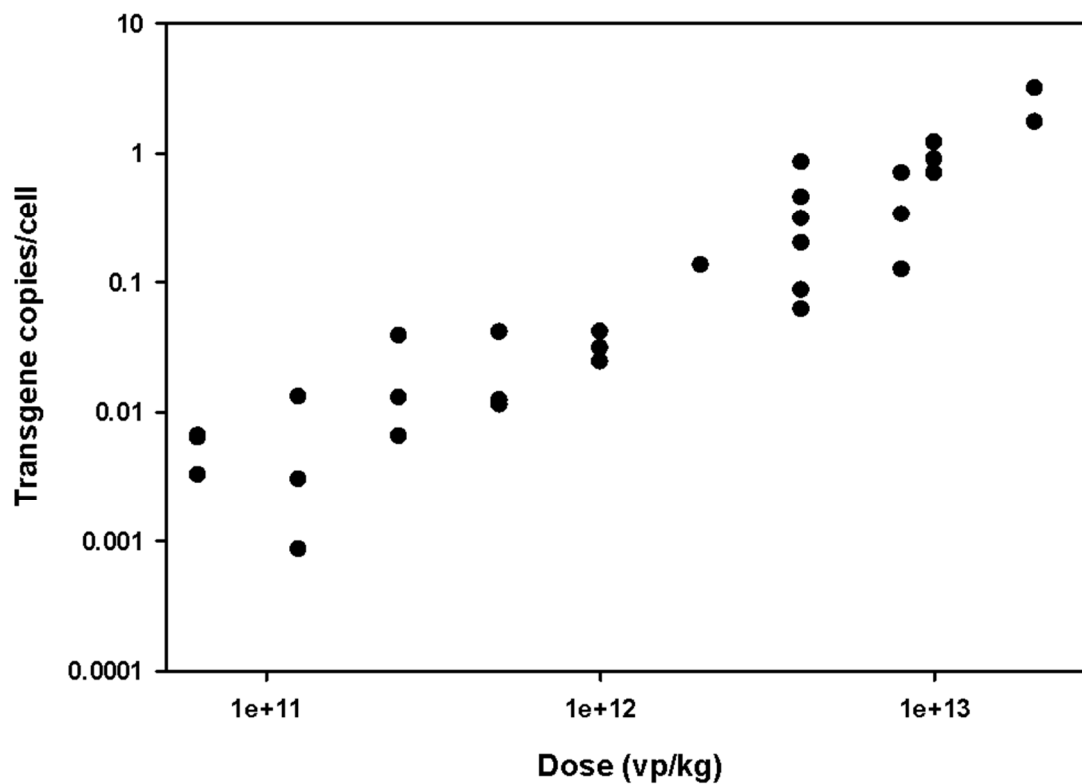


**Figure 2.5: *In vivo* viral genome copy number.** Quantitative PCR was used to determine the number of viral genomes in transduced livers. Primers directed against the FVIII A2 domain were used to determine the number of viral genome copies of this domain per cell for all mice receiving rAAV-HCR-ET3.



of hemophilia B have been conducted or currently are in progress, while none have been initiated for rAAV-FVIII vectors for testing in persons with hemophilia A.

To overcome these obstacles, several advancements in AAV-FVIII vector design have been reported. For example, Lu *et al* described an rAAV-FVIII construct incorporating a  $\beta$ -actin promoter with a cytomegalovirus enhancer and a bovine growth hormone poly(A) sequence that expressed FVIII at levels 3-5 fold higher than a comparable AAV construct utilizing a mini-thyrotropin promoter with a synthetic poly(A) sequence (133). The use of these large regulatory control elements resulted in a final transgene size of 5.8kb, which, similar to rAAV-HCR-ET3, was substantially oversized. Despite having no detectable vector genomes larger than 5.0kb, the optimized vector developed by Lu *et al* provided correction of FVIII levels in hemophilia A mice at a dose of  $2 \times 10^{11}$  vector genomes (vg)/mouse, or approximately  $8 \times 10^{12}$  vg/kg. Additionally, Arruda and colleagues recently described a minimally bioengineered hFVIII transgene delivered via an oversized (5.5 kb) rAAV vector achieving circulating FVIII expression up to 60% of normal at a dose of  $8 \times 10^{12}$  vg/kg (134). This bioengineering approach incorporates a single amino acid substitution which eliminates a furin cleavage site within human FVIII to mimic what occurs naturally in the B domain of canine FVIII. This substitution conferred a 2.5-fold increase in secreted single chain FVIII form, greater specific activity and improved hemostatic potency. Lastly, Nathwani and colleagues have developed a novel rAAV-FVIII vector that is reduced in size to 5.2 kb through promoter and polyadenylation sequence engineering and encodes a codon-optimized BDD hFVIII transgene that also incorporates a bioengineered linker containing additional N-glycan sequence motifs (135). The combination of these engineered elements resulted in a vector that mediated 10 to 20 fold higher expression of FVIII compared to the non-engineered vector. However, the exact mechanism(s) responsible for the improved expression were not determined.

In the present study, we sought to enhance the potency of rAAV-FVIII vectors through the integration of a fVIII molecule that has been bioengineered for more efficient cellular secretion, which is the known rate-limiting step in recombinant FVIII biosynthesis and presumably also exists

in gene therapy settings. This novel approach may be complimentary to the advancements described above by others in the field and combinations of the technologies, such as 1) reduction in AAV genome size through the use of smaller gene regulation elements like the ones described by Nathwani and colleagues or 2) the incorporation of the canine B-domain substitution described by Arruda and colleagues or 3) the insertion of N-glycan motifs into the FVIII B-domain linker sequence, which could potentially result in additive or synergistic improvements in vector performance. Regardless of these speculations, the present study demonstrates that rAAV-HCR-ET3 can achieve curative levels of FVIII activity *in vivo* using a minimal dose of  $1 \times 10^{12}$  vp/kg, which represents an 8-fold reduction in vector dose needed to achieve curative levels of circulating FVIII compared to the results obtained by the groups of Lu and Arruda discussed above, and doses comparable to that achieved with the vector developed by Nathwani and colleagues despite the substantially oversized nature of rAAV-HCR-ET3. As production of sustained therapeutic levels of FVIII remains a critical barrier to clinical gene therapy of hemophilia A and no recent transformational advances have been made in vector manufacturing or potency, transgene engineering approaches, such as that demonstrated by ET3, may provide the key innovation necessary to achieve clinical success. Furthermore, the reduced viral vector dose needed to achieve curative levels of FVIII represents a significant improvement in safety over other AAV-FVIII constructs through reduction in the viral antigen load delivered to the recipient, which previous and ongoing clinical trials have shown to initiate a cytotoxic immune response against transduced cells at vector doses as low as  $2 \times 10^{12}$  vp/kg (112).

Our laboratory has spent considerable effort studying the differential efficiency of FVIII biosynthesis, as well as other biochemical properties, of orthologous FVIII molecules. The knowledge gained has been applied to the bioengineering of enhanced FVIII molecules such as ET3/HP47 with markedly improved biosynthetic efficiency and increased stability following thrombin activation (119). Previously, we have described the improved performance of ET3 and other similar high expression FVIII sequence element containing constructs over standard human

BDD FVIII constructs in heterologous recombinant protein production systems as well as gene therapy applications involving  $\gamma$ -retroviral and lentiviral vector gene transfer into hematopoietic stem cells (118-120; 136-138). However, the current study is the first report utilizing the high expression sequence elements of porcine FVIII to boost FVIII levels in a liver-directed AAV-mediated gene therapy application. Consistent with data we have reported previously, the ET3 transgene enabled 20-fold higher expression compared to that achieved using the BDD human FVIII transgene in transiently transfected HepG2 cells. Furthermore, the enhanced expression conferred by the ET3 transgene compared to the BDD human FVIII transgene was recapitulated *in vivo* via hydrodynamic plasmid injection, where ET3 achieved 20-fold higher levels of circulating FVIII activity.

The bioengineered design of ET3 can be compared in some regards to a strategy currently being pursued in AAV clinical gene therapy of hemophilia B where constructs encoding a naturally occurring human coagulation factor IX molecule termed factor IX-Padua exhibit greater specific procoagulant activity than normal human FIX (139), and thus also increased vector potency. In the current study, the construct modifications implemented were designed to enhance expression/secretion efficiency, a bioengineering strategy which similarly increases vector potency. However, unlike the factor IX-Padua mutation, which is a naturally occurring mutation, ET3 is a non-naturally occurring FVIII chimera that substitutes the high-expression sequence identified in rpFVIII into BDD hFVIII (119).

When inserted into the rAAV-HCR-hAAT vector backbone, the expected genome size was 5.9 kb, which substantially exceeds the 4.7 kb size of endogenous AAV genomes. It seems likely that further improvement in both titer and potency could be garnered by reducing the vector genome size similar to what was described previously by Nathwani and colleagues (135). Unlike other, smaller, bioengineered vectors, such as that reported by the Nathwani group, molecular analysis of rAAV-HCR-ET3 revealed that there was no detectable full length transgene packaged into the vector (135). Rather, consistent with previous reports of oversized vectors, molecular analysis of

the rAAV-HCR-ET3 vector revealed that it packaged primarily as truncated transgene fragments, with no detectable viral transgenes larger than 5.0kb (47; 110) PCR analysis of the purified viral genomes revealed a packaging bias favoring the central portion of the transgene. This result is consistent with the current model of the AAV ssDNA transgene packaging from the 3' end of both sense and antisense strands, and, in the case of oversized transgenes, being truncated before packaging completely through a presently unknown mechanism. This model predicts that most viral particles will carry either a sense or antisense template both of which will contain A2-A3 domain transgene sequences, while the HCR-A1 transgene regions will only be carried by antisense coding viral particles, and the C1-C2-bGHPA transgene regions carried only by the sense coding viral particles. This differential prevalence of transgene region frequency, combined with the sub-5.0kb smear of viral ssDNA detected by Southern blot analysis, suggests a heterogeneous population of partially encoding viral transgenes. It is possible, therefore, that intracellular reassembly of the anti-sense viral transgenes containing the complete HCR promoter region and truncated FVIII template may lead to the production of dysfunctional FVIII protein products, presenting a potential safety concern by exposing treated individuals to novel immunological epitopes.

Previous work by the Nathwani lab with a similarly sized AAV-FVIII vector failed to detect either persistent truncated FVIII transgene or truncated FVIII protein in mice treated with the oversized vector (135). To alternatively investigate the presence of full-length FVIII mRNA in AAV treated mice, we performed RT-PCR analysis of mRNA transcripts (**Figure 2.3S**) in the livers of treated mice. This analysis showed the presence of the C2 domain of FVIII, an area found to be preferentially truncated in the packaged viral transgenes, which is only possible if the complete 5' sequence upstream of the interrogated 3' sequence region is present. These findings, coupled with the high specific activity of circulating FVIII in AAV-treated mice (**Figure 2.3f**), supports a model wherein, despite the truncated nature of the vector transgene, the majority of translated protein product contains the complete FVIII peptide sequence.

The differential prevalence of viral ssDNA transgene sequences in the product preparations necessitates considerations that must be taken into account when titering oversized rAAV vectors using PCR-based methods. The heterogeneous nature of the viral particles suggests that the quantity of a single region of ssDNA within the transgene may not be representative of entire viral genome. This brings to light an important safety consideration, as it has been shown in clinical trials that rAAV vector doses greater than  $2 \times 10^{12}$  vg/kg can induce acute liver toxicity due to capsid-targeted cytotoxic T cell-mediated destruction of transduced cells (51; 112; 140). In the present study, rAAV-HCR-ET3 was titered by quantitative protein analysis of DNA-containing viral particles. This approach provides an accurate estimation of the number of viral particles that contain DNA in the preparation, but does not account for the regions of transgene DNA that has been packaged. As there were no detectable full-length transgenes packaged within the rAAV capsids, titrating oversized rAAV vectors by either determination of viral particle number by mass or optical density, or by use of qPCR amplicons directed to a single viral genome segment, does not describe the heterogeneous nature of the vector genomes in the preparation. This presents a significant challenge to vector product manufacturing, characterization, and quality metrics for clinical product development comprising oversized AAV vector genomes.

Proviral rAAV-HCR-ET3 genomes persisted in the livers of treated mice for the duration of the study, between 11 and 50 weeks, as determined directly by qPCR and indirectly by the continuous detection of circulating FVIII activity. While the vector copy numbers obtained in the present study are substantially lower than those seen in studies using similar vectors (134; 135), in the previous studies, cellular DNA was collected soon after AAV administration, between 6 and 17 weeks. In the present study, vector doses that were comparable to those used in the previous studies were collected as long as 48 to 50 weeks after vector administration. The low vector copy numbers in the present study may be explained by loss of episomal AAV DNA over this extensive time period.

Despite its fragmented packaging, rAAV-HCR-ET3 provided complete ( $\geq 100\%$  normal) correction of the FVIII deficiency at doses as low as  $2 \times 10^{12}$  vp/kg. Additionally, doses as low as  $1 \times 10^{12}$  vp/kg provided lower, but still curative FVIII activity levels. Finally, a minimally effective dose of  $5 \times 10^{11}$  vg/kg was identified based on the criteria of achieving a sustained therapeutic levels of FVIII between 0.02 – 0.12 units/ml for more than 10 weeks post-vector administration. In addition to measurement of plasma FVIII activity, phenotypic correction was demonstrated by hemostatic challenge using the tail clip bleeding assay, which demonstrated dose responsive correction of bleeding diathesis. Although an overall reduction in bleeding was observed that trended toward significance in terms of a quantitative correlation between blood loss and vector dose or plasma FVIII activity level, previous experience with this assay in our laboratory has shown that blood loss does not directly correlate to FVIII activity levels in plasma. Furthermore, as others have shown, it frequently is observed that mice with levels of FVIII activity below the threshold of detection (1.6% of normal) fail to lose detectable amounts of blood. It is possible, therefore, that sub-detectable levels of FVIII activity may be sufficient for the correction of bleeding diathesis in this murine model.

Initial exposure to FVIII by persons with hemophilia A represents an immunologic challenge that can lead to the development of neutralizing humoral immunity in approximately 25% of persons with severe hemophilia A (111; 141). Since rAAV gene therapies are designed to provide a continuous source of the exogenous protein in treated individuals, this response presents a considerable safety and efficacy concern as these vectors are translated into human trials. Indeed, when administered to immune-competent macaques, rAAV encoding a codon optimized BDD human FVIII molecule resulted in the formation of neutralizing antibodies to FVIII (135). Furthermore, the incidence of anti-FVIII inhibitor formation in persons with hemophilia A is significantly greater than that of anti-FIX inhibitors in persons with hemophilia B (111). Thus, immunogenicity remains among the most significant safety concerns for all new hemophilia A therapeutics including gene therapies (142; 143). Despite the demonstrated safety in the ongoing

clinical trial of scAAV2/8-LP1-hFIXco for the treatment of hemophilia B, these results may not be predictive of safety in a similarly designed clinical trial for AAV-FVIII vectors for the treatment of hemophilia A (144). As there has not been a clinical trial of AAV gene therapy for hemophilia A completed to date, this issue can only be discussed at this time using preclinical data. In the present study, we utilized the C57BL/6 background exon-16 disrupted murine model of hemophilia A, a genetic background previously shown to produce higher anti-FVIII inhibitory antibodies than the Balb/c model of hemophilia A (145). Using this model, 2 animals developed inhibitory inhibitors to ET3, as evidenced by loss of FVIII activity and confirmed by ELISA and Bethesda assays. The two mice that developed anti-FVIII immune responses received the highest doses of virus ( $2 \times 10^{13}$  and  $1 \times 10^{13}$  vp/mouse) and exhibited supraphysiological levels of circulating FVIII prior to inhibitor development. This finding suggests that in immune-competent individuals, there may be an upper vector dose limit imposed by both the viral capsid antigen load and the plasma FVIII load (potency). The possibility remains that the unique porcine sequences known to be necessary for high-level expression in ET3 also conferred increased immunogenic risk and were the target of the anti-FVIII immune response observed. However, Lollar and colleagues recently performed a rigorous comparison of BDD rhFVIII and rpFVIII in the murine hemophilia A model, which revealed that the overall immunogenicities were similar with anti-A2 and anti-C2 constituting the majority of the inhibitors detected against each molecule (146). An important safety consideration in light of the high expression porcine sequences present in ET3 is that both plasma-derived and now rpFVIII products have been used clinically, the former for more than two decades, to treat acute bleeding following the development of anti-hFVIII inhibitors in the settings of congenital and acquired hemophilia A (147; 148). Therefore, there may be sufficient data available to support the risk/benefit case for transition to clinical safety (including immunogenicity) testing of ET3 delivered by AAV vector, lentiviral vector or intravenous infusion of the recombinant molecule.

As predicted by all previous gene transfer and recombinant protein expression studies, the ET3 transgene demonstrates high-level transgene product biosynthesis following liver-directed

rAAV delivery. The current data directly support the benefit of incorporating the high expression FVIII sequence elements encoded within ET3 into AAV gene transfer systems for treatment of hemophilia A. The rAAV-HCR-ET3 vector provided a long-term source circulating FVIII activity and correction of bleeding diathesis at vector doses lower than those of other bioengineered FVIII variants despite its larger size, making ET3 an ideal candidate transgene for incorporation into smaller AAV vector systems. However, due to the immune response exhibited by some mice against FVIII, additional immune modulation may be necessary to prevent the development of humoral immune response to FVIII. Previous data from our lab has shown that *ex vivo* genetic modification of hematopoietic stem cells (HSC) using a lentivector gene transfer platform promotes immune non-responsiveness to FVIII (149). While the immune nonresponsive profile induced by *ex vivo* HSC gene modification is desirable and this approach is predicted to be curative, the overall approach is clinically more complex than a single peripheral vein infusion of rAAV. Furthermore, the pre-conditioning regimens needed to attain therapeutic levels of cellular engraftment and protein expression pose additional risks. Therefore, it seems logical that different gene therapy strategies may be more amenable than others to application in distinct geographical, economically developed and clinically-advanced populations.

## **2.6 Acknowledgements**

This work was supported by grants from the National Institutes of Health; 1 U54 HL112309-01 and 1 R01 HL092179-01A2 to CBD and HTS, and T32GM008602 to HCB. CBD and HTS are co-founders Expression Therapeutics and own equity in the company. Expression Therapeutics owns the intellectual property associated with ET3. The terms of this arrangement have been reviewed and approved by Emory University in accordance with its conflict of interest policies.

## 2.7 Supplemental Information

**Supplemental Table 2.1**

A2	GAAGATGGGCCAACTAAATCAGATCCGCGGTGCCTGACCCGCTATTACT CTAGTTTC
C2	CACCTCCAAGGGAGGAGTAATGCCTGGAGACCTCAGGTGAATAATCCA AAAGAGTG
bGHPA	GTGCCTTCCTTGACCCTGGAAGGTGCCACTCCACTGTCCTTTCCTAATA AAATG

**Supplemental Table 2.1: Biotinylated probes used for detection of AAV-HCR-ET3 viral genomes** A cocktail of biotinylated probes was used for detection of AAV-HCR-ET3 viral genomes during Southern blot analysis.

**Supplemental Table 2.2**

Name	Sequence	Amplicon Length (bases)
HCR +	TTCGGTAAGTGCAGTGGAAG	
HCR -	GTCCTCGTCCGTATTTAAGC	191
Porcine A1 +	CCTGAAGAACATGGCTTCTC	
Porcine A1 -	TACCGGGAAGGACTTTATCG	133
Human A2 +	CTCACGGAATCACTGATGTC	
Human A2 -	TTGGCCCATCTTCTACAGTC	136
Porcine A3 +	TGGAGCAGCTCTGGGATTAC	
Porcine A3 -	GCAAATTCCCGGAAGACCAC	109
Human C1 +	TCAATGCCTGGAGCACCAAG	
Human C1 -	AGATGTAGAGGCTGGAGAAC	119
Human C2 +	CCTCCAAGGGAGGAGTAATG	
Human C2 -	CATCTTGACTGCTGGAGATG	169
bGHPA +	CCTTCTAGTTGCCAGCCATC	
bGHPA -	CCAGCATGCCTGCTATTGTC	199

**Supplemental Table 2.2: Primers used for regional transgene analysis** Primer sets spanning the length of the AAV-HCR-ET3 viral transgene were used for quantitative PCR analysis of the packaged ssDNA content of AAV-HCR-ET3 viral particles.

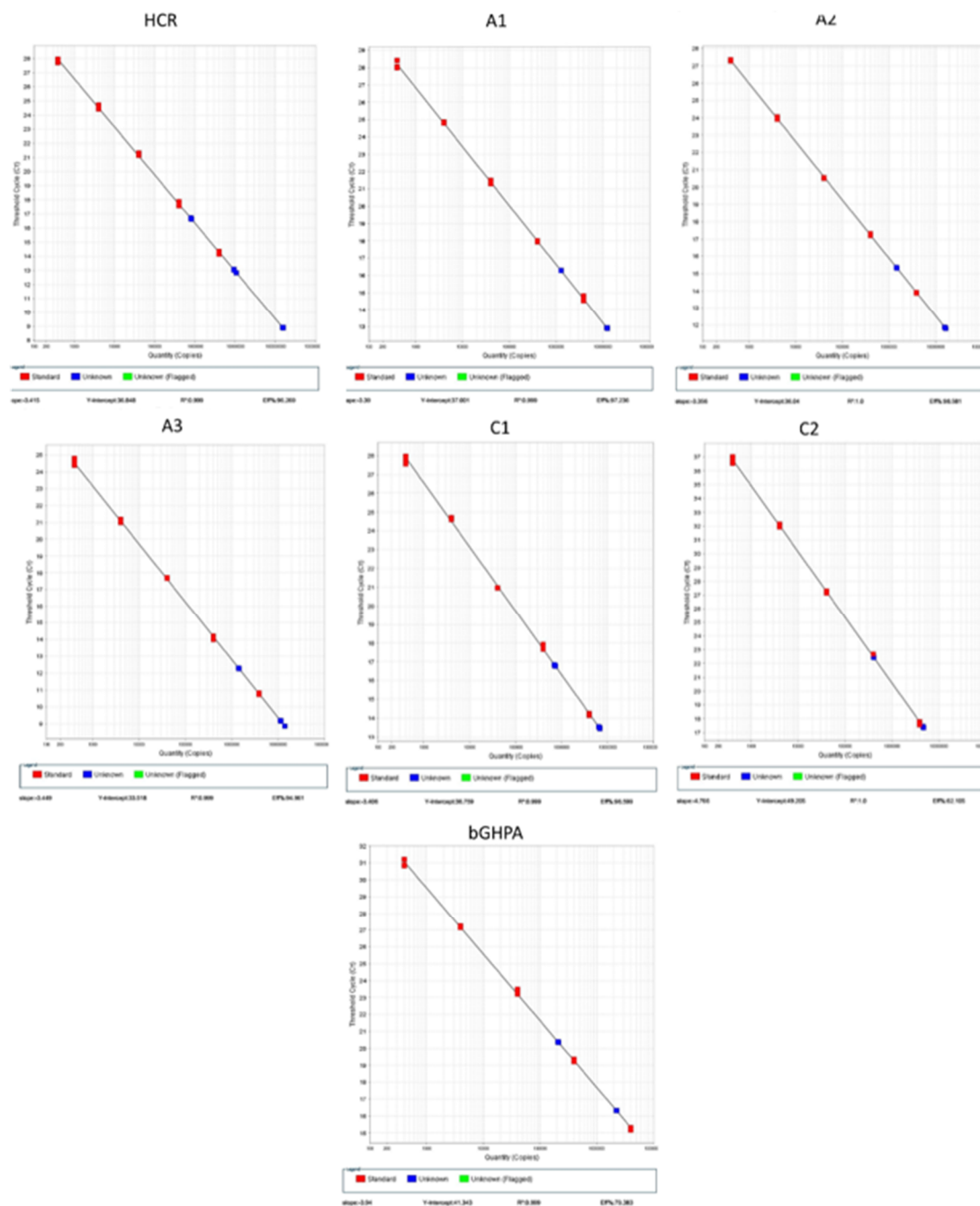
**Supplemental Table 2.3**

Mouse ID	Plasmid	Injection Time (seconds)	fVIII activity (U/mL)
355N	AAV-HCR-ET3	8	3.74
356R	AAV-HCR-ET3	10	7.80
357R	AAV-HCR-ET3	10	3.46
356L	AAV-HCR-HSQ	8	0.333
357N	AAV-HCR-HSQ	10	0.146
358L	AAV-HCR-HSQ	7	0.202

**Supplemental Table 2.3: Hydrodynamic injection of FVIII encoding AAV expression**

**plasmids** Mice were hydrodynamically injected with either AAV-HCR-ET3 or AAV-HCR-HSQ encoding expression plasmids. Individual injection times and resulting FVIII activity at 24 hours are shown.

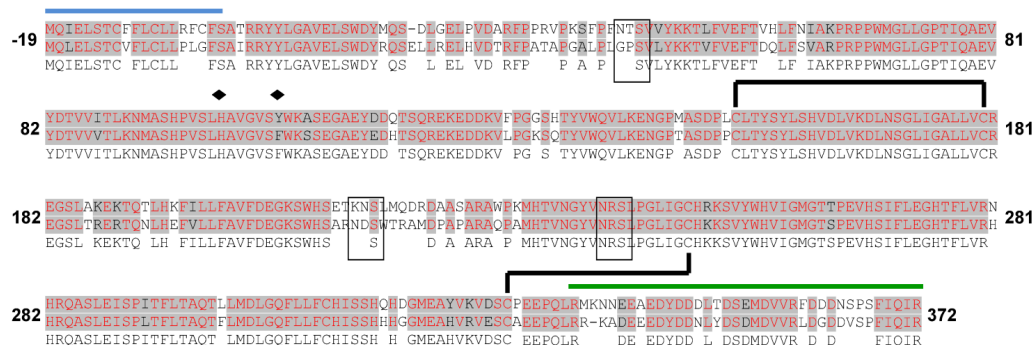
Supplemental Figure 2.1



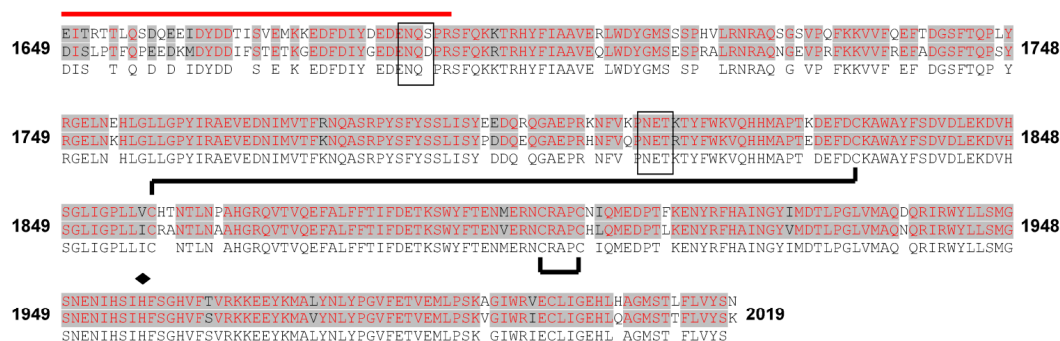
**Supplemental Figure 2.1: Standard curves for quantitative PCR analysis** To control for variation in primer efficiency during quantitative PCR analysis, standard curves of AAV-HCR-ET3 viral expression plasmid were generated for each primer set spanning the length of the AAV-HCR-ET3 transgene.

## Supplemental Figure 2.2

## A1 domain



## A3 domain



## Legend:

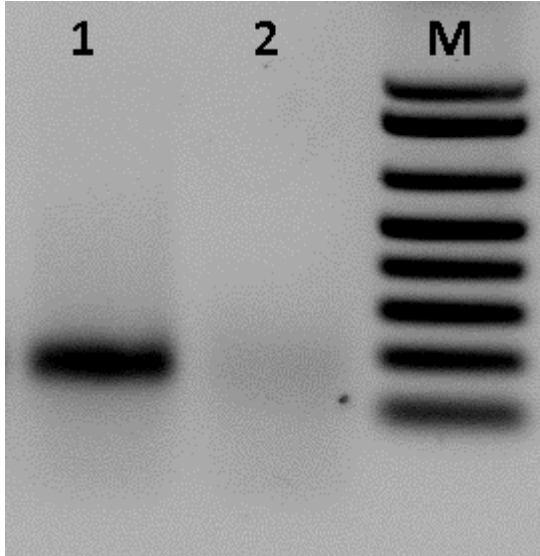
- signal peptide
- heavy chain acidic domain
- activation peptide
- disulfide linkages
- metal ion binding residues
- predicted N-linked glycan attachment sites

FVIII	Identity
Human	100%
ET3	91%

## Supplemental Figure 2.2: Sequence alignment of porcine-substituted domains of ET3 and HSQ

Amino acid sequence alignments for the signal peptide (black bar), A1 domain, heavy chain acidic domain (green bar), activation peptide (red bar) and A3 domain of human (top) and ET3 (bottom) fVIII are shown. Identical residues are distinguished by red type with gray background, similar residues are shown black type with gray background and all other residues are displayed in black

type with transparent background. Disulfide linkages are noted by the black lines connecting cysteine residues. Places where either human, ET3 or both sequences encode a N-linked glycosylation attachment site (N-X-S/T) are outlined with a black box. Additional amino acid differences in the synthetic linker sequence in ET3 and HSQ are not shown.

**Supplemental figure 2.3****Supplemental figure 2.3: ET3 C2 domain sequence RNA is present in liver of treated mice**

Reverse transcription PCR analysis of RNA isolated from livers of treated and untreated mice shows ET3 C2 domain sequence in a mouse treated with AAV-HCR-ET3 (lane 1) and no detectable ET3 C2 domain sequence in untreated control (lane 2).

## Chapter 3

### Liver-directed bioengineering of AAV-FVIII transgenes

Harrison C Brown<sup>1</sup>, Phillip M Zakas<sup>1</sup>, Stephan N George<sup>2</sup>, Ernest T Parker<sup>3</sup>, H Trent Spencer<sup>3</sup>,  
Christopher B Doering<sup>3</sup>

1 Graduate Program in Molecular and Systems Pharmacology, Laney Graduate School, Emory University,  
Atlanta, Georgia, USA.

2 Complex Carbohydrates Research Center, University of Georgia, Athens, Georgia, USA

3(Stephan, waiting)

3 Department of Pediatrics, Aflac Cancer and Blood Disorders Center, Emory University School of  
Medicine , Atlanta, Georgia, USA

Harrison Brown designed and conducted experiments, designed and cloned plasmids, analyzed  
data, performed animal procedures, performed computational analysis, and wrote the manuscript

Phillip Zakas characterized ancestral FVIII constructs

Stephan George clones plasmids and conducted experiments

Ernest Parker performed animal procedures

Trent Spencer and Chris Doering designed experiments and edited the manuscript

### 3.1 Abstract

Low-level protein biosynthesis frequently encumbers AAV gene therapies. This obstacle has particularly impacted AAV gene therapy for hemophilia A, where the intrinsically poor biosynthetic efficiency and large size of the coagulation factor VIII (FVIII) cDNA substantially impairs AAV vector potency. Codon optimization and synthetic promoter design are routinely utilized to increase the biosynthetic efficiency and decrease the transgene size of AAV-FVIII expression cassettes, however, these approaches have yet to realize an AAV vector of sufficient potency to provide curative levels of FVIII expression at clinically safe vector doses. To alleviate these constraints on AAV vectors for hemophilia A, we have generated a highly potent yet minimally sized promoter, which permits an AAV-FVIII expression cassette design of just 4883 base pairs, which is well within the optimal transgene length for AAV vector designs. Second, we have employed a novel tissue-directed modality of codon optimization. This strategy confers up to 7-fold greater increases in FVIII expression *in vivo* than traditional organism-level codon optimization strategies. Together these technologies, which are generalizable to all liver-directed AAV designs, have created an AAV-FVIII vector which provides curative levels of expression at  $1e11$  vector particles per kilogram in a murine model of hemophilia A.

### 3.2 Introduction

Hemophilia A is an X-linked bleeding disorder caused by a deficiency in coagulation factor VIII (FVIII). A growing body of clinical experience has supported the use of liver-directed adeno-associated virus (AAV) as a gene therapy vector for the treatment of hemophilia B, however, several obstacles have hindered the development of an AAV vector for hemophilia A (78; 82; 84; 150). These obstacles include the limited DNA packaging capacity of AAV for the large FVIII transgene (47; 48; 151; 152), and inefficient biosynthesis of human coagulation factor FVIII (98). Clinical experience with liver-directed AAV has shown a vector-dose limiting toxicity of  $2e12$  vector genomes (vg) per kilogram due to capsid-mediated cellular immunity directed toward AAV-

modified hepatocytes, resulting in loss of gene expression and transient hepatotoxicity (82; 84; 150). Due to this dose-limiting toxicity, it is critical that AAV-FVIII vectors confer efficacious levels of FVIII activity at doses below the  $2 \times 10^{12}$  vg/kg threshold.

While the precise packaging capacity of AAV is debated, it is accepted that vector genome sizes of 4.7-4.9 kilobases (kb) result in the most efficient transgene packaging and expression (47; 48; 151; 152). Due to the large size of the B-domain deleted (BDD) human FVIII (hFVIII) of 4.4kb and the necessary non-coding viral and regulatory control elements, AAV-FVIII vectors routinely exceed this ideal transgene length, resulting in suboptimal transgene packaging and delivery (152-154). An AAV-FVIII transgene minimally contains a promoter, the FVIII cDNA, a polyadenylation (polyA) signal, and AAV inverted terminal repeats (ITRs) flanking both sides of the cassette. Combined, these immutable elements, the ITRs and FVIII cDNA, occupy 4664bp of the 4900 bps available for optimal gene expression, leaving only 246bp for the promoter, polyA signal, and any intervening sequences. Currently utilized liver-specific promoters such as the hybrid liver promoter (HLP) and HCR-hAAT range in size from 250 to over 700 bases, which alone exceed the remaining capacity of the virus (154; 155). To alleviate this limitation, we utilized a combinatorial process of assembling and testing promoter and enhancer fragments to generate a novel 146bp promoter, designated the hepatic combinatorial bundle (HCB), which drives strong gene expression in hepatocytes despite its minimal size.

An additional factor that limits the efficacy of AAV-FVIII vectors is the low biosynthetic efficiency of the FVIII protein itself. FVIII is a large glycoprotein that is secreted at levels 2-3 orders of magnitude less efficiently than similarly sized glycoproteins (98). We have previously described a human/porcine chimeric FVIII molecule designated ET3 (previously HP47) which demonstrates 10-100 fold increased secretion compared to BDD hFVIII (HSQ) (99; 156). We sought to further improve the expression of both ET3 and HSQ by using a novel codon optimization strategy. Traditional codon optimization strategies utilize the entire genomic cDNA of a host species to derive the codon usage bias (CUB) of the organism as a whole, which is assumed to be

reflective of the physical tRNA pools within its cells, originally described as the “tRNA adaptation theory” (104-107). However, recent work has shown that the tRNA pools within different tissues vary, and suggests that the assumed prevalence of individual tRNA species derived from the host organism’s genomic cDNA may not be reflective of the tRNA pools within a particular tissue (108). We found that a previously-described CUB table generated from genes highly expressed within the liver exhibited greater deviation from the standard human CUB table than the standard murine CUB table, suggesting that codon optimization directed toward the specific tissue in which a gene is expressed may provide greater benefit than optimization to the CUB of the organism as a whole.

By combining these approaches, we have developed a 4.88kb AAV8-HSQ vector which provided 0.4 units (U)/mL of FVIII activity in a murine model of hemophilia A at a vector dose of  $1 \times 10^{11}$  vector genomes vg/kg, as well as a 4.91kb AAV8-ET3 vector which provided over 1.5 U/mL at the same dose. These vectors represent two of the most powerful AAV-FVIII vectors described to date, providing curative levels of FVIII expression at a vector dose 20-fold lower than the maximum clinically tolerated dose of  $2 \times 10^{12}$  vg/kg.

### 3.3 Materials and Methods

*Codon usage indexes:* The liver codon optimization table was previously described, utilizing sequences of highly and specifically expressed within hepatocytes (108). The myeloid optimization table was generated by examining previously published Affymetrix mRNA array data using the GSE16836 dataset (157). The myeloid CUB was determined from cDNA sequences from highly and specifically expressed utilizing the publically available Sequence Manipulation Suite (158). Individual codon usage bias of all human genes were determined using gene sequences retrieved from the Consensus CDS Sequence Project annotation of the GRCh38 reference genome (159).

*DNA synthesis:* The synthetic AAV2 expression cassette was constructed by Genscript Biotech Corporation and inserted into the pUC57 backbone. Promoter DNA sequences were

generated as linear dsDNA fragment gBlocks<sup>®</sup> by Integrated DNA Technologies, Inc. gBlocks<sup>®</sup> were cloned into the AAV vector using AgeI/SalI sites included in the gBlock design using the SalI-compatible XhoI site within the AAV vector. Complete FVIII DNA sequences were synthesized by Genscript. Codon optimization was performed using the Genscript Optimum Gene<sup>™</sup> algorithm using the standard human CUB index as the human codon optimization table or custom liver and myeloid CUB indexes. FVIII sequences were cloned into the AAV backbone using XhoI/NotI restriction sites. The sequence of ancestral FVIII node 53 (An53) was determined by ancestral sequence reconstruction as previously described and optimized to human and liver CUB tables using the OptimumGene<sup>™</sup> algorithm (160). The AAV-HLP-V3 was transgene sequence was generated from previously published sequence (154).

*tRNA expression plasmid:* The 6x tRNA expression sequence was synthesized by Genscript and inserted into the pUC57 backbone. tRNA sequences and chromosomal location were retrieved from the genomic tRNA database (161). Genomic sequences 200bp both upstream and downstream of the tRNA sequence itself were included to preserve the local genomic context as well as to capture local transcriptional regulators and proximal sequence elements.

*Transfection studies:* Low-passage HepG2 cells were plated at a density of 200,000 cells per well in 500 $\mu$ L DMEM/F12 supplemented with 10% fetal bovine serum and 1% penicillin/streptomycin in 6 well plates. 24 hours after seeding, cells were transfected using 1.5 $\mu$ L X2 transfection reagent (Mirus Bio) and 500ng plasmid. For tRNA cotransfection, 250ng of FVIII expressing plasmid was co-transfected with either 250ng of 6x tRNA or GFP control plasmid. The media was changed the following day, and supernatants were assayed for FVIII activity after 24 hours.

*FVIII activity measurements:* FVIII activity in conditioned supernatant was determined by activated partial thromboplastin reagent-based one-stage coagulation assay previously described (162). Briefly, 5 $\mu$ L of conditioned supernatant was diluted in 50 $\mu$ L FVIII-deficient plasma. 50 $\mu$ L of activated partial thromboplastin was then added and samples were incubated at 37 degrees for 4

minutes. Following incubation, 50 $\mu$ L of 20mM calcium was added. Time to clot formation was determined by automated viscometric measurement. FVIII activity was determined by linear regression analysis of the clotting time versus the logarithm of the reciprocal plasma dilution. FVIII activity in plasma samples was measured using the Diapharma Coatest SP<sub>4</sub> FVIII kit according to the manufacturer's instructions.

*Hydrodynamic Injections:* 250ng (ET3 and An53) or 500ng (HSQ) expression plasmid were diluted into Transit EE hydrodynamic injection solution (Mirus Bio) in a volume equivalent to 0.1mL/gram of the recipient mouse's weight. Plasmid was delivered as a single bolus into the tail vein over 5-10 seconds using 3mL syringes and 26 and 5/8 gauge needles. Mice were allowed to recover on heating pads for 30 minutes. Blood was drawn by the retroorbital method into citrated tubes 24 hours after injections.

*AAV production and titration:* AAV8 production was performed by Vigene Biosciences, Inc. Vector titers were determined in-house by a PCR method. Vector particles were DNase treated for 30 minutes, then DNase was inactivated by adding EGTA and heat inactivating at 65 degrees for 10 minutes. Packaged DNA was liberated by addition of Proteinase K and heated for 1 hour at 65 degrees. Proteinase K was then inactivated by heating at 95 degrees for 20 minutes. DNA concentration was determined by quantitative PCR using a standard curve generated from the appropriate AAV expression plasmid using primers directed toward the center of the viral transgene.

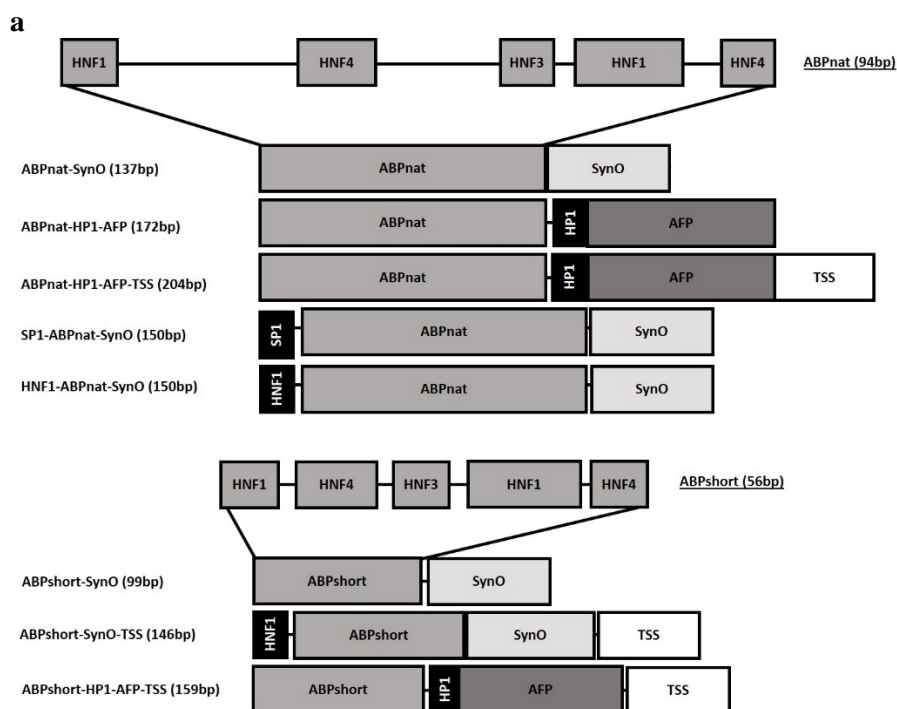
*Animal studies:* All animal studies were performed under the guidelines set by the Emory University Institutional Animal Care and Use Committee. Exon 16-disrupted mice back-crossed onto a C57BL/6 background were used as a model of hemophilia A (163). Hydrodynamic injections were performed in 8-12 week old mice of mixed sex. AAV studies were performed in 8-12 week old male mice. Bleeding was performed under anesthesia by retro-orbital method into citrated capillary tubes.

### 3.4 Results

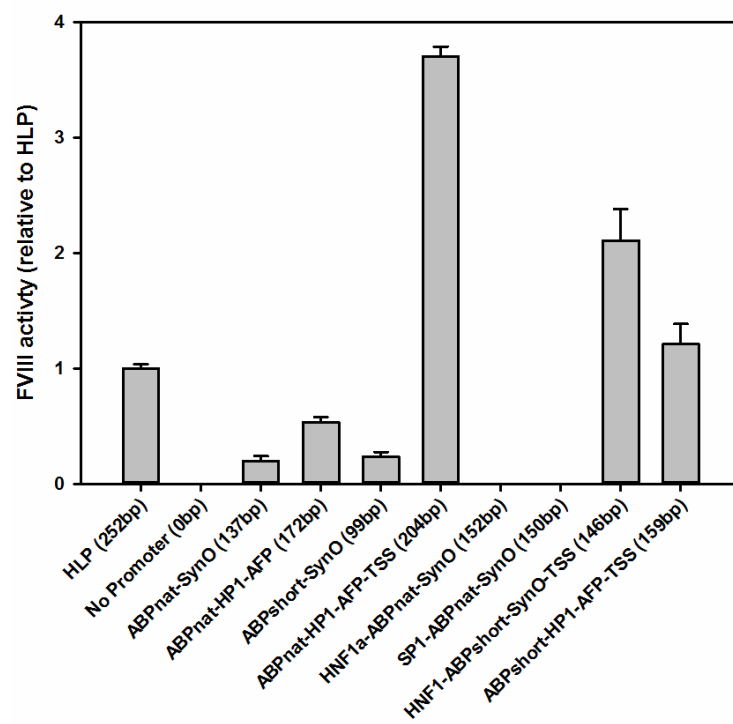
**Synthetic Promoter construction:** Ryffel *et al* previously reported that a 41bp fragment from the *Xenopus laevis* albumin 5' untranslated region (UTR) is by itself sufficient to drive gene transcription *in vitro* (164). This 41bp region, designated SynO, contains the hepatocyte-specific transcription factor (TF) binding site HP1 as well as a TATA box. Similarly, Godbout *et al* reported a 61bp fragment immediately 5' of the murine  $\alpha$ -fetoprotein gene (AFP) as also sufficient to drive gene expression (165). When inserted into a plasmid cassette driving GFP, these elements alone failed to drive detectable expression when transfected in HepG2 cells (data not show), however, this assay may have lacked sensitivity to detect low-level gene transcription. To increase the transcriptional power of these minimal promoters, we utilized an iterative process of modification, wherein fragments of the human 5'  $\alpha$ -microglobulin/Bikuni UTR enriched with liver-specific TF binding sites, designated ABP, were fused to the 5' ends of both SynO and AFP promoters, and the AFP promoter was additionally augmented with an HP1 TF binding site. We designed two ABP fragment variants, one of which included 94bp of native genomic sequence (ABPnat), and a second 61bp variant wherein non-TF binding regions were deleted (ABPshort), as identified by Rouet *et al* (166). These promoters were further modified with the inclusion of non-native transcription factor binding sites and transcription start site (TSS) motif. (**Figure 3.1a**)

These hybrid promoters were inserted into a cassette driving the expression of the high-expression FVIII variant ET3. The relative strength of these promoters was compared to the previously described 252bp hybrid liver promoter (HLP) which represents one of the shortest yet strongest liver-directed promoters described to date. When transfected into HepG2 cells, the ABPnat element fused to either SynO or AFP promoters drove detectable levels of FVIII expression, while the reduction of ABPnat to ABPshort did not impair gene expression. Inclusion of the TSS dramatically increased FVIII expression, while addition of the non-native TF binding sites HNF1a and SP1 in the context of the ABPnat enhancer diminished FVIII expression to undetectable levels.

Figure 3.1



**b**



c

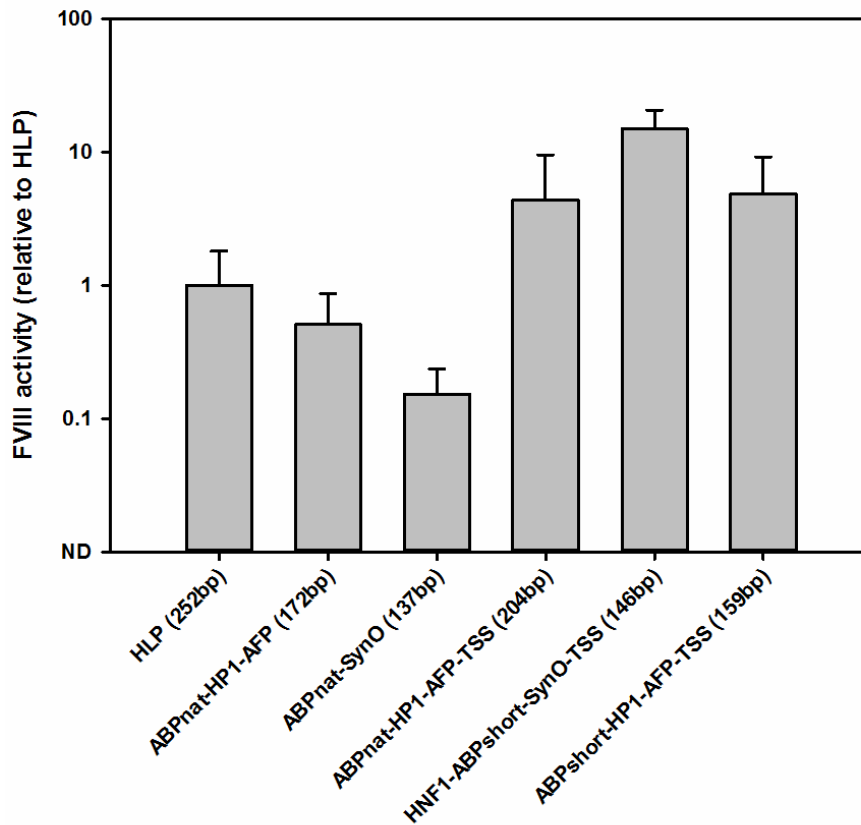


**Figure 3.1 Promoter design and testing.** (a) Novel, liver-directed promoters were constructed by assembly of discrete units designed for high transcriptional activity in the context of the liver. (b) To determine the relative strength of promoter designs, promoters driving the expression of ET3 were transfected into HepG2 cells, and FVIII activity was measured 48 hours post transfection. Activity is displayed relative to HLP. (c) To determine the strength of the promoters *in vivo*, plasmid was delivered by hydrodynamic injection to hemophilia A mice and plasma FVIII activity was measured by FVIII chromogenic assay. Activity is displayed relative to HLP.

Interestingly however, the HNF1 permitted robust gene expression when coupled with the ABPshort enhancer in the context of either SynO or AFP promoters. (**Figure 3.1b**)

From these data, five of these promoters were chosen for *in vivo* testing by hydrodynamic injection into the livers of hemophilia A mice. (**Figure 3.1c**) Both the ABPnat-AFP and ABPnat-SynO designs drove detectable FVIII expression, yet did not achieve the strength of the HLP promoter. In agreement with the *in vitro* data, inclusion of the TSS motif to ABPnat-AFP dramatically increased FVIII expression, achieving FVIII activity 4 fold higher than HLP. ABPshort coupled with either AFP-TSS or SynO-TSS permitted the highest *in vivo* FVIII expression of all plasmids tested. Due to its small size of only 146bp and strong *in vivo* activity of 14-fold that of HLP, ABPshort-SynO-TSS chosen as the final promoter design for our AAV vector design. For convenience, this promoter was renamed the hepatic combinatorial bundle (HCB).

**Tissue Specific Codon Optimization Index:** Previous work has revealed that the codon usage bias of genes highly and specifically expressed in the human liver differ from the codon usage bias of the entire human genome coding DNA sequence (CDS) (108). Furthermore, the codon usage bias of the liver is uniquely predictive of the physical tRNA content within liver tissue. Building on these observations, we utilized this liver directed CUB table to synthesize liver codon optimized (LCO) variants of HSQ, ET3, and the recently described ancestral FVIII protein An53 (160). As a control, we utilized a similar strategy as the Dittmar group to construct a codon usage bias table based on genes highly expressed in myeloid cells. This myeloid codon optimization (MCO) strategy was applied to both HSQ and ET3, while standard human codon optimization (HCO) was also applied to An53.

We first sought to quantify the deviation of the LCO and MCO CUB tables from the standard human CUB table. The CUB of an individual codon species within a coding sequence is given by formula 1, and the CUB deviation from human is given by formula 2.

$$\text{Formula 1: } CUBi = \frac{Ci}{Caa}$$

Where the codon usage bias of an individual codon species ( $CUBi$ ) is given by ratio of the number of times a single codon ( $Ci$ ) is utilized in a cDNA to the total number of synonymous codons ( $Caa$ ) coding for the corresponding amino acid are used within a coding sequence.

$$\text{Formula 2: } FD = \frac{CUBi_r}{CUBi_h}$$

Where  $FD$  is the fold difference of a single codon species with respect to human,  $CUBi_r$  is the codon usage bias of a single codon within the reference CUB table, and  $CUBi_h$  is the codon usage bias of the respective individual codon in the human CUB table.

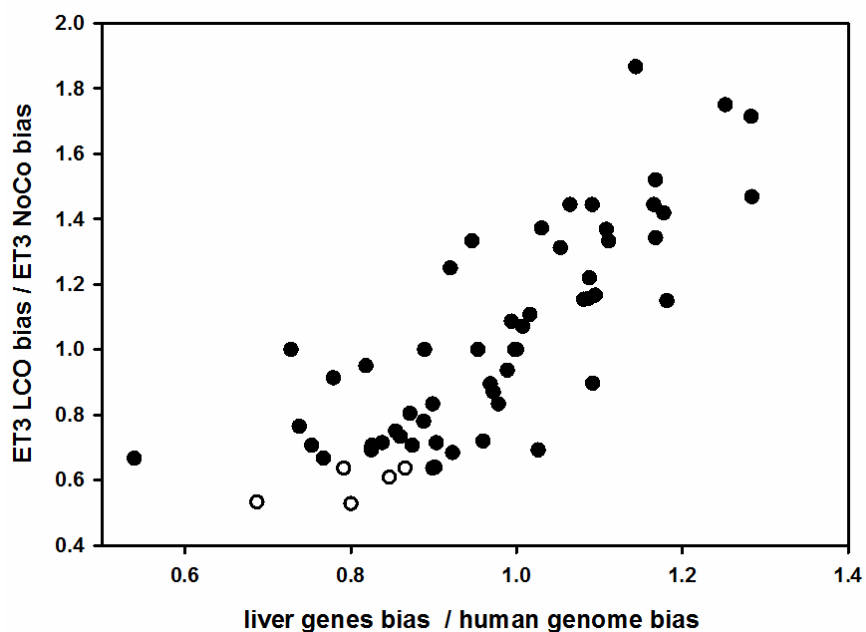
For comparison, we also quantified the deviation of the murine CUB table against the human CUB table. With respect to the human CUB table, the average  $FD$  of the liver and myeloid CUB tables were substantially greater than that of the murine CUB table. (**Figure 3.2a**). On average, murine  $FD$ s deviated from the human bias by just 1.04 fold per codon, whereas the liver and myeloid  $FD$ s significantly ( $p < 1e8$ ) showed over 3 times more deviation, with an average of 1.15 and 1.14 fold difference per codon, respectively.

While this analysis demonstrates the robust deviation of the tissue-directed CUB tables compared to human in relative terms, the absolute difference in magnitude of CUB must also be considered, which is given in formula 3.

$$\text{Formula 3: } AD_h = |CUBi_p - CUBi_h|$$



c



d

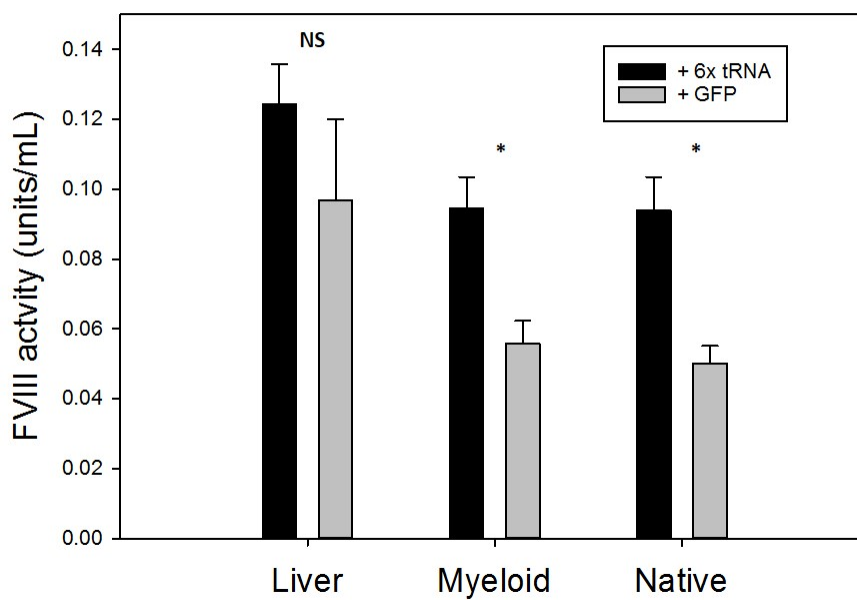


**Figure 3.2: Liver directed codon optimization.** (a) The fold difference in CUB of each codon in the liver, myeloid, and murine CUB tables over the same codon in the human CUB table. (b) The absolute difference codon usage bias of each codon in the liver CUB table versus the respective codon in the human CUB table. (\*  $p < 0.05$  by 2-way t-test,  $n = 43$  for liver CUB, 15453 for human CDS) (c) The correlation of the ratio of codon usage biases of the set of liver

genes to that of the entire human genomic coding sequence against the ratios of codon usage bias of ET3-LCO to that of ET3 non-codon optimized (NoCo). Open circles mark the six codon species with the lowest ET3 LCO to ET3-NoCo ratio. **(d)** Plasmids encoding ET3-LCO, ET3-MCO, and ET3-NoCo were cotransfected into HepG2 cells with either GFP expression plasmid or a plasmid encoding the six tRNAs predicted to be most limiting in to the expression of ET3-NoCo (n=3, \* =  $p < 0.05$ , error bars show standard deviation of the mean).

where  $AD_h$  is the absolute difference in magnitude of the  $CUB_i$  of a single codon species from an individual protein ( $CUB_{ip}$ ), from that of the respective codon in the human CUB table ( $CUB_{ih}$ ). The  $AD_h$  of each codon species was calculated for the list of 43 liver-specific genes, as well as for each individual gene in the human CDS.

The mean  $AD_h$  of  $CUB_{ip}$  from each of the 43 proteins from which the LCO CUB table was derived deviated by as much as .14 (ATC: liver .61, human .47) (**Figure 3.2b**). The mean of the  $AD_h$  of each codon species of the proteins from which the LCO CUB was generated was significantly greater than the mean  $AD_h$  of the human CDS in 22 codons (\* =  $p < 0.05$  by 2 way t-test). Together, these data strongly support that the codon usage of genes highly and uniquely expressed within a single tissue differ from that of the human CDS as a whole, and that a higher degree of variation may exist between tissues of a single organism than between orthologous species.

We next analyzed how closely the process of liver codon optimization of ET3 mimicked the naturally occurring biasing of the genes endogenously overexpressed within the liver. (**Figure 3.2c**) Mapping the correlation of the ratio of codon usage biases of the set of highly expressed liver genes to that of the entire human CDS against the ratios of codon usage bias of ET3 LCO to that of ET3 NoCo reveals a close correlation across all codons ( $r^2 = 0.65$ ). Effectively, this shows that the codons over-represented in the naturally liver optimized genes are similarly over-represented in our synthetically optimized ET3, and likewise, that the codons under-represented natively are also under-represented in ET3-LCO.

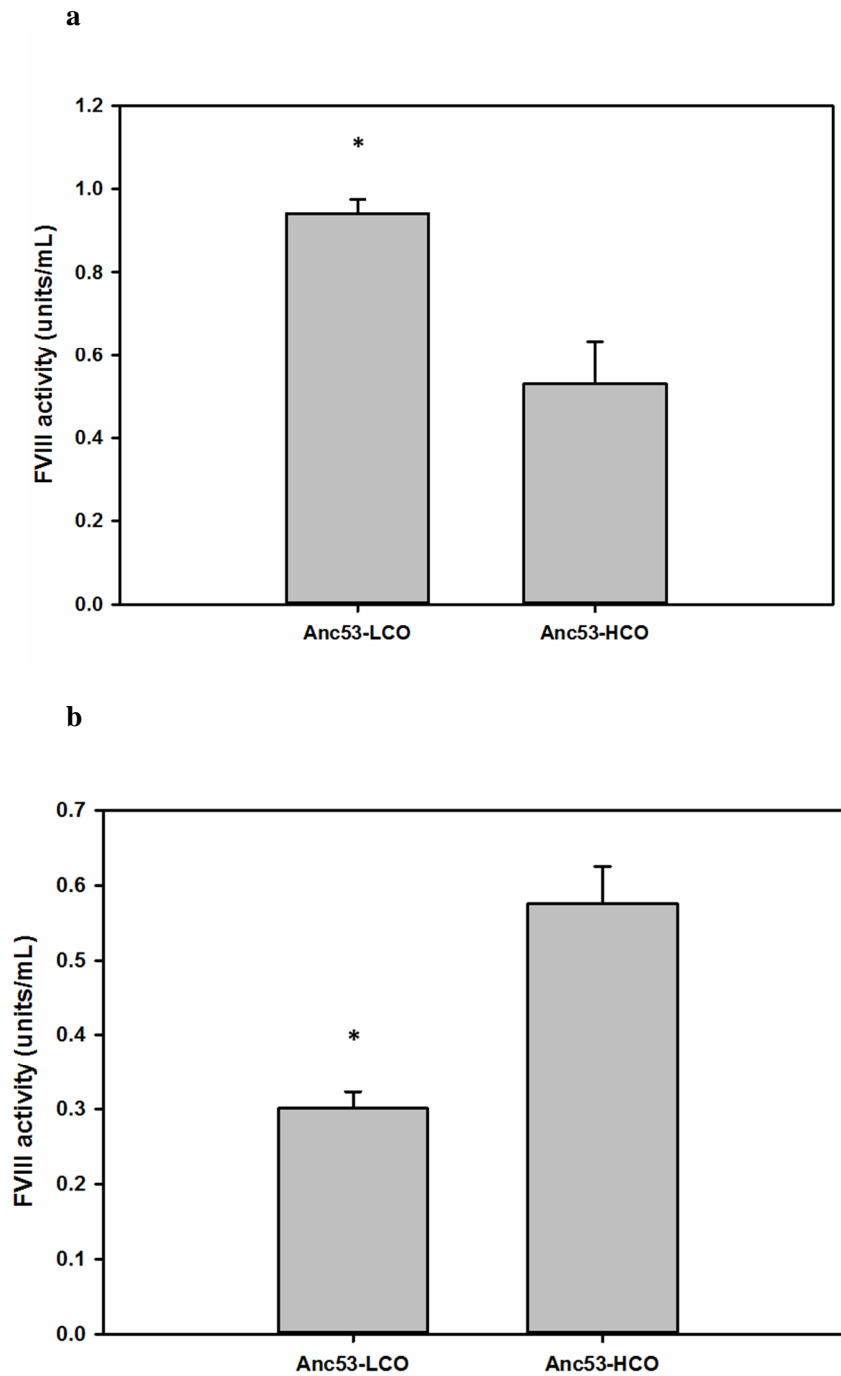
It has previously been shown that the codon usage bias of this set of 43 genes highly expressed in the liver is predictive of the physical tRNA pools within the tissue, where codons that are under-represented in the coding sequences have lower levels of tRNA isoacceptors within the

tissue, and codons used preferentially predict high levels of tRNA isoacceptor (108). The central assumption of codon optimization is that these tRNA levels are the rate limiting factor of protein translation, wherein cDNAs that frequently utilize codons with low-level cognate tRNAs suffer from inefficient translation. To test this hypothesis, we constructed a plasmid to over-express the 6 tRNAs that the ET3-LCO sequence predicts to be most limiting to the expression of ET3-NoCo, which are marked in open circles in **Figure 3.2d**. Plasmids encoding ET3-LCO, ET3-MCO, and ET3-NoCo were cotransfected into HepG2 cells with either the 6x tRNA plasmid or a GFP control. When cotransfected with GFP, ET3-LCO demonstrated 2-fold higher levels of FVIII expression than that of ET3-MCO or ET3-NoCo. When cotransfected with the 6x tRNA, ET3-LCO showed a slight but insignificant increase in FVIII expression ( $p = 0.41$  by 2-way t-test), while the expression of ET3-MCO and ET3-NoCo were elevated to that of non-tRNA supplemented ET3-LCO. (**Figure 3.2d**)

**In vitro testing of liver codon optimization:** To test if liver codon optimization provided benefit in the context of liver-directed expression over that of standard human codon optimization, An53-LCO and An53-HCO were transfected into HepG2 cells. As the sequence of An53 was predicted at the amino acid level, the native (NoCo) sequence was not available. In this system, An53-LCO expressed at levels nearly 2-fold greater than that of An53-HCO. (**Figure 3.3a**) To test if this effect was specific to liver derived cells, the same plasmids were then transfected into baby hamster kidney (BHK) cells. (**Figure 3.3b**) In this setting, ET3-LCO expressed at levels 2-fold lower than ET3-HCO, supporting that liver codon optimization provides benefit specifically in the context of liver-directed expression.

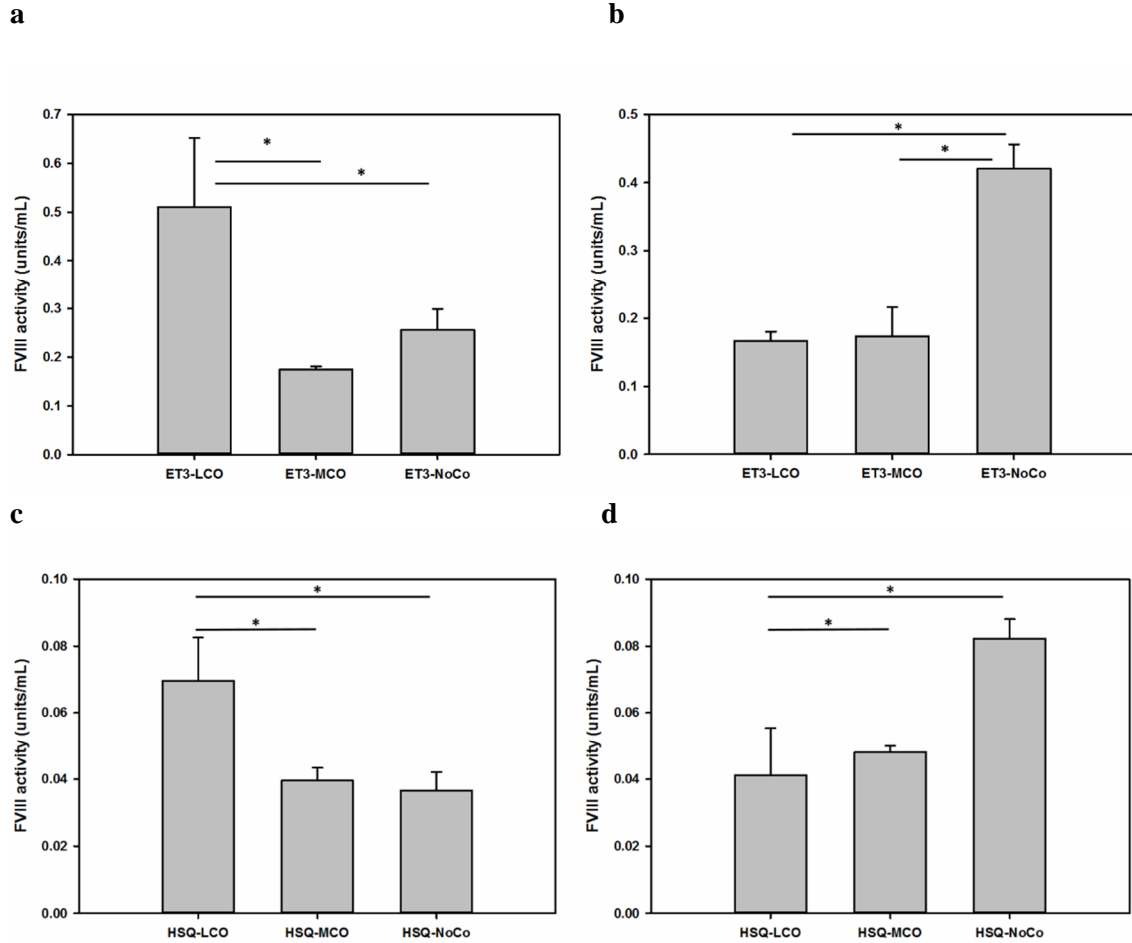
To further validate these findings, the same transfection studies were then performed using ET3-LCO, MCO, and NoCo as well as HSQ-LCO, MCO, and NoCo. When transfected into HepG2 cells, ET3-LCO and HSQ-LCO both showed significantly higher expression than either the MCO or NoCo cognates. (**Figures 3.4a,c**) When transfected into the BHK cells, both MCO and LCO

Figure 3.3



**Figure 3.3: Expression and tissue specificity of HCO versus LCO.** Anc53-HCO and Anc53-LCO were transfected into (a) HepG2 cells and (b) BHK cells FVIII activity from conditioned media was measured 48 hours after transfection (\* =  $p < 0.05$ ,  $n = 3$ , errors bars show standard deviation of the mean)

Figure 3.4



**Figure 3.4: Expression and tissue specificity of LCO, MCO, and NoCo designs.** ET3-LCO, ET3-MCO, and ET3-NoCo were transfected into (a) HepG2 cells and (b) BHK cells. HSQ-LCO, HSQ-MCO, and HSQ-NoCo were transfected into (c) HepG2 cells and (d) BHK cells. FVIII activity from conditioned media was measured 48 hours after transfection. (\* =  $p < 0.05$ ,  $n = 3$ , error bars show standard deviation of the mean)

optimization decreased FVIII expression relative to the non-optimized variants. (**Figures 3.4b,d**). Together, these data show that the liver codon optimization specifically provides benefit in the matched tissue, and through the MCO control that this optimization is not an artifact of optimization against a small subset of highly expressed genes. Further, they supports that removal of deleterious cis-acting RNA motifs, a process that was applied equally to the HCO, MCO and LCO designs, were not a significant source of increased expression.

**In vivo impact of tissue-specific codon optimization:** The benefit of liver codon optimization over other strategies was next compared *in vivo*. Expression plasmids carrying An53-HCO and An53-LCO were delivered by hydrodynamic injection to hemophilia A mice. In this system, An53-LCO provided a 7-fold increase in FVIII expression compared to An53-HCO. (**Figure 3.5a**) Next, ET3 and HSQ-LCO, MCO, and NoCo were delivered utilizing the same system. (**Figure 3.5b**) The benefit of LCO over MCO and NoCo was again observed by both ET3 and HSQ, with ET3-LCO providing 4-fold increase in expression over both MCO and NoCo (**Figure 3.5b**). HSQ-LCO raised FVIII to detectable levels compared to NoCo, representing a minimum of 6-fold improvement, and strongly but insignificantly trended toward 4-fold increase in expression over MCO. (**Figure 3.5c**). To ensure that these benefits were not due to altered expression kinetics, a time course experiment was performed using ET3 and HSQ LCO and NoCo. Our previous experience has shown that delivery linearized plasmid DNA provides prolonged gene expression compared to that of circular plasmid, however, maximum expression is not achieved for several days (data not shown). Linearized transgene DNA was delivered to by hydrodynamic injection to hemophilia A mice, and expression was monitored over the next two weeks. (**Figure 3.5d**) Over the course of the experiment, the benefit of LCO over NoCo was replicated, with ET3-LCO providing sustained 7-fold increase in FVIII expression, while HSQ-LCO again increased expression to detectable levels.

Figure 3.5

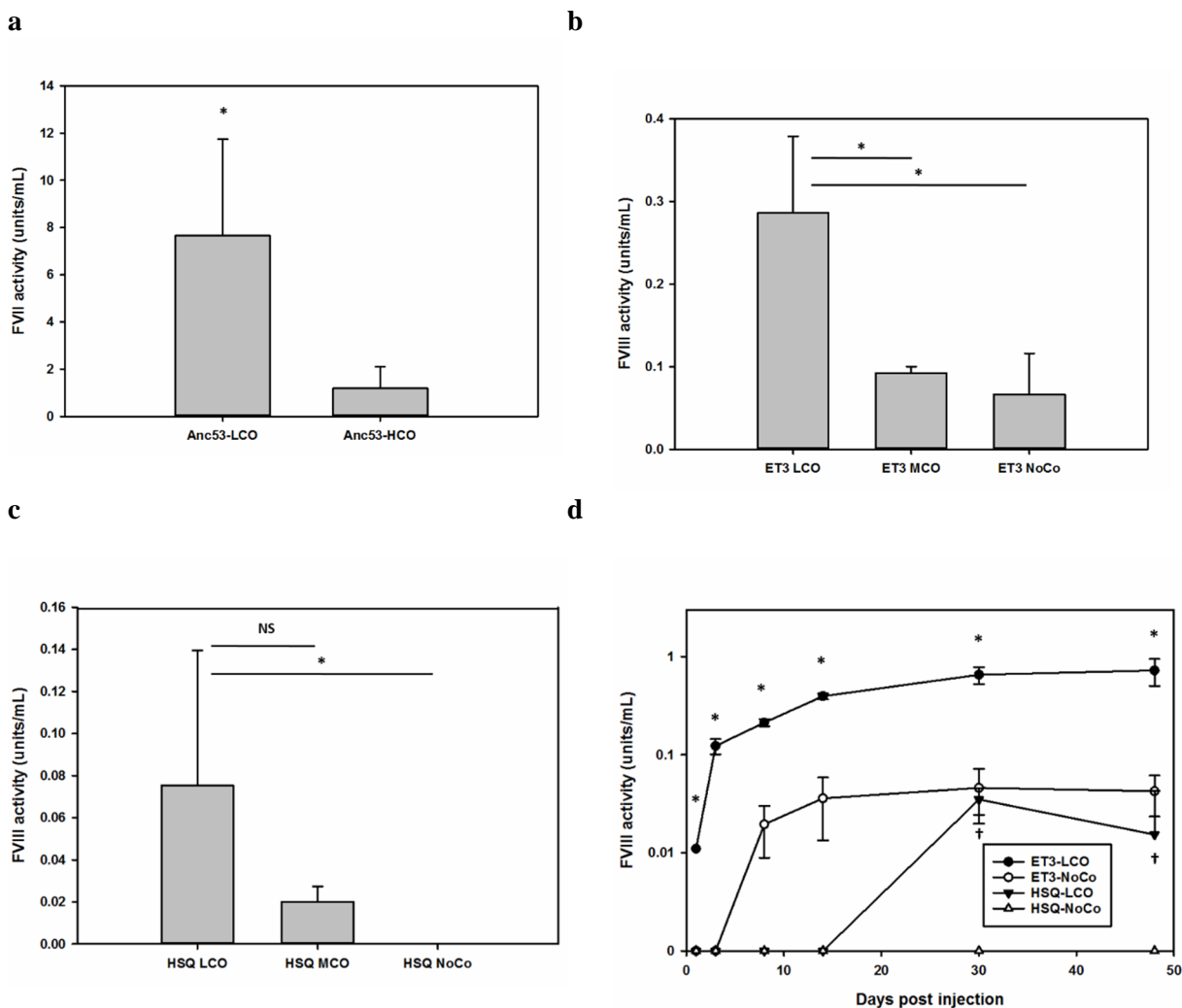


**Figure 3.5: In vivo expression of codon optimized designs.** (a) Anc53-HCO and Anc53-LCO, (b) ET3-LCO, ET3-MCO, and ET3-NoCo, (c) HSQ-LCO, HSQ-MCO, HSQ-NoCo plasmids were hydrodynamically injected into hemophilia A mice. Plasma levels of FVIII activity were measured 24 hours after injection. (d) Linearized ET3 and HSQ-LCO, MCO, and NoCo were hydrodynamically injected into hemophilia A mice. Plasma levels of FVIII activity were measured for 2 weeks post injection. (n = 3-5 per group, \* =  $p < 0.05$  [a-c], \* =  $p < 0.05$  ET3-LCO vs ET3-NoCo, † =  $p < 0.05$  HSQ-LCO vs HSQ-NoCo [d], error bars show standard deviation of the mean)

**AAV mediated delivery of optimized constructs:** AAV expression cassettes containing FVIII cDNAs and the synthetic promoters were constructed and packaged into AAV8 capsids. **(Figure 3.6a)** First, the benefit of HCO versus LCO strategies were compared in the context of liver directed gene therapy. To evaluate this, AAV8 Anc53-LCO and Anc53-HCO driven by the HLP promoter were synthesized.  $1e11$  vector genomes vg/kg of AAV8-HLP-An53k-LCO and AAV8-HLP-An53k-HCO were delivered intravenously to hemophilia A mice. In this system, the benefit of LCO over HCO was again recapitulated, with An53 LCO demonstrating persistent 4-5 fold greater FVIII activity over An53 HCO **(Figure 3.6b)**.

Optimized HSQ and ET3 constructs were also packaged into AAV8 capsids. These transgenes consisted of LCO FVIII designs driven by the HCB promoter and terminated by a minimal synthetic beta globin polyadenylation signal, flanked by AAV2 ITRs **(Figure 3.6a)**. At a size of 4882bp (HSQ) and 4912bp (ET3), to our knowledge these vectors are the shortest FVIII vectors described to date encoding full length BDD FVIII. As a control, these vectors were compared against AAV8-HLP-V3co also packed in AAV8 capsid. FVIII-V3co is a previously described high-expression, codon optimized human FVIII variant that contains a novel 17-aa peptide (V3) in which 6 glycosylation sites from the FVIII B domain were juxtaposed and then fused to the linker sequence joining the FVIII A3 and C1 domains, the addition of which was shown to increase FVIII expression 2-fold (154). AAV-HLP-V3co represents one of the most potent AAV-FVIII vectors described to date. When delivered to hemophilia A mice at a vector dose of  $1e11$  vg/kg, AAV-HCB-HSQ-LCO achieved persistent FVIII activity of approximately 0.4U/mL, which provided sustained expression greater than that of AAV-HLP-V3. At the same dose, AAV-HCB-ET3-LCO achieved persistent FVIII activity of over 1.5U/mL. **(Figure 3.6c)**.

To test the long term durability of FVIII expression conferred by the HCB promoter, a dose finding experiment was performed with high ( $1e12$ vg/k), medium ( $1e11$  vg/kg) and low ( $6.2e9$  vg/kg) was performed, with the notable addition of the minute virus of mice (MVM) intron added to the design **(Figure 3.6d)**. *In vivo* studies have suggested that the addition of the MVM intro to

Figure 3.6

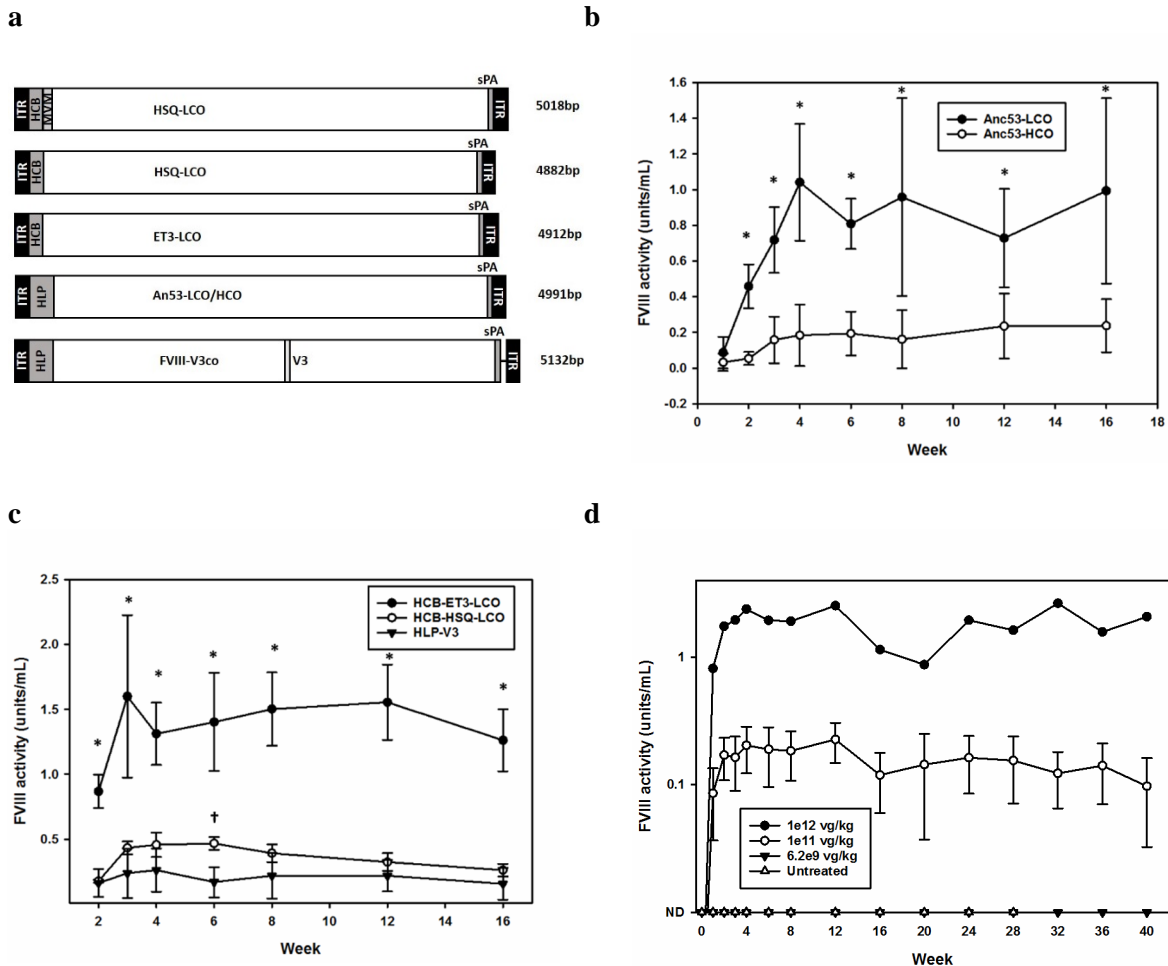


**Figure 6: AAV delivery of optimized FVIII cassettes.** (a) Schematics of transgene designs. (b)

1e11 vector genomes vg/kg of AAV8-HLP-An53k-LCO and AAV2/8-HLP-An53k-HCO were delivered intravenously to hemophilia A mice. (c) 1e11 vector genomes vg/kg of AAV8 HCB-

HSQ-LCO, AAV8-HCB-ET3-LCO, and AAV8-HLP-V3co were delivered intravenously to hemophilia A mice. (d) A long term, dose finding experiment was performed with varying doses

of AAV8-HCB-MVM-ET3-LCO (n = 3-5 per group [b.c], n = 1-3 per group [c], \* = p < 0.05 [b],

\* = p < 0.05 HCB-ET3-LCO vs HLP ET3, † = p < 0.05 HCB-HSQ-LCO vs HLP-V3 [c], error bars represent standard error of the mean)

represent standard error of the mean)

this design does not impact FVIII expression conferred by this cassette design (data not shown). Data out to 40 weeks post AAV injection show no decline in FVIII expression. While the FVIII conferred by this vector was lower than that seen in MVM-free variant, we attribute this to the additional size conferred by the MVM while itself providing no benefit in expression. From the optimization described herein, these vectors provide curative levels of FVIII expression at doses that are 20-fold lower than the maximum tolerated dose of  $2 \times 10^{12}$  vp/kg in a murine model of hemophilia.

### **3.5 Discussion**

Efforts to develop a clinical AAV vector product for hemophilia A have been hampered by the large size of the BDD FVIII cDNA (4374bp), the poor biosynthetic efficiency of FVIII, and vector dose limiting toxicity. Ideally, a clinical AAV-FVIII vector would be of sufficient potency to confer clinically beneficial (>1% of normal) or preferably curative (>40% of normal) circulating FVIII activity at a vector dose no higher than  $2 \times 10^{12}$  vp/kg, a dose which repeated clinical experience has revealed to be a dose limiting toxicity threshold caused by cytotoxic immunity directed against the gene modified hepatocytes. While pharmacological immune suppression has been utilized clinically to mitigate vector cytotoxicity, both responsive and prophylactic immune suppression has only partially mitigated vector mediated hepatotoxicity (78; 84; 150). Furthermore, this cellular immunity is directed specifically against the population of gene modified cells, causing a concurrent loss of protein expression associated with the cellular destruction.

Most recently, BioMarin Pharmaceutical has initiated a Phase 1/2 clinical trial of BMN 270, an AAV gene therapy vector for hemophilia A. This vector utilizes the HLP promoter driving human FVIII packaged in AAV5 capsid. Under their protocol, patients were dosed with low ( $6 \times 10^{12}$  vg/kg), medium ( $2 \times 10^{13}$  vg/kg), and high ( $6 \times 10^{13}$  vg/kg) vector doses. At the lowest vector dose, the single recipient in this cohort showed no detectable FVIII expression. However, at medium and high doses, patients showed dose-dependent benefit ranging from partial to complete phenotypic

correction. However, at these doses 6/8 patients predictably suffered from transaminitis that has been partially controlled through corticosteroid administration (167). While this trial represents a promising development in AAV therapy for hemophilia A, there remains a cogent need to develop AAV-FVIII vectors with improved pharmacodynamic properties. The goal of this study was to develop a state of the art vector with pharmacodynamics compatible with sufficient potency to confer curative levels of FVIII expression at clinically safe vector doses. Furthermore, reducing the viral vector dose required per patient would help reduce the per-patient cost of vector manufacture, which remains a bottleneck to clinical AAV therapy (168).

We previously described pre-clinical testing of a 5.86kb AAV8 vector encoding the bioengineered FVIII transgene ET3 that confers enhanced FVIII secretion efficiency (152). While this vector was of sufficient potency to partially or completely correct the hemophilia A phenotype at vector doses of  $5 \times 10^{11}$  to  $2 \times 10^{13}$  vp/kg, due to the large size of the transgene this vector suffered from substantial intraparticle heterogeneity and low yield vector manufacture. To reduce the size of this vector, we began by generating a completely synthetic AAV cassette, wherein unnecessary viral DNA remnants that have been present in early stage AAV vector designs was removed, leaving only the minimal AAV elements and enzyme restriction sites to allow simple substitution of discrete elements. This alone removed 210bp from our first generation vector design. We further substituted a 49bp synthetic polyadenylation (polyA) signal for our original 260bp bovine growth hormone polyA, removing an additional 211bp. While these modifications reduced the size of the vector transgene to 5.45kb, it remained substantially oversized. (**Supplemental Figure 3.1**)

To further reduce the size of the vector, we utilized an iterative “design, build, test” process to generate a minimally sized yet highly active promoter. In a process similar to that used to generate the previously described “super core promoter” (101), we utilized combinatorial assembly of previously-described elements to iteratively and empirically generate a promoter with the necessary size and strength required for a clinically oriented AAV-FVIII vector. Beginning with the SynO and AFP core elements, the impact of additional transcriptionally oriented modules

proved to not to be independently additive, but rather highly dependent on the interaction between specific modules present in a single design. As seen in the design where the ABP element was used in conjunction with SynO, when the ABPnat element was fused to the HNF1 TF binding motif, the resulting promoter lost detectable activity. However, when the ABPshort element was utilized in combination with the HNF1 element, activity of the SynO-based promoter restored. We attribute this to the exquisite complexity of the interaction and contextually dependent function of TFs, a process which remains difficult to define and methods for detecting these interactions in real time are only recently being realized (169; 170).

Through this iterative process, we arrived at an enhancer consisting of the HNF1 TF binding site proximal to the shortened ABP sequence. This enhancer is fused to the SynO core promoter which is modified with a defined transcription start site, a combination we designated the hepatic combinatorial bundle (HCB). At a total size of 146bp, this minimal promoter was shown to drive FVIII transcription at levels 2-fold higher than the 252bp HLP *in vitro* and 14-fold higher than HLP *in vivo* by hydrodynamic plasmid delivery. At this size, when substituted into our synthetic AAV transgene cassette, the HCB promoter results in an HSQ vector transgene of only 4883bp in length, which is expected to be compatible with complete transgene packaging and improved homogeneity and yield of vector product.

The second significant barrier to AAV gene therapy for hemophilia A is the poor biosynthetic efficiency of the mature FVIII protein itself, which is secreted at levels 2-3 orders of magnitude lower than similarly sized glycoproteins (98). This poor secretory efficiency has been spatially and temporally linked between inefficient trafficking from the ER to the Golgi due to induction of the unfolded protein response (99; 156). Our group and others have made efforts to improve the efficiency of secretion by bioengineering the protein itself. These approaches have included substitution of the FVIII A1/A3 domains with porcine FVIII sequences (ET3), inclusion of additional glycosylation sites within the truncated B-domain linker (V3), and reconstruction of ancestral FVIII protein sequences (An53). In the case of ET3, bioengineering the FVIII molecule

results in 10-100 fold more efficient protein expression. However, in all of these approaches, modification of the primary amino acid sequence and glycosylation patterns result in the possibility of the introduction of immunogenic neoepitopes. While the exogenous protein expression within liver has previously demonstrated a pro-tolerogenic environment, recent work casts doubt that this will translate to FVIII (170; 171). Therefore, development of both native FVIII and modified FVIII designs is warranted in the pursuit of a clinically viable transgene design.

With this in mind, we sought to create a platform that would benefit FVIII expression regardless of the precise primary amino acid sequence. Codon optimization has been routinely utilized in AAV vector designs, both in pre-clinical and now clinical studies. While this approach has been shown to confer benefit in some expression systems, recent studies quantifying the physical pools of tRNA within different tissues have shown that the primary assumption made by codon optimization, that the codon usage bias of an organism reflects the physical pool of available cognate tRNA, may not be reflective of an optimal strategy in certain tissues, including the liver. A commonly accepted causative factor for drift of codon usage bias across evolution is the tolerance of the protein product of particular cDNA for missense mutations (172-175), a mechanism which would allow for coadaptation of synonymous codon mutations and the tRNA milieu within a particular tissue to allow for optimal gene expression. When we investigated tissue-specific bias of genes highly expressed in human liver and myeloid lineage cells, we found that the drift in codon usage bias of these genes compared to the entire human CDS is in fact greater than the drift between the human and murine CDS codon usage biases. We therefore reasoned that codon optimizing to the target tissue of expression may offer benefit greater than that offered by optimization to the entire genome. Building on the work of Dittmar *et al*, we synthesized variants of HSQ, ET3, and An53 codon optimized for expression in the liver based on the codon usage bias of genes highly expressed within the liver, as well as controls optimized using the standard human codon index as well as a myeloid index.

*In vitro* studies showed the liver optimization specifically increased FVIII expression of all FVIII variants within HepG2 cells while decreasing FVIII expression in the non-hepatic BHK cell line relative to either human codon optimized or myeloid optimized variants. Importantly, these optimized constructs were all generated by the same algorithm but utilizing different codon usage indexes. While adjustment of the codon usage index and optimal codon distribution are central aspects of codon optimization, modern codon optimization algorithms also attempt to remove deleterious non-coding RNA motifs, such as destabilizing and structural features. By utilizing the same algorithm which was only adjusted by the codon usage index, these reciprocal experiments strongly suggests that the benefit of liver codon optimization is in fact due to the unique tRNA pool within the liver, and not simply the alteration of RNA motifs or artifact of optimizing to a small subset of genes.

When these codon optimized variants were delivered to the livers of hemophilia A mice by hydrodynamic injection, the benefit of liver codon optimization became more pronounced. When compared to the HCO variant, An53-LCO showed a 7-fold increase in FVIII expression. This benefit of liver optimization was again recapitulated by AAV-mediated delivery of An53, where LCO exhibited 4-5 fold benefit over HCO for the duration of the experiment. Likewise, when compared to the MCO or NoCo variants, HSQ and ET3-LCO both showed 4-fold improvement.

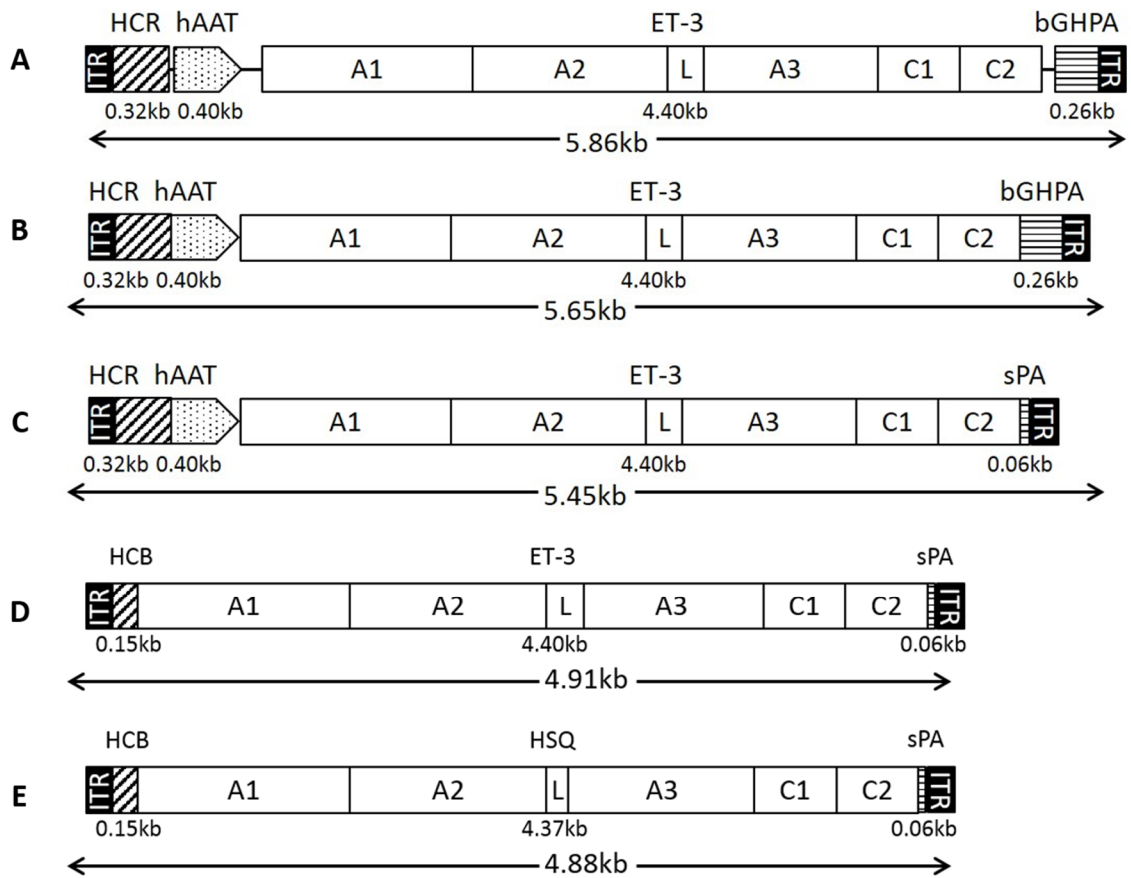
From this, the HepG2 model appears to have underestimated the benefit of liver optimization. tRNA dysregulation is emerging as an important factor driving the increased protein translation and proliferation in both primary cancer tissues as well as cancer derived cell lines (176; 177). In cancer derived cell lines, global tRNA levels have been shown to be elevated 3-5 fold over non-cancer derived cell lines, while in primary breast cancer tissue, tRNA levels were found to be elevated 10-fold over normal breast tissue (176). This expected difference in tRNA levels between the human liver carcinoma derived HepG2 cell line compared to those in the normal hepatocytes of hemophilia A mice may explain the attenuated benefit of LCO *in vitro* compared to the benefits observed *in vivo*, although this postulation will require further investigations.

Finally, our lead clinical candidate vectors, AAV-HCB-HSQ-LCO and AAV-HCB-ET3-LCO, were packaged into AAV8 capsid and delivered to hemophilia A mice at a dose of  $1 \times 10^{11}$  vg/kg. At this low vector dose, the HSQ vector infused mice expressed FVIII at 0.3-0.4 units/mL, which remained higher than that of HLP-V3co for the duration of the experiment. Much of the benefit of the AAV-HLP-V3co design was attributed to the substitution of the V3 linker, a novel 17aa linker that contains 6 glycosylation sites. When included in human FVIII designs, the V3 element increased FVIII expression 2-3 fold. We have now achieved greater levels of FVIII expression from the fully-human AAV-HCB-HSQ-LCO design, representing a significant step forward toward a clinically viable AAV-FVIII vector.

### **3.6 Acknowledgements**

This work was supported by grants from the National Institutes of Health; 1 U54 HL112309-01 and 1 R01 HL092179-01A2 to CBD and HTS, and T32GM008602 to HCB. CBD and HTS are co-founders Expression Therapeutics and own equity in the company. Expression Therapeutics owns the intellectual property associated with ET3. The terms of this arrangement have been reviewed and approved by Emory University in accordance with its conflict of interest policies.

## Supplemental Figure 3.1



**Supplemental Figure 3.1: Schematics of size reduction of AAV-FVIII transgenes** Vector schematics show (A) the initial vector design (AAV-HCR-ET3), (B) the size reduction conferred by removal of unnecessary DNA, (C) size reduction from the utilization of a more compact polyadenylation signal, (D) size reduction from the minimally sized HCB promoter, and (E) the shorter HSQ cDNA, which utilizes a shorter synthetic linker (L) than ET3.

## **Chapter 4**

### **General Discussion**

## 4.1 Collective Results

Despite nearly 15 years of experience with clinical applications of AAV for the treatment of the hemophilias, to date no vector has progressed beyond phase I/II clinical trials. While substantial progress has been made in the field of AAV-FIX vectors, AAV-FVIII vectors lag behind substantially. Development of AAV-FVIII vectors have been hampered by a unique set of obstacles unique to the FVIII protein itself. The large size of the FVIII cDNA and intrinsically poor biosynthetic efficiency of the FVIII protein itself have presented a substantial challenge in creating an AAV vector of sufficient potency to provide curative levels of FVIII expression at vector doses below the  $2 \times 10^{12}$  vp/kg limit imposed by cellular immunity directed against the capsid protein. While the ongoing BioMarin clinical trial of BMN 270, the first AAV-FVIII vector to reach human trials, represents a significant milestone in the field, the extremely high vector doses of  $6 \times 10^{13}$  vp/kg resulted in transaminitis which required extended steroid support to control. Due to these vector toxicities, the trial was suspended until a modified protocol was approved and the trial re-opened in October, 2016.

In chapter 1 we proposed several potential strategies for increasing vector potency to allow for successful application of clinically safe vector doses. It is well established that transgene cassettes that fit within the  $<5.0$ kb packaging capacity of AAV are of higher potency than oversized vectors. As all pre-clinical and now clinical AAV-FVIII vectors exceed this length, making reduction of the transgene size to fit within the optimal size of the AAV vector an attractive opportunity for not only increasing vector potency, but also improving vector manufacture and homogeneity. We also proposed that protein bioengineering and novel strategies of codon optimization may increase the biosynthetic efficiency of nascent FVIII proteins. By combining these strategies, we hypothesized that the potency of AAV-FVIII vectors may be increased to allow for efficacious expression of FVIII at clinically safe vector doses.

In Chapter 2, we investigated the integration of the bioengineered FVIII variant ET3 into an oversized AAV vector. The ET3 protein, which incorporates porcine FVII A1 and A3 domains,

has been previously shown in both recombinant protein and lentiviral gene therapies to increase FVIII expression by 10-100 fold, however, this was the first time this protein has been tested in the context of either AAV-mediated or liver-directed gene therapy. We demonstrated through hydrodynamic injection that the AAV-ET3 cassette recapitulated the increased FVIII expression over human FVII that has been observed in alternative expression systems. When packaged into AAV capsid, this vector was shown to confer high levels of FVIII expression at low vector doses, and provided complete correction of FVIII deficiency at doses as low as  $2 \times 10^{12}$  vp/kg. However, at 5.9kb in length, this vector was substantially oversized. Through molecular analysis of the AAV-FVIII genome of viral particles, we showed that this vector suffered from fragmented transgene packaging and vector particle heterogeneity.

In Chapter 3, we built on the knowledge gained from our first generation AAV-FVIII vector to generate a substantially improved transgene design. To decrease the size of the transgene, we utilized DNA synthesis technology to produce a vector cassette free from unnecessary DNA that persists in most off the shelf AAV designs. We additionally generated a novel 146bp promoter that retained higher gene expression activity than that of larger promoters frequently utilized in liver-directed AAV therapies. This design allowed for the construction of 4.88kb and 4.91kb AAV-HSQ and AAV-ET3 cassettes, respectively, which themselves represent a substantial step forward in AAV-FVIII technologies. We additionally employed a novel modality of codon optimization, where the codon usage bias was altered to reflect that of genes highly expressed within the liver. We showed that this codon optimization strategy increased FVIII expression 7-fold *in vivo* over traditional codon optimization strategies. When the liver codon optimized HSQ was inserted into our minimally sized AAV cassette and delivered to hemophilia A mice, it was found to be of greater potency than AAV-HLP-V3co, a vector design comparable to BMN 270 with the addition of the V3 linker peptide, which has been shown to increase vector potency by over 2-fold. The ET3 variant of this design was of even greater potency. Both our HSQ and ET3 vector designs represent a significant improvement over the state of the art BMN 270 vector.

## 4.2 Implications of Findings

The work presented herein confirm our initial hypothesis: that the oversized nature and poor biosynthetic efficiency of FVIII limit vector potency, and that these limits may be surmounted by novel bioengineering strategies. Previous studies have shown that murine models of AAV-FVIII expression in hemophilia A mice overestimate the levels of FVIII expression conferred by the identical vector administered at the same dose in non-human primates by approximately 20-fold (154). Therefore, we may estimate that a vector capable of conferring complete correction of FVII deficiency in non-human primates, including humans, must confer  $>0.4$  units/mL of FVIII expression in mice at vector doses at or below  $1e11$  vp/kg. Our optimized HSQ and ET3 vectors both achieved this stringent goal of curative level of FVIII expression at predictably safe vector doses.

If these results translate into non-human primates as predicted, clinical application of this vector will enable a new era of clinical management of hemophilia A. In 1916, Minot and Lee showed for the first time that infusion of whole blood from healthy donors could reduce bleeding times in hemophilic patients, for the first time enabling efficacious treatment options for this lethal disease. Since then, treatment options for the hemophilias have essentially used the same mechanism of action: protein replacement. While cryoprecipitates and recombinant protein expression technologies have enabled delivery of higher concentrations of clotting factors of greater purity and safety, the modality has remained the same. By infusing concentrates of the missing protein, patients experience temporary relief from FVIII/FIX deficiency. However, these proteins have a relatively short half-life, and even with tri-weekly prophylaxis, there is an intrinsic peak and valley nature to the levels of circulating clotting factor activity. While protein levels are high immediately after protein infusion, in the subsequent days following infusion activity may decline to only a few percent above normal. While this is sufficient to provide benefit, the risks associated with even the transiently low levels of clotting factor activity occurring between doses remain a cause for concern. What level of FVIII/FIX activity constitutes “protective” is likely

determined by individual needs, and area under the curve of coagulation factor levels are becoming recognized as a better predictor of prevention of hemarthrosis than the peak or trough levels of protein availability.

Now, 100 years after the work of Minot and Lee, AAV gene therapy approaches offer the first substantially different modality of correction of FVIII deficiency than that offered by protein replacement therapy. Under this paradigm, since the production of FVIII from the liver is continuous, this treatment no longer suffers from the same peak and valley levels of FVIII that protein replacement carries. This allows for continuously high and protective levels of FVIII expression, which provides constant protection against hemostatic challenge, which is not given by prophylactic protein replacement. This in itself represents a substantially improved therapy over the current standard of care.

Not only does AAV gene therapy offer constant levels of protein expression, it further offers solutions to many of the other problems that prevent 2/3 of hemophilia patients worldwide from receiving any care at all. The primary factor contributing to this is the high cost of treatment, which is as much as \$150,000 per patient year for prophylactic therapy. As a one-time treatment, AAV gene therapy has the potential to substantially reduce the cost of treatment. While there is currently minimal data to predict the cost of commercial gene therapy, it is reasonable to assume that initially the cost of AAV treatment for hemophilia will offer minimal cost savings over traditional prophylactic therapy. However, as the gene therapy market enters maturity and vector production costs are driven down, the cost of AAV-FVIII vectors may approach trivial on a per-patient basis. At this point in product lifecycle, there will likely emerge pricing solutions tailored to the means intended market, where developed nations will shoulder much of the burden of vector development and investment costs, whereas developing markets, where the need for improved therapy access is greatest, will benefit from low-cost treatment options with the potential to offer long-term correction of the disease with minimal further intervention. AAV vectors have been

shown to exhibit robust thermostability and resistance to degradation, which support the feasibility of global distribution to markets lacking advanced supply chain infrastructure.

Not only do AAV gene therapies offer the potential of a more efficacious yet less expensive durable treatment for hemophilia than protein replacement therapy, they additionally address the complications of poor patient compliance and potentially protein immunogenicity. As a single-dose treatment, the need for tri-weekly intravenous infusions are avoided, sparing the painful and intrusive nature of at-home prophylaxis. Furthermore, exogenous protein expression in the liver is well documented to encourage a pro-tolerogenic immune profile against the protein itself. This is well documented with FIX expression, however, the extension of these finds to FVIII remains uncertain.

For these reasons, AAV gene therapy for the hemophilias has remained an attractive yet elusive goal for the last 20 years. There has been substantial effort, both commercial and academic, to achieve this goal. The technologies presented herein offer solutions to many of the challenges that have constrained development of a clinically viable vector, and have enabled development of a vector that meets the long-standing goal of curative levels of FVIII expression at clinically safe vector doses.

#### **4.3 Limitations and future directions**

While this work has addressed many of the obstacles challenging the development of a suitable AAV-FVIII DNA cassette, this element represents only half of an AAV vector. The vector capsid, the protein shell that protects and directs the transgene cassette during its transport to the target cell, presents several challenges of its own. A primary concern in vector capsid design is pre-existing immunity to the vector capsid. As natural hosts to AAV, most humans have been exposed to the wildtype virus by adulthood. As such, 22-56% of humans are estimated to have pre-existing, inhibitory antibodies against AAV serotype 2, with antibodies frequently cross-reacting to other serotypes (49; 50). Developing either novel capsids, administration protocols, or methods of

subverting immune detection remain attractive and necessary goals in making a globally accessible AAV-FVIII vector.

Steroid administration during vector dose administration is a frequently utilized method of mitigating an immune response against the vector modified cells, however, this is a reactive rather than adaptive approach. Steroid administration exposes the patient to weeks or months of immune suppression and host of steroid-related side effects, while still only partially managing the associated transaminitis. Capsid protein engineering offers the potential to alter or remove the immunogenic epitopes present on AAV capsids. However, modification of these epitopes may alter the binding affinity of the virus for their natural receptors, either decreasing their binding strength or specificity. It is hoped that the development of novel capsids, or discovery of novel, naturally occurring serotypes, will produce a low immunogenicity capsid. An ultimate goal of this will be to develop a capsid or panel of capsids that will allow repeated administration of the vector. At present, the single dose administration of currently utilized AAV vectors results in immunogenic memory against the capsid, preventing subsequent vector administration. If multiple administrations were possible, FVIII expression could be increased by simply administering the vector multiple times. It is this limitation which necessitates vectors of high potency, a vector which could be administered an arbitrary number of times would not need to be of the same potency that is required of single-dose designs, however the cost saving and global accessibility of single-dose AAV vector would be compromised by this approach, leaving single-dose administration a more attractive goal.

However, the ability to administer vector multiple times would address an ongoing concern of non-integrating AAV vectors: the durability of expression. As a non-integrating vector, per-cell vector genome copy number conferred by AAV would be anticipated to decrease over time, as the liver is not terminally differentiated and hepatocytes undergo replacement throughout life. Current data involving the durability of liver-directed AAV gene therapy is limited to animal models, but data in dogs supports the durability of expression for at least 8 years, with the duration of the data

limited by the lifespan of the model (178). With the first human trials now underway, the durability of these vectors will need to be closely observed, and will be informative both of the needs for repeated vector administration as well as the marketability and pricing models of a durable, but not curative, vector.

It is easy to envision an integrating AAV-FVIII vector, wherein dual vector administration of AAV-FVIII and AAV-Rep would restore the integrating potential of the virus. AAV is known to integrate into a specific locus on human chromosome 19, providing it exquisite predictability and safety in terms of the potential for toxicities associated with insertional mutagenesis. By providing the AAV rep proteins *in trans* with the therapeutic vector, integration into this site could be achieved, allowing for duplication of the transgene with cellular division, sparing the dilution associated with non-integrated episomes. Alternatively, gene editing technologies, such as CRISPR/CAS9 offer an alternative method for permanent gene correction which would be inherited by daughter cells of the propagating hepatocyte. However, this approach would require tailoring to the mutation of the individual, with each mutation requiring a unique transgene design, each of which would require rigorous investigation of both its capability to correct the underlying mutation but also its off-target profile, which would substantially complicate the generalization of such a vector.

Importantly, much of the work presented herein is not limited to applications in AAV gene therapy for the hemophilias. AAV vectors are under development for inborn metabolic deficiencies such as ornithine transcarbamylase deficiency and alpha 1 antitrypsin deficiency, cystic fibrosis, Duchenne muscular dystrophy, macular degeneration, and many others. Our minimally sized yet highly potent expression liver-directed cassette stands to significantly improve options for vectors directed the inborn metabolic diseases of the liver, while our tissue-directed codon optimization strategy may benefit the expression of hard to express proteins in many tissues. However, the impact of tissue-specific codon optimization outside of the context of the liver needs to be addressed.

Our tissue specific codon optimization strategy may be substantially improved by direct measurements of the physical pools of tRNA within the target tissue. At present, we are forced to use the codon usage bias of genes highly expressed within a tissue as a predictor of the physical tRNA pools, however, these may not prove predictive in all tissues, and certainly at best only approximate the levels of tRNA. Due to the similarity and complex secondary structure of tRNA, robust and accurate quantification of their levels has only recently become possible, but remains a cumbersome and expensive task. As these technologies improve, we are hopeful that the content of the tRNA pool of many tissues and cell types will become available.

Finally, our findings have applications outside of gene therapy. As seen in our *in vitro* test of tissue-specific codon optimization, exogenous expression of FVIII is significantly impacted by the codon optimization strategy. Liver-directed optimization significantly increased FVIII expression in the tissue-matched HepG2 cells, but substantially decreased expression in the mismatched BHK cell line. Exogenous expression of FVIII in BHK and Chinese hamster ovary (CHO) cells is currently used in production of recombinant FVIII. Low-level FVIII expression in these systems is a significant contributor to the high cost of the protein products. By developing a BHK or CHO directed codon optimization strategy, preferably generated through direct measurement of tRNA levels, it may be possible to improve expression of FVIII or any protein exogenously expressed in these cells, potentially reducing the cost of production and increasing the availability of these therapeutics throughout the global market.

#### **4.4 Conclusions**

This thesis investigated the ability of targeted bioengineering efforts to increase the potency of liver-directed AAV-FVIII vector designs. By incorporating a high-expression bioengineered FVIII variant, a minimally sized expression cassette, and novel modality of codon optimization, we have substantially improved the potency of AAV-FVIII vectors. From data collected from a murine model of hemophilia treated with our vectors, we have generated two vectors, one HSQ and one ET3, which are predicted to be of suitable potency to offer complete

correction of hemophilia A at clinically safe vector doses. These developments may offer improved access to care for hemophilia throughout the world, and may be generalized to AAV gene therapy vectors for diseases beyond the hemophilias.

## References

1. 2015. *Cellular & Gene Therapy Products*.  
<http://www.fda.gov/BiologicsBloodVaccines/CellularGeneTherapyProducts/ucm2005904.htm>
2. Wirth T, Parker N, Yla-Herttuala S. 2013. History of gene therapy. *Gene* 525:162-9
3. 2012. *uniQure's Glybera® First Gene Therapy Approved by European Commission*.  
<http://www.uniquire.com/news/167/182/>
4. Griffith F. 1928. The Significance of Pneumococcal Types. *The Journal of hygiene* 27:113-59
5. Hershey AD, Chase M. 1952. Independent functions of viral protein and nucleic acid in growth of bacteriophage. *The Journal of general physiology* 36:39-56
6. Avery OT, MacLeod CM, McCarty M. 1944. Studies on the Chemical Nature of the Substance Inducing Transformation of Pneumococcal Types : Induction of Transformation by a Desoxyribonucleic Acid Fraction Isolated from Pneumococcus lype III. *The Journal of Experimental Medicine* 79:137-58
7. Szybalska EH, Szybalski W. 1962. Genetics of human cell line. IV. DNA-mediated heritable transformation of a biochemical trait. *Proceedings of the National Academy of Sciences of the United States of America* 48:2026-34
8. Sambrook J, Westphal H, Srinivasan PR, Dulbecco R. 1968. The integrated state of viral DNA in SV40-transformed cells. *Proceedings of the National Academy of Sciences of the United States of America* 60:1288-95
9. Terheggen HG, Lowenthal A, Lavinha F, Colombo JP, Rogers S. 1975. Unsuccessful trial of gene replacement in arginase deficiency. *Zeitschrift fur Kinderheilkunde* 119:1-3

10. Giri I, Danos O, Yaniv M. 1985. Genomic structure of the cottontail rabbit (Shope) papillomavirus. *Proceedings of the National Academy of Sciences of the United States of America* 82:1580-4
11. Blaese RM, Culver KW, Miller AD, Carter CS, Fleisher T, et al. 1995. T lymphocyte-directed gene therapy for ADA- SCID: initial trial results after 4 years. *Science (New York, N.Y.)* 270:475-80
12. Bordignon C, Notarangelo LD, Nobili N, Ferrari G, Casorati G, et al. 1995. Gene therapy in peripheral blood lymphocytes and bone marrow for ADA- immunodeficient patients. *Science (New York, N.Y.)* 270:470-5
13. 2016. *Gene Therapy Clinical Trials Worldwide*.  
<http://www.wiley.com/legacy/wileychi/genmed/clinical/>
14. Shimamura M, Nakagami H, Taniyama Y, Morishita R. 2014. Gene therapy for peripheral arterial disease. *Expert opinion on biological therapy* 14:1175-84
15. Alton E, Armstrong DK, Ashby D, Bayfield KJ, Bilton D, et al. 2016. Efficacy and Mechanism Evaluation. In *A randomised, double-blind, placebo-controlled trial of repeated nebulisation of non-viral cystic fibrosis transmembrane conductance regulator (CFTR) gene therapy in patients with cystic fibrosis*. Southampton (UK): NIHR Journals Library. Number of.
16. Konstan MW, Davis PB, Wagener JS, Hilliard KA, Stern RC, et al. 2004. Compacted DNA nanoparticles administered to the nasal mucosa of cystic fibrosis subjects are safe and demonstrate partial to complete cystic fibrosis transmembrane regulator reconstitution. *Human gene therapy* 15:1255-69
17. Kamimura K, Kanefuji T, Yokoo T, Abe H, Suda T, et al. 2014. Safety assessment of liver-targeted hydrodynamic gene delivery in dogs. *PloS one* 9:e107203

18. Zhang W, Solanki M, Muther N, Ebel M, Wang J, et al. 2013. Hybrid adeno-associated viral vectors utilizing transposase-mediated somatic integration for stable transgene expression in human cells. *PLoS one* 8:e76771
19. Anguela XM, Sharma R, Doyon Y, Miller JC, Li H, et al. 2013. Robust ZFN-mediated genome editing in adult hemophilic mice. *Blood* 122:3283-7
20. Murlidharan G, Sakamoto K, Rao L, Corriher T, Wang D, et al. 2016. CNS-restricted Transduction and CRISPR/Cas9-mediated Gene Deletion with an Engineered AAV Vector. *Molecular therapy. Nucleic acids* 5:e338
21. Sarkis C, Philippe S, Mallet J, Serguera C. 2008. Non-integrating lentiviral vectors. *Current gene therapy* 8:430-7
22. Chodisetty S, Nelson EJ. 2014. Gene therapy in India: a focus. *Journal of biosciences* 39:537-41
23. Cattoglio C, Facchini G, Sartori D, Antonelli A, Miccio A, et al. 2007. Hot spots of retroviral integration in human CD34+ hematopoietic cells. *Blood* 110:1770-8
24. Kvaratskhelia M, Sharma A, Larue RC, Serrao E, Engelman A. 2014. Molecular mechanisms of retroviral integration site selection. *Nucleic acids research* 42:10209-25
25. Naldini L, Blomer U, Gallay P, Ory D, Mulligan R, et al. 1996. In vivo gene delivery and stable transduction of nondividing cells by a lentiviral vector. *Science (New York, N.Y.)* 272:263-7
26. De Palma M, Montini E, Santoni de Sio FR, Benedicenti F, Gentile A, et al. 2005. Promoter trapping reveals significant differences in integration site selection between MLV and HIV vectors in primary hematopoietic cells. *Blood* 105:2307-15
27. Crystal RG. 2014. Adenovirus: the first effective in vivo gene delivery vector. *Human gene therapy* 25:3-11

28. Hendrickx R, Stichling N, Koelen J, Kuryk L, Lipiec A, Greber UF. 2014. Innate immunity to adenovirus. *Human gene therapy* 25:265-84
29. Raper SE, Chirmule N, Lee FS, Wivel NA, Bagg A, et al. 2003. Fatal systemic inflammatory response syndrome in a ornithine transcarbamylase deficient patient following adenoviral gene transfer. *Molecular genetics and metabolism* 80:148-58
30. Pearson S, Jia H, Kandachi K. 2004. China approves first gene therapy. *Nature biotechnology* 22:3-4
31. Muzyczka N. 1992. Use of adeno-associated virus as a general transduction vector for mammalian cells. *Current topics in microbiology and immunology* 158:97-129
32. Carter BJ. 2004. Adeno-associated virus and the development of adeno-associated virus vectors: a historical perspective. *Molecular therapy : the journal of the American Society of Gene Therapy* 10:981-9
33. Samulski RJ, Muzyczka N. 2014. AAV-Mediated Gene Therapy for Research and Therapeutic Purposes. *Annual review of virology* 1:427-51
34. Muzyczka N, Berns KI. 2015. AAV's Golden Jubilee. *Molecular therapy : the journal of the American Society of Gene Therapy* 23:807-8
35. Berns KI, Linden RM. 1995. The cryptic life style of adeno-associated virus. *BioEssays : news and reviews in molecular, cellular and developmental biology* 17:237-45
36. Wu Z, Asokan A, Samulski RJ. 2006. Adeno-associated virus serotypes: vector toolkit for human gene therapy. *Molecular therapy : the journal of the American Society of Gene Therapy* 14:316-27
37. Zincarelli C, Soltys S, Rengo G, Rabinowitz JE. 2008. Analysis of AAV serotypes 1-9 mediated gene expression and tropism in mice after systemic injection. *Molecular therapy : the journal of the American Society of Gene Therapy* 16:1073-80

38. Grieger JC, Samulski RJ. 2005. Packaging capacity of adeno-associated virus serotypes: impact of larger genomes on infectivity and postentry steps. *Journal of virology* 79:9933-44
39. Edelstein M. 2016. *Gene Therapy Clinical Trials Worldwide*.  
<http://www.abedia.com/wiley/vectors.php>
40. Berns KI, Rose JA. 1970. Evidence for a single-stranded adenovirus-associated virus genome: isolation and separation of complementary single strands. *Journal of virology* 5:693-9
41. Sonntag F, Kother K, Schmidt K, Weghofer M, Raupp C, et al. 2011. The assembly-activating protein promotes capsid assembly of different adeno-associated virus serotypes. *Journal of virology* 85:12686-97
42. Duan D, Sharma P, Yang J, Yue Y, Dudus L, et al. 1998. Circular Intermediates of Recombinant Adeno-Associated Virus Have Defined Structural Characteristics Responsible for Long-Term Episomal Persistence in Muscle Tissue. *Journal of virology* 72:8568-77
43. Xie Q, Bu W, Bhatia S, Hare J, Somasundaram T, et al. 2002. The atomic structure of adeno-associated virus (AAV-2), a vector for human gene therapy. *Proceedings of the National Academy of Sciences of the United States of America* 99:10405-10
44. Bartlett JS, Wilcher R, Samulski RJ. 2000. Infectious Entry Pathway of Adeno-Associated Virus and Adeno-Associated Virus Vectors. *Journal of virology* 74:2777-85
45. Douar A-M, Poulard K, Stockholm D, Danos O. 2001. Intracellular Trafficking of Adeno-Associated Virus Vectors: Routing to the Late Endosomal Compartment and Proteasome Degradation. *Journal of virology* 75:1824-33

46. Ferrari FK, Samulski T, Shenk T, Samulski RJ. 1996. Second-strand synthesis is a rate-limiting step for efficient transduction by recombinant adeno-associated virus vectors. *Journal of virology* 70:3227-34
47. Dong JY, Fan PD, Frizzell RA. 1996. Quantitative analysis of the packaging capacity of recombinant adeno-associated virus. *Human gene therapy* 7:2101-12
48. Hirsch ML, Wolf SJ, Samulski RJ. 2016. Delivering Transgenic DNA Exceeding the Carrying Capacity of AAV Vectors. *Methods in molecular biology (Clifton, N.J.)* 1382:21-39
49. Calcedo R, Vandenberghe LH, Gao G, Lin J, Wilson JM. 2009. Worldwide epidemiology of neutralizing antibodies to adeno-associated viruses. *The Journal of infectious diseases* 199:381-90
50. Jeune VL, Joergensen JA, Hajjar RJ, Weber T. 2013. Pre-existing Anti-Adeno-Associated Virus Antibodies as a Challenge in AAV Gene Therapy. *Human Gene Therapy Methods* 24:59-67
51. Mingozi F, Anguela XM, Pavani G, Chen Y, Davidson RJ, et al. 2013. Overcoming Preexisting Humoral Immunity to AAV Using Capsid Decoys. *Science translational medicine* 5:194ra92-ra92
52. Peyvandi F, Garagiola I, Young G. 2016. The past and future of haemophilia: diagnosis, treatments, and its complications. *Lancet (London, England)* 388:187-97
53. Rosner F. 1969. Hemophilia in the Talmud and rabbinic writings. *Annals of internal medicine* 70:833-7
54. Hoyer LW. 1994. Hemophilia A. *The New England journal of medicine* 330:38-47
55. Otto JC. 1996. An account of an hemorrhagic disposition existing in certain families. *Clinical orthopaedics and related research*:4-6

56. Minot GR, Taylor FH. 1947. Hemophilia; the clinical use of antihemophilic globulin. *Annals of internal medicine* 26:363-7
57. Biggs R, Douglas AS, Macfarlane RG, Dacie JV, Pitney WR, Merskey. 1952. Christmas disease: a condition previously mistaken for haemophilia. *British medical journal* 2:1378-82
58. Mannucci PM. 2002. Hemophilia and related bleeding disorders: a story of dismay and success. *Hematology. American Society of Hematology. Education Program*:1-9
59. Makris M, Garson JA, Ring CJ, Tuke PW, Tedder RS, Preston FE. 1993. Hepatitis C viral RNA in clotting factor concentrates and the development of hepatitis in recipients. *Blood* 81:1898-902
60. Evatt BL. 2006. The tragic history of AIDS in the hemophilia population, 1982-1984. *Journal of thrombosis and haemostasis : JTH* 4:2295-301
61. Gitschier J, Wood WI, Goralka TM, Wion KL, Chen EY, et al. 1992. Characterization of the human factor VIII gene. 1984. *Biotechnology (Reading, Mass.)* 24:288-92
62. Choo KH, Gould KG, Rees DJ, Brownlee GG. 1982. Molecular cloning of the gene for human anti-haemophilic factor IX. *Nature* 299:178-80
63. Monahan-Earley R, Dvorak AM, Aird WC. 2013. Evolutionary origins of the blood vascular system and endothelium. *Journal of thrombosis and haemostasis : JTH* 11 Suppl 1:46-66
64. Jagadeeswaran P, Gregory M, Day K, Cykowski M, Thattaliyath B. 2005. Zebrafish: a genetic model for hemostasis and thrombosis. *Journal of thrombosis and haemostasis : JTH* 3:46-53
65. Kehrel B, Wierwille S, Clemetson KJ, Anders O, Steiner M, et al. 1998. Glycoprotein VI is a major collagen receptor for platelet activation: it recognizes the platelet-activating

- quaternary structure of collagen, whereas CD36, glycoprotein IIb/IIIa, and von Willebrand factor do not. *Blood* 91:491-9
66. Nieswandt B, Brakebusch C, Bergmeier W, Schulte V, Bouvard D, et al. 2001. Glycoprotein VI but not alpha2beta1 integrin is essential for platelet interaction with collagen. *The EMBO journal* 20:2120-30
67. Jackson SP. 2007. The growing complexity of platelet aggregation. *Blood* 109:5087-95
68. Dahlback B. 2000. Blood coagulation. *Lancet (London, England)* 355:1627-32
69. Berntorp E, Boulyjenkov V, Brettler D, Chandy M, Jones P, et al. 1995. Modern treatment of haemophilia. *Bulletin of the World Health Organization* 73:691-701
70. Hacker MR, Geraghty S, Manco-Johnson M. 2001. Barriers to compliance with prophylaxis therapy in haemophilia. *Haemophilia : the official journal of the World Federation of Hemophilia* 7:392-6
71. Evatt BL. 1998. Public health and international health-care development for persons with haemophilia: operation improvement and operation access. *Haemophilia : the official journal of the World Federation of Hemophilia* 4 Suppl 2:54-8
72. Eldar-Lissai A, Hou, Q., Krishnan, S. 2014. The Changing Costs of Caring for Hemophilia Patients in the U.S.: Insurers' and Patients' Perspectives. *Blood* 124(21), 199
73. Ehrenforth S, Kreuz W, Scharrer I, Linde R, Funk M, et al. 1992. Incidence of development of factor VIII and factor IX inhibitors in haemophiliacs. *Lancet (London, England)* 339:594-8
74. Di Michele DM. 2011. Immune tolerance induction in haemophilia: evidence and the way forward. *Journal of thrombosis and haemostasis : JTH* 9 Suppl 1:216-25
75. Colowick AB, Bohn RL, Avorn J, Ewenstein BM. 2000. Immune tolerance induction in hemophilia patients with inhibitors: costly can be cheaper. *Blood* 96:1698-702

76. Tarantino MD, Cuker A, Hardesty B, Roberts JC, Sholzberg M. 2016. Recombinant porcine sequence factor VIII (rpFVIII) for acquired haemophilia A: practical clinical experience of its use in seven patients. *Haemophilia : the official journal of the World Federation of Hemophilia*
77. Plug I, Mauser-Bunschoten EP, Brocker-Vriends AH, van Amstel HK, van der Bom JG, et al. 2006. Bleeding in carriers of hemophilia. *Blood* 108:52-6
78. Kay MA, Manno CS, Ragni MV, Larson PJ, Couto LB, et al. 2000. Evidence for gene transfer and expression of factor IX in haemophilia B patients treated with an AAV vector. *Nature genetics* 24:257-61
79. Manno CS, Chew AJ, Hutchison S, Larson PJ, Herzog RW, et al. 2003. AAV-mediated factor IX gene transfer to skeletal muscle in patients with severe hemophilia B. *Blood* 101:2963-72
80. Jiang H, Pierce GF, Ozelo MC, de Paula EV, Vargas JA, et al. 2006. Evidence of multiyear factor IX expression by AAV-mediated gene transfer to skeletal muscle in an individual with severe hemophilia B. *Molecular therapy : the journal of the American Society of Gene Therapy* 14:452-5
81. Herzog RW, Yang EY, Couto LB, Hagstrom JN, Elwell D, et al. 1999. Long-term correction of canine hemophilia B by gene transfer of blood coagulation factor IX mediated by adeno-associated viral vector. *Nature medicine* 5:56-63
82. Manno CS, Pierce GF, Arruda VR, Glader B, Ragni M, et al. 2006. Successful transduction of liver in hemophilia by AAV-Factor IX and limitations imposed by the host immune response. *Nature medicine* 12:342-7
83. Mingozzi F, Maus MV, Hui DJ, Sabatino DE, Murphy SL, et al. 2007. CD8(+) T-cell responses to adeno-associated virus capsid in humans. *Nature medicine* 13:419-22

84. Nathwani AC, Tuddenham EG, Rangarajan S, Rosales C, McIntosh J, et al. 2011. Adenovirus-associated virus vector-mediated gene transfer in hemophilia B. *The New England journal of medicine* 365:2357-65
85. Gao GP, Alvira MR, Wang L, Calcedo R, Johnston J, Wilson JM. 2002. Novel adeno-associated viruses from rhesus monkeys as vectors for human gene therapy. *Proceedings of the National Academy of Sciences of the United States of America* 99:11854-9
86. McCarty DM, Monahan PE, Samulski RJ. 2001. Self-complementary recombinant adeno-associated virus (scAAV) vectors promote efficient transduction independently of DNA synthesis. *Gene therapy* 8:1248-54
87. UniQure B. *uniQure Presents Updated Clinical Data in Patients with Severe Hemophilia B Demonstrating up to 9 Months of Sustained Levels of Factor IX Activity and Therapeutic Effect.* <http://www.uniqure.com/news/320/182/uniQure-Presents-Updated-Clinical-Data-in-Patients-with-Severe-Hemophilia-B-Demonstrating-up-to-9-Months-of-Sustained-Levels-of-Factor-IX-Activity-and-Therapeutic-Effect.html>
88. Monohan P. 2011. A Phase 1 Open-Label, Ascending-Dose trial of AskBio009 in Patients with Severe Hemophilia B. Recombinant DNA Advisory Committee
89. Simioni P, Tormene D, Tognin G, Gavasso S, Bulato C, et al. 2009. X-linked thrombophilia with a mutant factor IX (factor IX Padua). *The New England journal of medicine* 361:1671-5
90. Shire P. 2016. *Second Quarter 2016 Results Webcast.* <http://investors.shire.com/quarterly-results/year-2016.aspx>

91. Wang Lea. 2016. A Dose-Escalating Preclinical Study to Determine the Efficacy, MED, and Safety of a Clinical Candidate Vector in a Mouse Model of Hemophilia B. In *American Society of Gene and Cell Therapy*, p. Abstract #227. Washington, DC
92. Therapeutics S. *Spark Therapeutics Announces Updated Data from First Cohort in Hemophilia B Phase 1/2 Trial Demonstrating Consistent, Sustained Therapeutic Levels of Factor IX Activity*. <http://ir.sparktx.com/phoenix.zhtml?c=253900&p=irol-newsArticle&ID=2177020>
93. Pasi J. Interim results of an open-label, Phase 1/2 study of BMN 270, an AAV5-FVIII gene transfer in severe hemophilia A. *Proc. World Federation of Hemophilia World Congress, Orlando, Florida, 2016*:
94. Salganik M, Aydemir F, Nam H-J, McKenna R, Agbandje-McKenna M, Muzyczka N. 2014. Adeno-Associated Virus Capsid Proteins May Play a Role in Transcription and Second-Strand Synthesis of Recombinant Genomes. *Journal of virology* 88:1071-9
95. Yang Q, Mamounas M, Yu G, Kennedy S, Leaker B, et al. 1998. Development of novel cell surface CD34-targeted recombinant adenoassociated virus vectors for gene therapy. *Human gene therapy* 9:1929-37
96. Grifman M, Trepel M, Speece P, Gilbert LB, Arap W, et al. 2001. Incorporation of tumor-targeting peptides into recombinant adeno-associated virus capsids. *Molecular therapy : the journal of the American Society of Gene Therapy* 3:964-75
97. Perabo L, Endell J, King S, Lux K, Goldnau D, et al. 2006. Combinatorial engineering of a gene therapy vector: directed evolution of adeno-associated virus. *The journal of gene medicine* 8:155-62

98. Kaufman RJ, Pipe SW, Tagliavacca L, Swaroop M, Moussalli M. 1997. Biosynthesis, assembly and secretion of coagulation factor VIII. *Blood coagulation & fibrinolysis : an international journal in haemostasis and thrombosis* 8 Suppl 2:S3-14
99. Doering CB, Healey JF, Parker ET, Barrow RT, Lollar P. 2004. Identification of porcine coagulation factor VIII domains responsible for high level expression via enhanced secretion. *The Journal of biological chemistry* 279:6546-52
100. Brown HC, Gangadharan B, Doering CB. 2011. Enhanced Biosynthesis of Coagulation Factor VIII through Diminished Engagement of the Unfolded Protein Response. *The Journal of biological chemistry* 286:24451-7
101. Juven-Gershon T, Cheng S, Kadonaga JT. 2006. Rational design of a super core promoter that enhances gene expression. *Nature methods* 3:917-22
102. Hershberg R, Petrov DA. 2009. General rules for optimal codon choice. *PLoS genetics* 5:e1000556
103. Qian W, Yang J-R, Pearson NM, Maclean C, Zhang J. 2012. Balanced Codon Usage Optimizes Eukaryotic Translational Efficiency. *PLoS genetics* 8:e1002603
104. Garel JP, Mandel P, Chavancy G, Daillie J. 1970. Functional adaptation of tRNAs to fibroin biosynthesis in the silk gland of *Bombyx mori* L. *FEBS Letters* 7:327-9
105. Garel J-P. 1976. Quantitative adaptation of isoacceptor tRNAs to mRNA codons of alanine, glycine and serine. *Nature* 260:805-6
106. Gouy M, Gautier C. 1982. Codon usage in bacteria: correlation with gene expressivity. *Nucleic acids research* 10:7055-74
107. Dong H, Nilsson L, Kurland CG. 1996. Co-variation of tRNA abundance and codon usage in *Escherichia coli* at different growth rates. *Journal of molecular biology* 260:649-63

108. Dittmar KA, Goodenbour JM, Pan T. 2006. Tissue-specific differences in human transfer RNA expression. *PLoS genetics* 2:e221
109. High KA, Aubourg P. 2011. rAAV Human Trial Experience. In *Adeno-Associated Virus*, ed. RO Snyder, P Moullier:429-57: Humana Press. Number of 429-57 pp.
110. Grieger JC, Samulski RJ. 2005. Packaging Capacity of Adeno-Associated Virus Serotypes: Impact of Larger Genomes on Infectivity and Postentry Steps. *Journal of Virology* 79:9933-44
111. Ehrenforth S, Kreuz W, Linde R, Funk M, Güngör T, et al. 1992. Incidence of development of factor VIII and factor IX inhibitors in haemophiliacs. *The Lancet* 339:594-8
112. Mingozi F, High KA. 2013. Immune responses to AAV vectors: overcoming barriers to successful gene therapy. *Blood* 122:23-36
113. Heinz S, Schüttrumpf J, Simpson J, Pepperkok R, Nicolaes G, et al. 2009. Factor VIII-eGFP fusion proteins with preserved functional activity for the analysis of the early secretory pathway of factor VIII. *Thrombosis and Haemostasis* 102:925-35
114. Dorner A, Bole D, Kaufman R. 1997. The relationship of N-linked glycosylation and heavy chain-binding protein association with the secretion of glycoproteins. *J Cell Bio* 105:2665-74
115. Swaroop M, Moussalli M, Pipe SW, Kaufman RJ. 1997. Mutagenesis of a Potential Immunoglobulin-binding Protein-binding Site Enhances Secretion of Coagulation Factor VIII. *Journal of Biological Chemistry* 272:24121-4
116. Pipe SW, Morris JA, Shah J, Kaufman RJ. 1998. Differential Interaction of Coagulation Factor VIII and Factor V with Protein Chaperones Calnexin and Calreticulin. *Journal of Biological Chemistry* 273:8537-44

117. Brown HC, Gangadharan B, Doering CB. 2011. Enhanced Biosynthesis of Coagulation Factor VIII through Diminished Engagement of the Unfolded Protein Response. *Journal of Biological Chemistry* 286:24451-7
118. Doering CB, Healey JF, Parker ET, Barrow RT, Lollar P. 2002. High Level Expression of Recombinant Porcine Coagulation Factor VIII. *Journal of Biological Chemistry* 277:38345-9
119. Doering CB, Healey JF, Parker ET, Barrow RT, Lollar P. 2004. Identification of Porcine Coagulation Factor VIII Domains Responsible for High Level Expression via Enhanced Secretion. *Journal of Biological Chemistry* 279:6546-52
120. Dooris K, Denning G, Gangadharan B, Javazon E, McCarty D, et al. 2009. Comparison of Factor VIII Transgenes Bioengineered for Improved Expression in Gene Therapy of Hemophilia A. *Molecular therapy : the journal of the American Society of Gene Therapy* 20:465-78
121. Manno CS, Arruda VR, Pierce GF, Glader B, Ragni M, et al. 2006. Successful transduction of liver in hemophilia by AAV-Factor IX and limitations imposed by the host immune response. *Nature medicine* 12:342-7
122. Hirsch ML, Li C, Bellon I, Yin C, Chavala S, et al. 2013. Oversized AAV Transduction Is Mediated via a DNA-PKcs-independent, Rad51C-dependent Repair Pathway. *Molecular therapy : the journal of the American Society of Gene Therapy*
123. Wu Z, Yang H, Colosi P. 2009. Effect of Genome Size on AAV Vector Packaging. *Molecular therapy : the journal of the American Society of Gene Therapy* 18:80-6
124. Gonçalves M. 2005. Adeno-associated virus: from defective virus to effective vector. *Virology Journal* 2

125. Doering CB, Parker ET, Healey JF, Craddock HN, Barrow RT, Lollar P. 2002. Expression and Characterization of Recombinant Murine Factor VIII. *Thrombosis and Haemostasis* 88:450-8
126. Ayuso E, Mingozi F, Montane J, Leon X, Anguela XM, et al. 2010. High AAV vector purity results in serotype- and tissue-independent enhancement of transduction efficiency. *Gene therapy* 17:503-10
127. Bi L, Lawler AM, Antonarakis SE, High KA, Gearhart JD, Kazazian HH. 1995. Targeted disruption of the mouse factor VIII gene produces a model of haemophilia A. *Nature genetics* 10:119-21
128. Qian J, Borovok M, Bi L, Kazazian HH, Hoyer LW. 1999. Inhibitor Antibody Development and T Cell Response to Human Factor VIII in Murine Hemophilia A. *Thrombosis and Haemostasis* 81:240-4
129. Parker ET, Healey JF, Barrow RT, Craddock HN, Lollar P. 2004. Reduction of the inhibitory antibody response to human factor VIII in hemophilia A mice by mutagenesis of the A2 domain B-cell epitope. *Blood* 104:704-10
130. Meeks SL, Healey JF, Parker ET, Barrow RT, Lollar P. 2009. Non-classical anti-factor VIII C2 domain antibodies are pathogenic in a murine in vivo bleeding model. *Journal of Thrombosis and Haemostasis* 7:658-64
131. Kasper C, Aledort L, Aronson D, Counts R, Edson J, et al. 1975. Proceedings: A more uniform measurement of factor VIII inhibitors. *Thromb Diath Haemorrh* 34
132. Davidoff AM, Ng CYC, Zhou J, Spence Y, Nathwani AC. 2003. Sex significantly influences transduction of murine liver by recombinant adeno-associated viral vectors through an androgen-dependent pathway. *Blood* 102:480-8

133. Lu H, Chen L, Wang J, Huack B, Sarkar R, et al. 2008. Complete Correction of Hemophilia A with Adeno-Associated Viral Vectors Containing a Full-Size Expression Cassette. *Human gene therapy* 19:648-54
134. Siner JI, Iacobelli NP, Sabatino DE, Ivanciu L, Zhou S, et al. 2013. Minimal modification in the factor VIII B-domain sequence ameliorates the murine hemophilia A phenotype. *Blood* 121:4396-403
135. McIntosh J, Lenting PJ, Rosales C, Lee D, Rabbanian S, et al. 2013. Therapeutic levels of FVIII following a single peripheral vein administration of rAAV vector encoding a novel human factor VIII variant. *Blood* 121:3335-44
136. Doering CB, Denning G, Dooriss K, Gangadharan B, Johnston JM, et al. 2009. Directed Engineering of a High-expression Chimeric Transgene as a Strategy for Gene Therapy of Hemophilia A. *Molecular therapy : the journal of the American Society of Gene Therapy* 17:1145-54
137. Gangadharan B, Parker ET, Ide LM, Spencer HT, Doering CB. 2006. High-level expression of porcine factor VIII from genetically modified bone marrow-derived stem cells. *Blood* 107:3859-64
138. Spencer HT, Denning G, Gautney RE, Dropulic B, Roy AJ, et al. 2011. Lentiviral Vector Platform for Production of Bioengineered Recombinant Coagulation Factor VIII. *Molecular therapy : the journal of the American Society of Gene Therapy* 19:302-9
139. Finn JD, Nichols TC, Svoronos N, Merricks EP, Bellenger DA, et al. 2012. The efficacy and the risk of immunogenicity of FIX Padua (R338L) in hemophilia B dogs treated by AAV muscle gene therapy. *Blood* 120:4521-3
140. Elizabeth M. Parzych HL, Xiangfan Yin, Qin Liu, Te-Lang Wu, Gregory M. Podsakoff, Katherine A. High, Matthew H. Levine, and Hildegund C.J. Ertl. 2013. Effects of

- Immunosuppression on Circulating Adeno-Associated Virus Capsid-Specific T cells in Humans. *Human gene therapy* 24
141. LW H. 1995. The incidence of factor VIII inhibitors in patients with severe hemophilia A. In *Inhibitors to coagulation factors*:35-45: Plenum. Number of 35-45 pp.
142. Wight J, Paisley S. 2003. The epidemiology of inhibitors in haemophilia A: a systematic review. *Haemophilia : the official journal of the World Federation of Hemophilia* 9:418-35
143. Astermark J, Altisent C, Batorova A, Diniz MJ, Gringeri A, et al. 2010. Non-genetic risk factors and the development of inhibitors in haemophilia: a comprehensive review and consensus report. *Haemophilia : the official journal of the World Federation of Hemophilia* 16:747-66
144. Nathwani AC, Tuddenham EGD, Rangarajan S, Rosales C, McIntosh J, et al. 2011. Adenovirus-Associated Virus Vector–Mediated Gene Transfer in Hemophilia B. *New England Journal of Medicine* 365:2357-65
145. Qadura M, Waters B, Burnett E, Chegeni R, Hough C, et al. 2011. Immunoglobulin isotypes and functional anti-FVIII antibodies in response to FVIII treatment in Balb/c and C57BL/6 haemophilia A mice. *Haemophilia : the official journal of the World Federation of Hemophilia* 17:288-95
146. Healey JF, Parker ET, Barrow RT, Langley TJ, Church WR, Lollar P. 2009. The comparative immunogenicity of human and porcine factor VIII in haemophilia A mice. *Thrombosis and Haemostasis* 102:35-41
147. Ciavarella N, Antoncicchi S, Ranieri P. 1984. Efficacy of porcine factor VIII in the management of haemophiliacs with inhibitors. *British Journal of Haematology* 58:641-8

148. Kempton CL, Abshire TC, Deveras RA, Hoots WK, Gill JC, et al. 2012. Pharmacokinetics and safety of OBI-1, a recombinant B domain-deleted porcine factor VIII, in subjects with haemophilia A. *Haemophilia : the official journal of the World Federation of Hemophilia* 18:798-804
149. Ide LM, Iwakoshi NN, Gangadharan B, Jobe S, Moot R, et al. 2010. Functional aspects of factor VIII expression after transplantation of genetically-modified hematopoietic stem cells for hemophilia A. *The journal of gene medicine* 12:333-44
150. Nathwani AC, Reiss UM, Tuddenham EG, Rosales C, Chowdary P, et al. 2014. Long-term safety and efficacy of factor IX gene therapy in hemophilia B. *The New England journal of medicine* 371:1994-2004
151. Wu Z, Yang H, Colosi P. 2010. Effect of Genome Size on AAV Vector Packaging. *Molecular Therapy* 18:80-6
152. Brown HC, Wright JF, Zhou S, Lytle AM, Shields JE, et al. 2014. Bioengineered coagulation factor VIII enables long-term correction of murine hemophilia A following liver-directed adeno-associated viral vector delivery. *Molecular therapy. Methods & clinical development* 1:14036
153. Lu H, Chen L, Wang J, Huack B, Sarkar R, et al. 2008. Complete Correction of Hemophilia A with Adeno-Associated Viral Vectors Containing a Full-Size Expression Cassette. *Human gene therapy* 19:648-54
154. McIntosh J, Lenting PJ, Rosales C, Lee D, Rabbanian S, et al. 2013. Therapeutic levels of FVIII following a single peripheral vein administration of rAAV vector encoding a novel human factor VIII variant. *Blood* 121:3335-44
155. Nathwani AC, Gray JT, Ng CY, Zhou J, Spence Y, et al. 2006. Self-complementary adeno-associated virus vectors containing a novel liver-specific human factor IX expression

- cassette enable highly efficient transduction of murine and nonhuman primate liver. *Blood* 107:2653-61
156. Brown HC, Gangadharan B, Doering CB. 2011. Enhanced biosynthesis of coagulation factor VIII through diminished engagement of the unfolded protein response. *The Journal of biological chemistry* 286:24451-7
157. Ancuta P, Liu KY, Misra V, Wacleche VS, Gosselin A, et al. 2009. Transcriptional profiling reveals developmental relationship and distinct biological functions of CD16+ and CD16- monocyte subsets. *BMC genomics* 10:403
158. Stothard P. 2000. The sequence manipulation suite: JavaScript programs for analyzing and formatting protein and DNA sequences. *BioTechniques* 28:1102, 4
159. Harte RA, Farrell CM, Loveland JE, Suner MM, Wilming L, et al. 2012. Tracking and coordinating an international curation effort for the CCDS Project. *Database : the journal of biological databases and curation* 2012:bas008
160. Zakas PM, Brown HC, Knight K, Meeks SL, Spencer HT, et al. 2016. Enhancing the pharmaceutical properties of protein drugs by ancestral sequence reconstruction. *Nature biotechnology*
161. Chan PP, Lowe TM. 2009. GtRNAdb: a database of transfer RNA genes detected in genomic sequence. *Nucleic acids research* 37:D93-7
162. Doering C, Parker ET, Healey JF, Craddock HN, Barrow RT, Lollar P. 2002. Expression and characterization of recombinant murine factor VIII. *Thromb Haemost* 88:450-8
163. Bi L, Lawler AM, Antonarakis SE, High KA, Gearhart JD, Kazazian HH, Jr. 1995. Targeted disruption of the mouse factor VIII gene produces a model of haemophilia A. *Nature genetics* 10:119-21

164. Ryffel GU, Kugler W, Wagner U, Kaling M. 1989. Liver cell specific gene transcription in vitro: the promoter elements HP1 and TATA box are necessary and sufficient to generate a liver-specific promoter. *Nucleic acids research* 17:939-53
165. Godbout R, Ingram R, Tilghman SM. 1986. Multiple regulatory elements in the intergenic region between the alpha-fetoprotein and albumin genes. *Molecular and cellular biology* 6:477-87
166. Rouet P, Raguenez G, Tronche F, Yaniv M, N'Guyen C, Salier JP. 1992. A potent enhancer made of clustered liver-specific elements in the transcription control sequences of human alpha 1-microglobulin/bikunin gene. *The Journal of biological chemistry* 267:20765-73
167. Pasi J. Interim results of an open-label, Phase 1/2 study of BMN 270, an AAV5-FVIII gene transfer in severe hemophilia A. *Proc. World Federation of Hemophilia 2016 World Congress, Orlando, Florida, 2016:*
168. Ayuso E. 2016. Manufacturing of recombinant adeno-associated viral vectors: new technologies are welcome. *Molecular therapy. Methods & clinical development* 3:15049
169. Fuda NJ, Ardehali MB, Lis JT. 2009. Defining mechanisms that regulate RNA polymerase II transcription in vivo. *Nature* 461:186-92
170. Gebhardt JCM, Suter DM, Roy R, Zhao ZW, Chapman AR, et al. 2013. Single Molecule Imaging of Transcription Factor Binding to DNA in Live Mammalian Cells. *Nature methods* 10:421-6
171. Cao O, Dobrzynski E, Wang L, Nayak S, Mingle B, et al. 2007. Induction and role of regulatory CD4+CD25+ T cells in tolerance to the transgene product following hepatic in vivo gene transfer. *Blood* 110:1132-40

172. Drummond DA, Wilke CO. 2009. The evolutionary consequences of erroneous protein synthesis. *Nature reviews. Genetics* 10:715-24
173. Akashi H. 1994. Synonymous Codon Usage in *Drosophila Melanogaster*: Natural Selection and Translational Accuracy. *Genetics* 136:927-35
174. Stoletzki N, Eyre-Walker A. 2007. Synonymous codon usage in *Escherichia coli*: selection for translational accuracy. *Molecular biology and evolution* 24:374-81
175. Shah P, Gilchrist MA. 2010. Effect of Correlated tRNA Abundances on Translation Errors and Evolution of Codon Usage Bias. *PLoS genetics* 6:e1001128
176. Pavon-Eternod M, Gomes S, Geslain R, Dai Q, Rosner MR, Pan T. 2009. tRNA over-expression in breast cancer and functional consequences. *Nucleic acids research* 37:7268-80
177. Winter AG, Sourvinos G, Allison SJ, Tosh K, Scott PH, et al. 2000. RNA polymerase III transcription factor TFIIC2 is overexpressed in ovarian tumors. *Proceedings of the National Academy of Sciences of the United States of America* 97:12619-24
178. Niemeyer GP, Herzog RW, Mount J, Arruda VR, Tillson DM, et al. 2009. Long-term correction of inhibitor-prone hemophilia B dogs treated with liver-directed AAV2-mediated factor IX gene therapy. *Blood* 113:797-806